INFORMATION TO USERS

This manuscript has been reproduced from the microfilm master. UMI films the text directly from the original or copy submitted. Thus, some thesis and dissertation copies are in typewriter face, while others may be from any type of computer printer.

The quality of this reproduction is dependent upon the quality of the copy submitted. Broken or indistinct print, colored or poor quality illustrations and photographs, print bleedthrough, substandard margins, and improper alignment can adversely affect reproduction.

In the unlikely event that the author did not send UMI a complete manuscript and there are missing pages, these will be noted. Also, if unauthorized copyright material had to be removed, a note will indicate the deletion.

Oversize materials (e.g., maps, drawings, charts) are reproduced by sectioning the original, beginning at the upper left-hand corner and continuing from left to right in equal sections with small overlaps.

Photographs included in the original manuscript have been reproduced xerographically in this copy. Higher quality 6" x 9" black and white photographic prints are available for any photographs or illustrations appearing in this copy for an additional charge. Contact UMI directly to order.

Bell & Howell Information and Learning
300 North Zeeb Road, Ann Arbor, MI 48106-1346 USA

UMI®
800-521-0600

CYCLIC BEHAVIOR OF COHESSIONLESS GRANULAR MEDIA USING THE COMPACT STATE CONCEPT

Ali Noorzad

A Thesis

in

The School for Building

(Civil Engineering Program)

Presented in Partial Fulfillment of the Requirements
For the Degree of Doctor of Philosophy at
Concordia University
Montreal, Quebec, Canada

February 1998

ABSTRACT

CYCLIC BEHAVIOR OF COHESIONLESS GRANULAR MEDIA USING THE COMPACT STATE CONCEPT

Ali Noorzad, Ph.D.
Concordia University, 1998

Soil densification may lead to buildup of excess pore water pressure, which causes the soil to lose its strength and resulting in, possibly, the instability of the system. For this reason the concept of compact state, defined as the state that all granular will eventually assume when subjected to large number of stress cycles, is postulated.

The proposed constitutive model used in describing the stress-strain characteristics of the soil is the extended CANAsand model: an elasto-plastic material with a non-associated flow rule along with the concept of bounding surface plasticity possessing ultimate state and compact state. The model is capable of realistically simulating stress-strain behavior of sands under monotonic and cyclic, drained and undrained loading conditions. The numerical results indicate that samples looser than the critical void ratio have a very high potential to collapse upon loading. Deposits denser than the critical void ratio could also liquefy as the tendency to contract exists even in these deposits. Dilatation manifests itself only if the deposit is subjected to large amplitude cyclic loading. Such high stress loading cycles are not likely to occur very often in nature.

The present research focuses on the modification of CANAsand model (to incorporate the compact state) and its application to two particular problems in the domain of large displacements. These are:

(i) The quasi-static behavior of seabed sand deposit under the action of a standing wave is investigated. The simulation results of seabed sands are given and the influence of the wave amplitude and the wave length for a wide range of void ratio are discussed.

(ii) An upper bound solution of the sand blow phenomenon that has received attention of the geotechnical and earthquake engineers is also presented. The application of the ID (Integro-Differential) technique for plane strain problems is discussed. Some numerical experiments are carried out by the computer in order to provide an assessment of the performance of a system composed of a surficial clay layer and supported by a deposit of sand.

Dedicated to

Prof. Hormoz B. Poorooshasb

who inspired many aspects of my life

ACKNOWLEDGEMENTS

The author would like to express his sincere appreciation to his supervisor and dissertation committee chairman, Professor Hormoz B. Poorooshasb, for his invaluable guidance, encouragement, inspiration, and continuous support throughout his Ph. D. studies at Concordia University. Without his valuable advice, most dynamic and encouraging personality this work would not have been completed.

Many hours of fruitful discussion on constitutive modeling and theoretical soil mechanics with Professor Poorooshasb deserve special recognition. I believe that those hours of discussion have significantly contributed to my desire for a dedicated academic life.

I also wish to acknowledge Professor N. Miura of Saga University, Japan for his kindness, assistance and advice while I was visiting as a research fellow at Saga University, Japan.

The research was financially supported by the Ministry of Culture and Higher Education of Iran, the Ministry of Energy of Iran and Natural Science and Engineering Research Council (NSERC) of Canada. Their support is gratefully acknowledged.

The author would like to express his gratitude to his parents and family whose unconditional love and support have made it possible for him to pursue advanced studies. I will always remember my father as being the first and one of the best teachers I have ever had.

I would also like to thank my wife, daughter and son for their endless patience, supreme devotion and understanding during the entire period of my studies at Concordia University.

TABLE OF CONTENTS

LIST OF FIGURES

1

INTRODUCTION

1.1 MOTIVATION FOR THE STUDY

Engineering is concerned with understanding, analyzing, and predicting the way in which real devices, structures, and pieces of equipment will behave in use. It is rarely possible to perform an analysis in which full knowledge of the object being analyzed permits a complete and accurate description of the object to be incorporated in the analysis. Understanding of the behavior of real objects, in particular soils, is improved if intelligent simplifications of reality are made and analyses are performed using simplified models.

One problem that has received an extensive attention in the field of geotechnical engineering is the liquefaction phenomenon. Liquefaction is associated with large deformation as a result of decreased shear strength in saturated cohesionless soils. A phenomenon wherein a saturated sand loses a large percentage of its shear resistance due to the monotonic or to the cyclic loading, and flows in a manner resembling a liquid until shear stresses acting on the mass are as low as its reduced resistance.

Liquefaction of soil has been recognized as a major cause of substantial damages to the public facilities, lifeline and residential buildings. Extension damages to port facilities, utilities, highway and high-rise residential and office structures during earthquakes have attracted geotechnical engineers to explore and study the mechanism of

liquefaction and its consequences in relation to large strains and instability of constructed facilities.

1.2 STATEMENT OF THE PROBLEM

Engineering structures are subjected to "normal loading conditions" and "exceptional loading conditions." The exceptional loading conditions include transient loads, which are variable in time as for their magnitude and direction. These transient loads may be divided into two categories. First, those that must be treated as true dynamic cases, such as earthquake loading. Second, those cases which, in view of their rather slow, but nevertheless transient mode of action, may be treated as a quasi-static situation. However, it is worth noting that certain differences exist between earthquake excitation and ocean wave loading, although both are cyclic in nature.

Liquefaction problems are frequently encountered in the field of geotechnical engineering. Two common problems in this field included: (i) wave - induced liquefaction, (ii) earthquake - induced liquefaction.

(i) The ocean wave-induced response of seafloor deposits has received considerable attention in marine geotechnical engineering. In view of the complexity of the general problem and associated uncertainties many simplifying assumptions have been made. Zienkiewicz and Bettess (1982) have shown that a typical seabed problem under wave loading in which the period of wave is no shorter than 10 seconds and the wave length is of the order of 10m, can be assimilated to slow-motion phenomenon. It may therefore be rational to omit the inertia terms from the governing equations.

When ocean waves propagate over a seabed, they impose a periodical water pressure on the surface of seabed. Although the real nature of ocean waves is very complex, the wave-associated pressure on the surface of the seabed may be evaluated with the relatively simple and generally most useful theory of ocean surface wave propagation, namely the small amplitude theory known as the Airy wave theory. The approximation with the small amplitude wave theory can be considered reasonable, when the fundamental properties of a group of irregular waves are expressed by a superposition of the sinusoidal waves.

The evaluation of response and the integrity of the soils in front of the structure subjected to the action of wave storms for various nearshore installations involved in ocean resource exploitation (buried pipelines, gravity and platform structures) as well as coastal development (rubble mound and caisson-type breakwaters) is to be analyzed. This is done as a free field analysis. That is, the presence of the protective unit is ignored and the problem is solved as if no such structure existed. This simplifying assumption is the most stringent condition imposed but is necessary in view of the rather complex nature of the problem. The results obtained using this simplification are then used to interpret the behavior of the structure.

(ii) Realizing the significance of soil liquefaction, a major task of the geotechnical engineer is to determine the susceptibility of a particular site of interest to liquefaction. When strong ground shaking or earthquake occurs, a film of water is created between the sand deposit and the overlying thin loose soil deposit leading to the instability of the system. Passage of earthquake waves opens fissures, violently forcing out the water and

with it large quantities of sand. The loose soil layer may become liquid and subsequently settle into a denser state. This phenomenon is known as sand blows, which has been observed at many sites subjected to earthquake loading.

The production of sand blows or sand volcanoes begins at the base of the relatively fine-grained surface soil layer and propagates to the surface, where they emerge explosively some time after the vibratory disturbance that initiated the process. The original ground surface underlying the sand blows is commonly depressed, owing to the displacement of sand and water from the subsurface onto the surface. This mechanism of sand blows has been observed to occur in nature in the few minutes following an earthquake.

Penick (1981) quoted an observer of the great New Madrid earthquakes: "Great amounts of liquid spurted into the air, it rushed out in all quarters... ejected to the height from ten to fifteen feet, and falling in a black shower, mixed with the sand.... The whole surface of the country remained covered with holes, which resembled so many craters of volcanoes...."

Prediction of this phenomenon requires an understanding of fundamental soil behavior under earthquake loading conditions, which is typically of cyclic nature. The study is of importance as it relates to the "dynamic liquefaction" of sand deposits. The present study addresses this aspect and aims to develop a new method for dynamic analyses in conjunction with the Integro-Differential (ID) technique (Poorooshasb et al., 1996 a, b, and c). The ID technique is a simple analytical tool that can be used in the evaluating and solving a certain problems encountered in geomechanics.

1.3 PURPOSE OF THE STUDY

The objective of the present study is to investigate the problem of soil liquefaction and its consequences, such as the permanent deformation and large strains leading to the instability of the structure. To study the above mentioned problems in a qualitative manner, it is necessary:

- To describe a mathematical formulation for analyzing soil liquefaction and deformation in soil system.

- To develop a constitutive model to define the behavior of the soil under various stress and strain. Constitutive equations are derived by modifying of CANAsand model using the new concept, the compact state, to assess the applicability of CANAsand model in simulating the cyclic behavior of sand in loose and dense state.

- To establish efficient computational means of numerical approximation incorporating the proposed constitutive model with the aid of the ID (Integro-Differential) technique to find the distribution of stress and strain in the soil system.

It is obvious that meaningful answers can only be achieved if all three aspects are simultaneously tackled. Bearing in mind the difficulties and limitations of the experimental evaluations of the magnitude and patterns of stress-strain within a sample, the present study is only concerned with information acquired from theoretical analysis and computer tests in order to have a qualitative idea of the developed model.

1.4 STRUCTURE OF THE THESIS

The sequence of the material covered in this dissertation is as follows. The thesis consists of six chapters. Following the introductory chapter which explains the objective and scope of the study a review of some of the major works which have already been done in the area of soil plasticity models is presented in Chapter 2 to introduce the motivations of the present research.

In Chapter 3 the main characteristics of the critical state line are presented and discussed. It is followed by introducing the concept of compact state. Then a brief summary of the CANAsand model, which is based on the bounding surface plasticity incorporating a non-associated flow rule, is provided. Next, the extension of the CANAsand model is made using the compact state concept. Finally typical simulation results of cyclic loading on sandy soils are illustrated and analyzed. This chapter serves as an essential background for some of the material discussed in other sections of the present study.

Chapter 4 is concerned with the nature of loads imposed by standing waves on the seabed deposits. First it is attempted to review the historical development of the major methodologies for the wave-induced liquefaction analysis while emphasizing the merits and limitations of each method. The rest of this chapter consists of an explanation of the elasto-plastic model used to provide an analytical solution to wave loading. The influence of wave amplitude, wave length and the pertinent physical properties of the seabed deposit under standing wave loading are discussed.

The mechanism of sand blows phenomenon is presented in Chapter 5. First a briefly review of the ID technique, as it applies to the present study, is presented. Then the dynamic response of a sand layer under horizontal earthquake excitation is investigated using the ID technique. The results of the numerical simulation incorporating various void ratios of the sandy layer are compared and discussed. The conclusion reached in relation to the subject in question closes the chapter.

Finally, the main conclusions drawn from the present study are given in the last chapter (Chapter 6), which also outlines the need for future research in this field.

2

HISTORICAL REVIEW OF PLASTICITY IN SOIL MECHANICS

2.1 INTRODUCTION

Any material body deforms when it is subjected to external forces. The deformation is called elastic if it is reversible and time independent, that is, if the deformation vanishes instantaneously as soon as the forces are removed. The deformation is called plastic if it is irreversible or permanent. The traditional soil mechanics textbooks contain various definitions of plasticity. Materials whose shearing resistance is independent of the degree of deformation are called plastic materials; the term "plastic flow" indicates continuous deformation at constant state of stress (Terzaghi, 1943).

The treatise by Hill (1950) clarified the nature of plastic deformation in metals, and the extent to which such deformations were amenable to analytical prediction. Despite earlier usage in soil mechanics, there seems to be no good reason for departing from the definitions of elastic and plastic components of deformation which are used in other branches of solid mechanics. Elastic deformations are recoverable on completion of a closed cycle of loading and unloading, during which energy is conserved. On the other hand, plastic deformations are permanent, and as they proceed, energy is dissipated. As a consequence of these different properties, during elastic deformations, increments of strain occur in the direction of the increments of applied stress whereas during plastic deformations, increments of strain occur in the direction of the current stress and during a

small increment are therefore only marginally affected by the direction of the stress probe.

The start of the decade 1950-1960 formed a watershed in the development of soil mechanics as a scientific discipline on two accounts. On the first account it heralded a new era in laboratory testing of soils regarding both the quality of the data, and the sophistication and variety of apparatus and experimental methods that have since become available. Secondly, this period coincided with considerable research activity in the field of plasticity theory. During the last few decades, there has been a continuous and increasing interest in developing constitutive models of soils. Recent research in soil mechanics is directed toward a better understanding of the stress-strain behavior of soils, within the framework of the principles of continuum mechanics.

2.2 CLASSICAL THEORY OF PLASTICITY: A HISTORICAL OUTLINE

The history of plasticity theory dates back to 1864 when Tresca published his yield criterion based on his experimental results on punching and extrusion which led him to state that a metal yielded plastically when the maximum shear stress attained a critical value. Since then, over 130 years, tremendous progress has been made by many researchers who have established the cornerstones for the theory. Now developments in plasticity theory is an active field of mechanics in general and of soil mechanics in particular.

In classical plasticity, the failure surface is adopted as the yield surface when the state of stress reaches that surface. A state of stress below the failure surface denotes elastic behavior. Thus one-failure surface defines the yielding of the material. The first

attempt to formulate the stress-strain relationship for plastic deformation was made by Saint-Venant (1870). He worked on the plane plastic strain problem using Tresca's criterion and assumed the work hardening to be zero. For the first time he proposed that the principal axes of the strain increment coincided with the axes of principal stress. The generalization of Saint-Venant's idea for the three dimensional case between stress and plastic strain rate was done by Levy (1871) and independently by von Mises (1913). In 1928, von Mises used octahedral shear or distortion energy criterion and developed a constitutive relation based on the normality concept that relates the plastic strain rate to the yield surface. The von Mises yield criterion implies that the plastic behavior begins when the distortional energy reaches a critical value.

Since Levy's work remained unknown outside of his country at that time, the theory is called the Levy-Mises theory of plasticity and can be stated as follows:

- The elastic strain is so small as to be negligible.
- The direction of principal plastic strain increment tensor coincides with the principal directions of the stress tensor. This is known as coaxiality.

$$\dot{\varepsilon}_{ij} = \dot{\lambda} S_{ij} \tag{2.1}$$

where $\dot{\lambda}$ is a proportional parameter, and is determined from the yield criterion, $\dot{\varepsilon}_{ij}$ is the strain rate and S_{ij} is the deviatoric stress. The Levy-Mises equation is usually called the flow rate of plasticity because it resembles the constitutive equation of a viscous fluid. The flow rate is even generalized to imply any constitutive equation for plastic strain rate, $\dot{\varepsilon}^{p}$, and the plastic deformation is thus called plastic flow.

Prandtl (1927) and Reuss (1930) proposed relationships similar to Levy-Mises equation for the plastic strain rate. Plastic deformation is isochoric and the rate of plastic

deformation is still assumed to be coaxial with the deviatoric stress. Equation 2.1 can be rewritten in terms of plastic stress-strain relationship. That is, the following proportionality under the principal strain increment and principal deviatoric stress can be generated:

$$\frac{\dot{\varepsilon}_1^p}{S_1} = \frac{\dot{\varepsilon}_2^p}{S_2} = \frac{\dot{\varepsilon}_3^p}{S_3} = \dot{\lambda} \tag{2.2}$$

where subscripts 1, 2 and 3 denote the principal directions of plastic strain increments and deviatoric stresses.

In the 1950's major advances were made in the theory of plasticity by the creation of (i) the limit theorem which was presented by Drucker et al. (1951, 1952), (ii) the concepts of normality and (iii) the idea of the stability of a system, Drucker (1959). All these have led to a rigorous basis for the theory and a platform from which other notable developments have sprung.

2.3 PLASTICITY IN SOIL BEHAVIOR MODELING

Plasticity theory has to a large extent been developed on the basis of observed behavior of metals, and the principles embodied in classical plasticity theory apply particularly well for such materials. Various types of materials respond in quite different ways to applications of stresses. This has not always been recognized, and many of the principles of plasticity theory have often been used uncritically in the development of constitutive models for materials which exhibit patterns of behavior different from those observed for metal. This situation may have developed due to a lack of knowledge about the behavior of such materials under general three-dimensional stress and strain conditions. In particular, frictional materials such as soil, show behavior patterns quite

different from those of metallic materials. The time-independent behavior of both types of materials may be characterized by elasticity theory, work-hardening and work-softening plasticity theory. However, the differences in observed behavior result in fundamentally different constitutive models for metals and frictional materials. The major differences as well as the similarities in behavior of metals and frictional materials are reviewed by Lade (1988).

Historically, the criteria for the yielding of plastic solids, mainly soils, had been proposed by Coulomb (1773). The Coulomb criterion is certainly the best known failure criterion in soil mechanics that takes into consideration the effect of the hydrostatic pressure on the strength of granular materials. Utilizing the simple ideas of the theory of perfect plasticity, Meyerhof (1951) proposed the conventional methods for estimating the ultimate bearing capacity of footings. However, the implications of perfect plasticity in the soil mechanics problems involving deformation are far-reaching and unexpected (Drucker and Prager, 1952). Because the Coulomb criterion is not mathematically convenient in three-dimensional situations due to the existence of corners (singularities), the perfect plasticity model of the Drucker-Prager type (1952) is the simplest model which approximates the Coulomb yield criterion.

Since most geological materials experience yielding from the very beginning, it is necessary to define the yield function for the continuous yielding behavior leading towards the failure, peak, critical or ultimate condition.

One of the major advances in the application of plasticity theory was made by Drucker et al. (1957). They were concerned with the limitations of perfect plasticity when applied to a frictional material with a Mohr-Coulomb failure criterion. The

limitation came about because the failure envelope was treated as a yield envelope, and the normality condition implied an unacceptably large rate of dilation at failure. Moreover, the implication was that this rate was always applied, which was in conflict with the experimental evidence that in some cases soils reduce in volume during yield. To overcome these deficiencies, they proposed the idea of using a "cap" type yield function to define the continuous yielding of soils.

There are two important innovations in the Drucker et al. (1957) studies. The first is that the introduction of the idea that the usual consolidation curve is a case of work hardening stress-strain relationship, and to associate this with successive yield envelopes. As a consequence of the first innovation, the second is that when the soil is an isotropically normally consolidated condition, then an increase in mean effective stress causes yield. This argument led to the proposal of a circular yield envelope fitted to the Mohr-Coulomb envelope, or more generally a spherical cap fitted to the cone in principal stress space obtained by revolution of the Mohr-Coulomb envelope. Insufficient experimental evidence at the time did not allow a more elaborate choice of shape for this additional part of the yield envelope. However, this work-hardening model was a major step toward a more realistic representation of soil behavior.

The introduction of work-hardening plasticity into soil mechanics led in turn to generation of the family of soil models developed at Cambridge. The additional feature which has been an integral part of all these models has been the concept of critical state, Poorooshasb (1961) which had previously been referred to as critical void ratio (Roscoe et al., 1958). The line of critical state is the locus of failure points for all shear tests under both drained and undrained conditions. This line has the crucial property that at this

critical state large shear distortions occur without any change in state parameters. Roscoe et al. (1958) emphasized the need to incorporate void ratios as an essential parameter in the models.

Despite the use of plasticity concept and terminology in the work of Roscoe et al. (1958), a complete stress-strain theory based on the theory of plasticity was not achieved. Later, Roscoe and Poorooshasb (1963) studied the behavior of a sample of normally consolidated clay when subjected to a triaxial compression test. They proposed an incremental stress-strain theory for the medium and alluded to the possibility of applying the concept of a potential function to facilitate the formulation of the flow rule. Although their particular representation of the above function was incorrect, the paper led to the valuable comment by Calladine (1963) who examined the experimental results and showed that normally consolidated clay is a strain work-hardening plastic material. Roscoe et al. (1963) utilized Callandine's suggestion and established an equation of the yield locus of a normally consolidated clay. The resultant yield locus had a bullet shape in stress space and was derived by using a basic energy equation that specifies how an externally applied energy is divided between that part stored and that dissipated. The dissipated energy depends on the soil's frictional constant so that this fundamental parameter plays an important role in the construction of the model. This model was later named "Cam-clay" by its developers, Roscoe et al. (1963).

The original Cam-clay model predicts larger shear deformations than those observed for small levels of shear stress. In order to overcome this limitation, a modified version of the Cam-clay model was suggested by Burland (1965) replacing the bullet-shaped surface of the Cam-clay model with an elliptic shape and subsequently was

extended by Roscoe and Burland (1968). The model is an isotropic, nonlinear elastic strain hardening plastic model. The model presented by Roscoe and Burland (1968) is called by them "modified" Cam-clay to distinguish it from the "original" Cam-clay model. This "original" model has been much less used for numerical analysis than the "modified" model and the qualifier "modified" will be omitted subsequently.

In the Cam-clay model the elastic and plastic behavior is completely specified by only four basic soil constants: the compression index (λ), the swelling index (κ), the frictional constant (M), and the position of the critical state line (μ). It is also assumed that yield loci and plastic potentials are identical and elliptical in the p:q effective stress plane;

$$f = \psi = (q/p_0)^2 - M^2[(p/p_0)(1-p/p_0)] = 0 \tag{2.3}$$

where ψ is plastic potential and f is yield surface. p_o is a strain-hardening parameter and scales the size of any particular member of the family. The yield locus was found by integrating a linear relationship for dilatancy of the soil, i.e.,

$$\frac{d\varepsilon_p^p}{d\varepsilon_q^p} = \frac{2\eta}{M^2 - \eta^2}; \eta = \frac{q}{p} \tag{2.4}$$

where $d\varepsilon_p^p (= d\varepsilon_1^p + d\varepsilon_3^p)$ and $d\varepsilon_q^p (= 2/3(d\varepsilon_1^p - d\varepsilon_3^p))$ are the plastic volumetric strain and plastic triaxial shear strain respectively. p is the mean effective stress and q is the deviator stress, which are defined as:

$$p = \frac{1}{3}(\sigma_1 + 2\sigma_3) \tag{2.5}$$

$$q = \sigma_1 - \sigma_3 \tag{2.6}$$

where σ_1 is the major principal stress and σ_3 is the minor principal stress.

DiMaggio and Sandler (1971) proposed the cap model that is similar to the critical state model, except that a composite failure yield surface replaces the critical state line. Again, the yield surfaces allows for continuous yielding (a movable cap) whose position is a function of the plastic volumetric history of the material, and at failure, the failure envelope is used as separate yield surface. The model is based on isotropic plasticity with associated flow rule and its mathematical formulation satisfies the Drucker's postulate for stability, uniqueness and continuity. The cap model was initially developed for sands but later has been extended to other materials such as clays (Sandler et al., 1976).

Both the Cam-clay and Cap models can suffer from various limitations: (a) for states of stress below the critical state line, only compressive volumetric strains are predicted, and dilative strains are predicted only if the locus of the critical state points is used as yield surface. Since many materials exhibit volume increase (dilation) before the critical state or peak stress is reached, the model cannot predict such behavior; (b) the yield surface is circular in the principal stress space; (c) the hardening or yielding is defined through total volumetric plastic strains (or void ratio), thus the definition of hardening does not include the effect of deviatoric plastic strains; (d) the yield surface intersects the mean effective stress (p) axis orthogonally. Hence, the coupled effect of the mean pressure on shear strains is not included; and (e) if the failure surface is used in computations, the model involves singularity at the intersection of yield surface and failure surface, which may cause computational difficulties.

In view of the above limitations, the isotropic hardening model cannot reproduce the hysteretic behavior under unloading-reloading path. In such a model, the yield

surface expands uniformly with plastic deformation, so that the size of elastic region, controlled by the maximum stresses that have been applied, becomes very large. Only elastic deformation is allowed in the isotropic hardening models during unloading. However, it is generally observed from many soil tests that during unloading, both elastic and plastic deformations occur before the stress is fully reversed. Experimental observations show that truly elastic response is probably only associated with rather small changes in stress after a change in stress path direction: kinematic hardening models allow this character of response to be reproduced.

Prager (1955, 1956) first introduced the idea that yield surface translates without rotation in the stress space in the direction of the strain increment. This model, known as the kinematic hardening model, was improved upon by Ziegler (1959). Ziegler (1959) modified Prager's hardening rule and assumed the rate of translation to take place in the direction of the reduced-stress vector. Later Iwan (1967), starting from a one-dimensional model, generalized it for multi-dimensional cases in the stress space by assuming a collection of yield surfaces arranged in a series-parallel combination instead of the usual single surface. Each one of the yield surfaces obeys a linear work-hardening law of the Prager (1956) type, but the combined effect gives rise to a non-linear hardening law and can effectively model the Bauschinger effect. Independently, Mroz (1967, 1969) proposed a similar model introducing the concept of a field of work-hardening moduli. This field is defined by a configuration of surfaces of constant work-hardening moduli in the stress space. To do so, he postulated that the response of material is governed by a collection of nested yield surfaces, with each surface obeying a linear kinematic hardening rule. He also proposed a new rule of kinematic hardening,

which is different from those of Prager and Ziegler. However, because of the results obtained in some experiments by Philips and Tang (1972), the adequacy of the different kinematic hardening rules perhaps should be reconsidered.

The idea of these nested yield surface kinematic hardening models can be introduced with the aid of circles in the $\sigma_1 - \sigma_2$ plane, as shown in Fig. 2.1. Figure 2.1(a) shows the surfaces at the initial state and the loading path OE and unloading followed by the reverse loading path EK. Conversion of the qualitative model shown in Figure 2.1 to a quantitative model requires assumptions about the way in which the yield surfaces changes in size and translates on any particular stress increment. It is desirable that translation should allow yield surfaces to touch but not to intersect. It is convenient to assume that all the nesting yield surfaces have the same shape. However, some care is necessary in setting up the equations because in general the yield surfaces will change in size at the same time as they translate (Hashigushi, 1986).

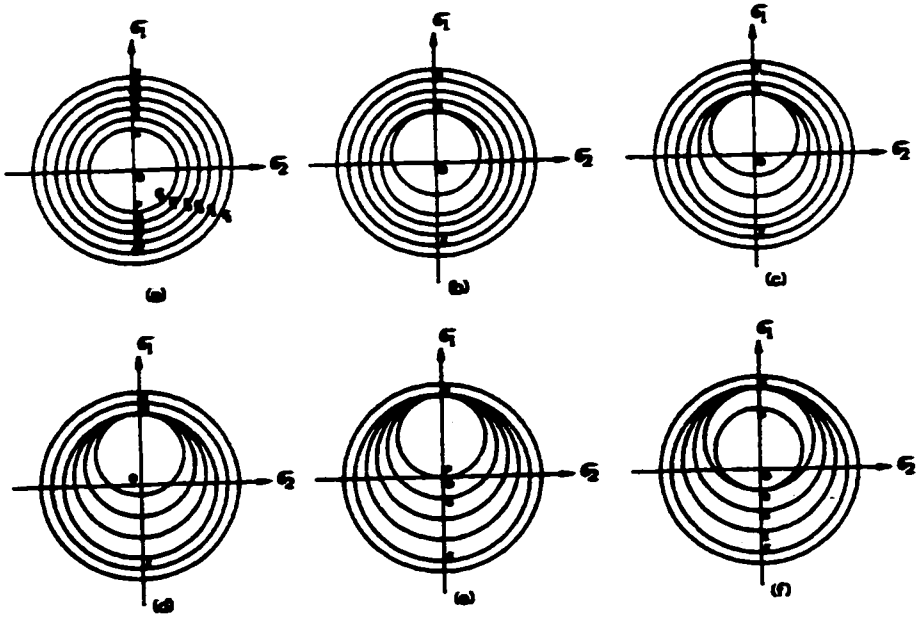

Figure 2.1 Illustration of multi-yield surfaces model

Isotropic and kinematic hardening (mixed hardening) occur simultaneously that may provide a more realistic representation of soil behavior under reverse, and particularly cyclic loading condition (Chen and Huang, 1994).

Joyner and Chen (1976) studied the application of the Iwan/Mroz multisurface model in calculating the response of earth dams subjected to earthquake loading. The model performance has been found to be particularly promising for such cases. Later, within the same multisurface framework, Prevost (1977) formulated a constitutive model for the undrained behavior of clays under both monotonic and cyclic loading conditions. He utilized the von Mises type of nested yield surfaces with the associated flow rule. Each yield surface was allowed to evolve through a combination of isotropic and kinematic hardening rule. Prevost (1978) has also extended his undrained model to that for drained conditions, by taking into account the effect of hydrostatic pressure on the shape of the yield surfaces. In this model, it is assumed that the current size of yield surface and the hardening modulus are functions of the plastic volumetric strains or the plastic shear distortions. Therefore, the model allows each surface to translate and expand as plastic loading occurs. A non-associated flow rule is adopted for the inner surfaces, while the associated flow rule is used for the outermost surface. Strain softening is admitted for the outermost surface only.

In a subsequent paper, Prevost (1985) proposed a multi surface plasticity model which accurately describes shear non-linear hysteretic behavior, including shear stress induced anisotropy. Yielding is controlled by a family of nested yield surfaces which describe cones in principal stress space with circular cross sections perpendicular to the hydrostatic axis as shown in Figure 2.2. A non-associative flow rule for the dilatational

component of stress, depending on the effective stress ratio, allows dilation and compaction under shear stress. In using multiple conical yield surfaces it is possible to realistically model soil with a vanishingly small elastic region by diminishing the size of the inner yield surface. However, for a stress path that follows the axis of the yield surfaces, the model allows soil to deform only elastically. Also, the model does not accurately characterize the plastic behavior of soil under hydrostatic loading. Later Lacy and Prevost (1987) modified the Prevost's model to include volumetric yielding of soil under hydrostatic loading.

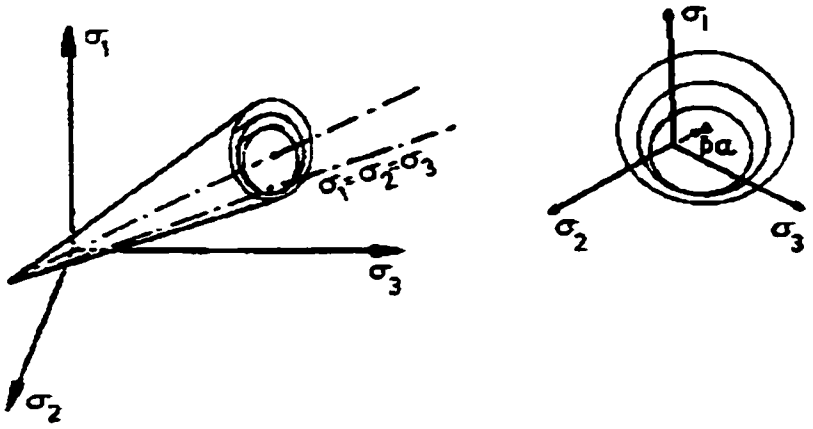

Figure 2.2 Conical yield surfaces in principal stress space

A kinematic hardening model in which 10 nesting yield surfaces are introduced is described by Prevost and Griffiths (1988). They used yield surfaces, which are cones in principal stress space with a common apex (which may or may not coincide with the stress region). In deviatoric (constant mean stress) planes the cones all project as non-concentric circles. Prevost and Griffiths (1988) also assumed deviatoric normality of plastic strain increment vectors, but a nonassociated flow was assumed to govern the link between volumetric and distortional effects. In order to allow volumetric strains to occur

under isotropic compression, an innermost yield surface of zero dimension, located at the current stress state, was assumed. Movement of this yield surface is accompanied only by volumetric plastic strains. A great deal of initial anisotropic information can be included in the choice of positions and sizes of 10 yield surfaces, and a lot of detail of stress history can be memorized by the model.

All of these models discussed have definite advantages, however none have the smooth transition from elastic to fully plastic state for reversed loading which is observed experimentally on most materials. Among the new concepts in plasticity is that of the "bounding surface", originally introduced by Dafalias and Popov (1975), using the plastic internal variables concept and subsequently in a more general formulation by Dafalias and Popov (1976) and independently by Krieg (1975) in conjunction with an enclosed yield surface for metal plasticity. Compared with the multisurface model, this model uses only two surfaces, namely, a bounding surface and loading surface, defines a continuous variation of the plastic modulus between these two surfaces (rather than a piecewise constant plastic moduli field which was discussed earlier by Mroz (1972) and applied to analyze plastic strain accumulation under cyclic torsion and tension). The bounding surface bears a similarity with the outer surface used in the field of work-hardening moduli formulation, but it is not equivalent and in general provides a simpler constitutive model.

Much simpler models of anisotropic strain-hardening plasticity have been developed for soils based on the bounding surface concept introduced earlier for metals. A bounding/yield surface plasticity formulation for soils was fully developed by Mroz et al. (1978, 1979) within the triaxial space of critical state soil mechanics. This is further

elaborated by Mroz and Norris (1982). The extended formulation, covering a general stress state, is presented by Pietruszczak and Mroz (1983). The bounding surface, referred to as the consolidation surface, is assumed to reflect isotropic properties of the material and is constituted, in a natural way, by the initial consolidation process. Since, dense granular materials show a strong tendency to dilate prior to failure. Mroz and Pietruszczak (1983) generalized the Pietruszczak and Mroz (1983) model to include this effect in the contest of a combined volumetric-deviatoric hardening. In this extended version, applicable to sand, the bounding surface (referred to as configuration surface) is assumed to reflect the degree of initial compaction of the material. Consequently, the extent of this surface, prior to imposition of any external load, depends on the initial void ratio.

Two different direct bounding surface formulations within the framework of critical state soil plasticity were also presented qualitatively by Dafalias and Herrmann (1980) for the case of zero elastic range and quasi-elastic range (Dafalias, 1979). In Dafalias and Herrmann (1980) model the bounding surface formulation were used to describe the behavior of clay under cyclic loading by abandoning yield surface (zero elastic range) within the bounding surface. They used a simple radial mapping rule in order to define the variation of the hardening modulus. For each actual stress point within (or on) the bounding surface, a corresponding conjugate or "image" point on the surface is specified as the intersection of the surface with the straight (radial) line connecting the origin with the current stress point. The actual hardening modulus is then assumed to be a function of the hardening modulus on the bounding surface, at the conjugate point, and the distance between the actual stress point and its conjugate. A

generalization and further analysis of this model were developed by Dafalias and Herrmann (1982, 1986) in a general stress space by means of stress invariants under various conditions of monotonic, cyclic, drained and undrained loadings. They also showed that their proposed model has the ability of reproducing observed behavior of normally and over-consolidated clay in the triaxial space. In a subsequent development, Anandarajah and Dafalias (1986) extended Dafalias and Herrmann's isotropic model to an anisotropic model for clays by incorporating a rotational hardening (Hashiguchi, 1979) and a distortional hardening. For anisotropically consolidated soils, the initial yield function and plastic potential in the stress space undergo a rotation as a result of previous anisotropical stress history. It may be considered that the subsequent yield surface expands, translates, and rotates in the stress space when general loadings are applied to a soil sample. It was shown that the results obtained from the model under triaxial undrained loading and K_o loading/unloading condition agree quite well with those measured experimentally.

The aforementioned developments by Prevost (1977 and 1978), Mroz et al. (1978, 1979 and 1981), Pietruszczak and Mroz (1981), Dafalias and Herrmann (1980, 1982, and 1986), and Anandarajah and Dafalias (1986) employed some new concepts of plasticity in order to develop constitutive models within the framework of critical state soil mechanics. In other words, it was shown that the critical state framework is an appropriate framework to construct a reasonable model for clays. Such a conclusion is hardly applicable to granular cohesionless media. Recognizing the limitations of critical state models in simulating the behavior of sands, many investigators have attempted to modify the basic ingredients of critical state models. These efforts have led to

developments of numerous constitutive models for cohesionless soils during the last two decades. In the following a brief review of major developments will be presented.

It is usually assumed in classical plasticity theory that the plastic potential function takes the same form as the yield function, i.e., associated flow is employed. Experimental evidence from tests on several types of frictional materials have clearly indicated that the use of associated flow rules results in prediction of too large volumetric expansion. To characterize the volume change correctly, it is necessary to employ a non-associated flow rule. The plastic potential surfaces therefore do not coincide with the yield surfaces. Poorooshasb et al. (1966, 1967) were among the first who showed that the deformation of sand in the triaxial shear defines a family of yield loci in the stress space which is completely different from the plastic potential curves established for the same sand. Poorooshasb et al. (1967) have suggested a method of approach for determining the yield loci using triaxial shear tests. This method consists of performing triaxial drained tests employing different stress paths involving loading, unloading and reloading and marking, in the two dimensional stress space, the points at which yielding begins to occur. By connecting these points, it is possible to find the function by which a yield law is defined. Poorooshasb et al. suggested that an approximate description of the yielding of sand could be obtained by assuming that the yield loci were lines of constant stress ratio $\eta = q / p$ =constant. Later, Poorooshasb (1971) has shown that for the sand he tested using a triaxial apparatus the yield function is determined uniquely irrespective of the density and stress path given by:

$$f = \eta + mLnp \tag{2.7}$$

where m is a constant and for a particular sand he used it was chosen 0.6.

Tatsuoka and Ishihara (1974) followed the same procedure that was proposed by Poorooshasb et al. (1967) to define the yield function on loose samples of Fuji sand in triaxial compression. They concluded that the yield loci change to some extent depending upon the density of the sample, with looser samples requiring greater deviator stress to cause yielding under a given mean principal stress. Based on their observation, it was found that the type of yield loci suggested in Granta gravel model (Schofield and Wroth, 1968) does not appear to duplicate real behavior.

Based on experimental studies on Monterey No. 0 sand in cubical triaxial tests, Lade and Duncan (1973) concluded that the normality condition is almost satisfied on the deviatoric plane, but not on the triaxial plane. From these observations, Lade and Duncan (1975) developed a non-associative elastoplastic model, based on the failure criterion which can be expressed in a simple combination of stress invariants, i.e.,

$$f = I_1^3 - \kappa_1 I_3 = 0 \tag{2.8}$$

where I_1 and I_3 are respectively the first and third invariants of the stress tensor, and κ_1 is a value of stress level at failure depends on the density of sands.

From experimental observations, Lade and Duncan (1975, 1976) introduced the plastic potential function ψ that is expressed in a similar form to that of the yield function. The plastic strain increment vectors can in fact be determined from this plastic potential function.

$$\psi = I_1^3 - \kappa_2 I_3 = 0 \tag{2.9}$$

in which κ_2 has a constant value which depends on a given stress level and is related to the directions of the plastic strain increment in the triaxial plane for both the triaxial compression and extension conditions. Comparisons between the results predicted by

equation (2.8) were in a good agreement with the published results of the cubical triaxial tests performed by Ko and Scott (1968).

Later Lade (1977) modified his original model to include the post peak behavior of dense sands by introducing an empirical work-softening law in addition to the work-hardening law previously used in the original model. In this model, a spherical yield cap, similar to those of the generalized cap models, was added in the original model to allow for continuous yielding of the material. These two different kinds of yield loci are used to describe the yielding properties of shear strains and dilatancy. In this isotropic double hardening model, it is assumed that these two kinds of yielding take place independently; there is no coupling between shear deformations with accompanying dilatancy and deformations due to isotropic compression. In reality, there is probably some kind of coupling between these two different kinds of deformation. This two-surface model also involves a singularity at the intersection of the cap and failure surface.

Recently, Kim and Lade (1988) and Lade and Kim (1988a and b) have proposed the use of single surface yield (and potential) functions for describing hardening or continuous yielding of geologic materials. This approach is considered similar to the hierarchical single surface (HISS) approach developed previously by Desai et al. (1986) and recently implemented in a finite element code (Desai et al., 1991).

The nonassociated flow rule in Lade and Kim model (1988) is derived from a plastic potential whose shape in the principal stress space resembles a cigar with an asymmetric cross-section. Yielding occurs along a single, isotropic yield surface shaped as an asymmetric teardrop and the yield function is expressed as the product of two functions. The yield surface describes a contour of constant plastic work because plastic

work is used as the hardening parameter (Huang, 1980). The transition from hardening to softening occurs abruptly at the peak failure point.

There are some differences between Lade and Kim model and Desai et al. Model, e.g., (1) Lade and Kim approach defines a separate failure surface, which in the HISS approach is a subset of the compact single surface function, (2) the number of constants in Lade and Kim model required is greater than in the HISS approach. For instance, the total number of elastic and plastic constants in the δ_1-nonassociative model (Frantziskonis et al., 1986) is 8, whereas for the comparable nonassociative Lade and Kim model is 12, (3) the damage/softening response in the HISS approach is based on a consistent definition of damage function that leads to incorporation of damage due to microcracking and discontinuous nature of the material damage and subsequent softening (Frantziskonis and Desai, 1987), whereas in the Lade and Kim approach, softening is incorporated in the continuum sense involving contraction of the yield surface.

Nova and Wood (1979) developed a constitutive model for sand in axisymmetric conditions. The model is characterized by a single yield surface with isotropic hardening and a non-associated flow rule. Hardening depends on both volumetric and deviatoric plastic strains.

Vermeer (1978) proposed a double hardening model similar to that suggested by Lade (1977) using Rowe's stress-dilatancy relation (1962). Row originally deduced his stress-dilatancy relation from minimum energy considerations of particle sliding. A distinct feature of Vermeer's model was the shape of deviatoric (shear) yield surface, which was chosen in accordance with the experimental findings of Poorooshasb et al. (1966, 1967) and Tatsuoka and Ishihara (1974). Similar to Lade's model (1977), the

major shortcoming in Vermeer's model was the assumption of elastic response during unloading and reloading which made the model not suitable for simulation of the cyclic behavior of sands. Difficulties arise, however, when stress path change directions.

Ghaboussi and Momen (1979, 1982) were among the first who developed a material model that is capable of representing the cyclic behavior of sands. Their proposed model consists of a failure surface and a yield surface. The conical type of failure surface forms an asymptotic envelope of the yield surface, which undergoes a combination of isotropic and kinematic hardening. A non-associative flow rule is used and the volumetric plastic strain and dilatancy of the soil are determined by a semi-empirical rule. It was shown that the model simulation of undrained tests was capable of representing the experimental results, which were reported by Castro (1969) and Ishihara et al. (1975) with a reasonable degree of accuracy only if the membrane penetration effects are included. It was also found that membrane penetration could significantly influence the results of undrained tests.

In a recent work, Lade and Inel (1997) developed a rotational kinematic hardening model, which incorporates rotation and intersection of yield surfaces. The basis for the rotational kinematic model is an extension to isotropic single hardening model (Kim and Lade, 1988; Lade and Kim, 1988a and b). This elasto-plastic model employs a nonassociated flow rule derived from a plastic potential whose shape in principal stress space resembles an asymmetric cigar with smoothly rounded triangular cross-sections in octahedral planes. During primary loading the isotropic teardrop shaped yield surface is active. When stress-reversal occurs, the pseudo-hydrostatic axis defining the position of the rotated kinematic surface passes through the stress reversal point. In

this manner, both the orientation and the size of the kinematic surface is determined by the stress reversal point. The capability of the new model was examined by comparing predictions with experimental data for stress paths involving large stress reversals in the triaxial tests on loose, cylindrical specimens of Santa Monica Beach sand (Inel and Lade, 1997). Within the scatter of test results, the proposed model was shown to capture the behavior of sand with reasonable accuracy.

Although numerous constitutive models have been developed during the last decade, a few of them possess interesting features and are worthy of mentioning. The term "generalized plasticity" was introduced by Zienkiewicz and Mroz (1984) in an attempt to provide a basis for the formulation of general plastic models without the need to think in terms of yield surfaces and plastic potentials. Although the models that emerge have ingredients of their own which are rather similar to these. Classical elastic-plastic models can be seen as special cases of these generalized plasticity models, which in turn also have close similarities with bounding surface plasticity models. Instead of a yield surface dividing stress space into elastic and plastic regions, a field of unit vectors is defined in order that unloading processes (which are not necessarily elastic processes) and loading processes can be distinguished. This also allows loading processes to be strain softening ones. Instead of a plastic potential, two fields of unit vectors are defined, which specify the flow rules for loading and unloading processes, respectively.

The application of generalized plasticity to the generation of model for the cyclic loading of sands in axisymmetric triaxial tests is presented by Pastor et al. (1985). Pastor and Zienkiewicz (1986) and Pastor et al. (1990) discuss the details of this formulation and show how the typical behavior of sand under complex loading can be reproduced

with physical constants identified (8-10 is sufficient for most sands). To account for both initial and stress-induced anisotropic fabric, Pastor (1991) introduced an extension of Zienkiewicz and Mroz (1984) model for isotropic granular soil which was previously applied to sands under earthquake loading conditions and showed good agreement with experimental results (Zienkiewicz et al., 1985; Pastor and Zienkiewicz, 1986) and centrifuge model tests (Zienkiewicz et al., 1990). Pastor's (1991) approach to the modeling of anisotropic behavior is accomplished by introducing a new set of "modified invariants" which are dependent on stress and on a tensor which is a measure of material microstructure. These invariants are used in definitions of loading-unloading direction and of plastic modulus. Model predictions have been checked against experimental data on Fuji River sand reported by Yamada and Ishihara (1979, 1981) that exhibits a very strong initial anisotropy caused by the natural process of deposition through water, and shown to reproduce behavior satisfactorily.

Two surface plasticity theory would be one of the most reasonable and the simplest models to describe the anisotropic hardening. Poorooshasb and Pietruszczak (1985, 1986) proposed a generalization of the deviatoric hardening concept in the context of bounding surface plasticity. They developed a two-surface model for sand extended to the general effective stress space incorporating a non-associative flow rule and the idea of reflected plastic potential (Pande and Pietruszczak, 1982). In this formulation the bounding surface reflects the isotropic properties of the material and is assumed to be created by any active loading process imposed upon virgin material. For all stress histories confined to the interior of the bounding surface, a simplified memory structure (similar to Dafalias and Popov, 1975) has been incorporated in which only the events

maximum load intensity reflect upon subsequent material behavior. Such one-level structure is modeled by introducing the concept of a "yield" surface which encloses the elastic domain (usually infinitesimally small) and incorporating the framework of kinematic hardening, i.e., allowing this surface to move within the domain enclosed by the bounding surface. In Poorooshasb and Pietruszczak (1985) model, the kinematics of the yield surface is formulated in such a manner as to ensure a smooth transition (without intersection) with the bounding surface. The simplified scheme is shown in Figure 2.3.

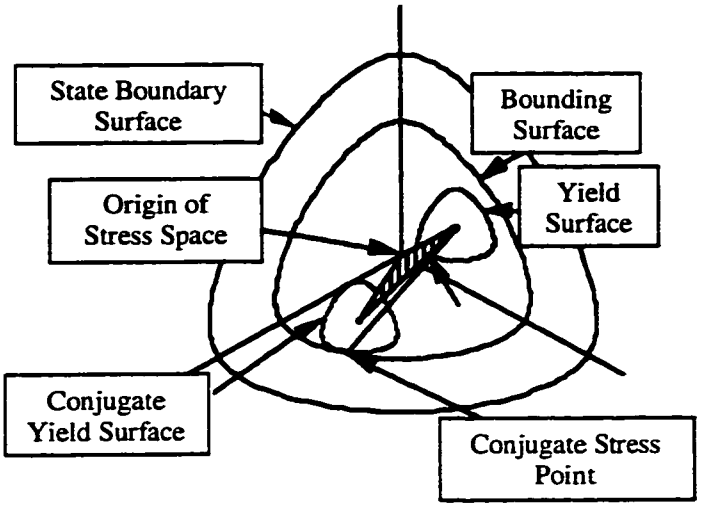

Figure 2.3 Bounding surface, yield and conjugate surfaces

Once the appropriate evolution law has been formulated, the response of the material is described by the flow rule implemented in the context of the actual "yield" surface and the local plastic potential. The proposed model has been proved to be applicable for both loose and dense sands, in particular, liquefaction can adequately be simulated. The model is fairly complicated mainly because of the kinematic of the yield surface, mostly due to incorporation of Lode angle in the formulation of the yield surface and the bounding surface. An alternative scheme has been proposed by Pietruszczak and Stolle (1987) by considering a circular section (independent of the Lode angle) for the

yield surface in the p plane. This modification simplified the kinematics of the yield surface, however, the complexity due to local potentials was not removed.

Bartlett (1986) also developed an isotropic bounding surface plasticity model for sand within the framework of critical state soil mechanics. He assumed associated flow rule and with the bounding surface given by an elliptical shape in the effective stress plane, closely similar to that of the Cam-clay yield locus but with a modification to allow the model to take account of different ratio q/p mobilized at failure in compression and extension (and for other non-axiymmetric combinations of principal stresses) and also to allow the bounding surface not to pass through the origin if desired. The size of the bounding surface is assumed to depend only on plastic volumetric strains. A radial mapping rule was used to find the image of current stress state on the bounding surface.

Motivated to provide a unified critical state approach, Crouch and Wolf (1994a and b) and Crouch et al. (1994) proposed a volumetric plastic strain hardening formulation based on the bounding surface plasticity model for isotropic clays by Dafalias and Herrmann (1986). The new features are both radial and deviatoric mapping rules to define the loading surface and the use of an apparent normal consolidation line for sands. A non-associated flow rule incorporating a subelliptic plastic potential surface and a kinked (bilinear) critical state line is used. A series of simulations showed satisfactory agreement with the experimental strain-controlled triaxial compression data on Sacramento River sand reported by Lee and Seed (1967) over a wide range of cell pressures and initial void ratios for both drained and undrained tests. The proposed model, however, had no provision for sufficiently accurate cyclic loading response simulation.

More recently, Manzari and Dafalias (1997) developed a constitutive model for sands in a general stress space. The two-surface formulation of plasticity in deviatoric stress-ratio space is coupled with the state parameter concept (Roscoe and Poorooshasb, 1963; Been and Jefferies, 1985) as an essential variable arising in a critical state soil mechanics framework. In the process, these two independent are coupled together on the basis of modifications of the recent proposition by Wood et al. (1994) relating peak stress ratio and state parameter. The model also includes features such as softening of sands at states denser than critical as they dilate in drained loading, softening of sands looser than critical in undrained loading, and the pore-water pressure increase under undrained cyclic loading. It was shown that the model is capable of simulating the material response under monotonic and cyclic, drained and undrained loading conditions.

In closing, in the last two decades rapid progress has been made in developing of elasto-plastic models for the solution of complex geotechnical engineering problems. In view of the recognition of the need for realistic constitutive models for reliable solutions of the problems, activities toward theoretical and experimental research and implementation of the models have witnessed significant continuing growth. Despite the apparent diversity of the various models, unifying trends may exist. Possibly the most attractive feature of the models is their simplicity and their foundation on concepts and data which are well established and understood by the geotechnical engineering community. As J.W. Gibbs wrote in his letter of acceptance of the Rumford Medal in 1881: "One of the principal objects of theoretical research in any department of knowledge is to find the point of view from which the subject appears in its greatest simplicity".

3

THE COMPACT STATE OF THE COHESIONLESS GRANULAR MEDIA

3.1 INTRODUCTION

The behavior of soils under conditions of dynamic loading is of obvious interest to structural engineers. Earthquakes are among the most disastrous natural phenomena, which cause major destruction and damage to various types of structures. The resistance of cohesionless soils tends to decrease under earthquakes, particularly when the soils are saturated. It is to be noticed that the cohesionless soil is brought to a critical state, resulting deformation could be unlimitedly large, producing a flow type failure and sudden loss of strength in short-term loading and hence this condition is called liquefaction in the broad sense of the word. The term liquefaction was used for the first time by Hazen (1920) to explain the mechanism of flow failure of the hydraulic-filled Calaveras Dam in California. Although this term was originally used to describe the flow of an earth dam under static gravitational loads, it was later extended to dynamic loads.

It is generally observed that the basic mechanism of liquefaction in a deposit of loose saturated sand during earthquakes is the progressive build up of excess pore water pressure due to application of cyclic shear stresses induced by the upward propagation of shear waves from the underlying rock formation. A soil element in level ground is subjected to a confining stress due to the weight of the overlying soil prior to any earthquake loading. When a number of cyclic loading is applied in the event of an earthquake, the element of sand tends to reduce its volume. However, since the duration

of the cyclic stress application is so short, there is not enough time for drainage of water. At this state, the pore water pressure builds up to a full extent in which it approaches a value equal to the initially existing confining stress, thereby reaching a condition of no effective stress or intergranular stress as if they were floating in water.

Increasing concern of damage and destruction caused by liquefaction of sandy soils subjected to earthquake loading has arisen the need for investigating the mechanism in which loss of strength is recognized as a result of progressive development of pore pressures within saturated sand, to prevent or mitigate future seismic damage. Attention was focused on the liquefaction problem for the first time as a result of wide spread ground failures during the 1964 earthquake in Niigata, Japan. Most of the damage in Niigata can be attributed to liquefaction induced by the earthquake. The recent example in North America is the extensive damage caused by liquefaction in the Marina district in San Francisco during the Loma Prieta earthquake of 1989 (Finn, 1993).

Recent major shaking events such as the 1995 Hyogoken-Nanbu earthquake in Kobe, Japan, demonstrated the damaging effects of liquefaction and associated reduction of soil strength. Liquefaction-induced failures during the recent earthquake at the reclaimed port island in Kobe, caused financial losses that were estimated in the billions of dollars. Elgamal et al. (1996) utilized the surface and downhole acceleration records at Port Island, Kobe, Japan during the 1995 earthquake to investigate the involved dynamic site response characteristics. Those records were used to obtain direct estimates of the corresponding soil shear stress and strain histories. The analysis showed that at shallow elevations, soil stiffness and strength were found to sharply decrease during the

earthquake, presumably due to excess pore-pressure buildup, indicating a liquefied condition.

The mechanism of liquefaction for the case of sand is now well understood and the susceptibility of its occurrence can be estimated with a reasonable degree of confidence. The present state-of-art on liquefaction behavior of cohesionless soils has come to a stage that reasonable estimates of liquefaction potential can be made based on laboratory testing or even from simple field investigations and experience during the past earthquakes, as well as numerical and analytical solutions.

Terzaghi (1956) was among the first who attempted to explain liquefaction phenomenon. He referred to the phenomenon of sudden or static liquefaction of loose sands due to minor triggering mechanism as spontaneous liquefaction. Castro (1969, 1987) defined liquefaction as the behavior of saturated, loose sand when increasing pore pressures due to undrained shear decrease the effective stress resulting in a reduction in the shear resistance to a constant value, called steady state.

A number of different methods are available for the analysis of the dynamic response of saturated cohesionless soils to seismic loading. The methods differ in the simplifying assumptions that are made in the representation of the constitutive relations. The cyclic stress approach and the cyclic strain approach are the theoretical and experimental work, which commonly used for evaluation of liquefaction potential of soils. Cyclic stress approach may be classified into two main categories: total stress methods and effective stress methods. Seed and Idriss (1967) reported the first total stress analysis of saturated sands subjected to earthquake loading. Cyclic stress approach (Seed and Idriss, 1981) is based on the premise that the development of pore water

pressure in saturated sand subjected to a given cyclic shear stress history, is mainly a function of relative density and the initial effective stress acting on the sand. The total stress approach is unable to take into account the influence of pore water pressure generation on the shear stiffness of the soil.

Since 1976, there has been growing interest in the development and application of effective stress methods of dynamic response analysis due to the potential deficiency of the total stress approach. (Finn et al., 1977; Zienkiewicz et al, 1978; Ishihara and Towhata, 1982; Dickmen and Ghaboussi, 1984). However, because of a lack of data from suitably instrumented structures in the field it has not been possible to validate the quantitative predictive capabilities of the methods.

Dobry et al. (1982) introduced cyclic strain approach as an alternative to the cyclic stress approach. This approach is based on the premise that pore water pressure build up during shear loading is controlled mainly by the magnitude of the cyclic shear strain. They concluded that relative shear modulus rather than relative density is the main parameter controlling pore water pressure build up in the field.

3.2 BACKGROUND

3.2.1 The Concept of Critical Void Ratio

The phenomenon of sand changing its behavior from "solid" to "liquid" was recognized in the early stage of soil mechanics' development. The potential for liquefaction of saturated sands under seismic loading conditions has been extensively investigated. One of the first attempts to explain the liquefaction phenomenon in sandy soils was made by Casagrande (1936) and is based on the concept of Critical Void Ratio

(C.V.R.). Casagrande coined the term "critical void ratio" or "critical density," which is the void ratio or density of a soil subjected to continuous shear under neither dilating nor contracting behavior. Roscoe et al. (1958) extended the Casagrande concept of critical void ratio and critical density by defining a state, at which the soil continues to deform at constant stress and constant void ratio. Any further increment of shear distortion will not result in any change of void ratio. Realizing that this particular situation was a special case in the state space, Poorooshasb (1961) called it the "critical state." It has been suggested that an element of soil undergoing uniform shear distortion eventually reaches a critical state condition in which it can continue to distort without further change of void ratio or of the effective stresses.

3.2.2 The Steady State of Deformation

Utilizing the Casagrande's concept of critical void ratio, Poulos (1981) introduced the concept of steady state of deformation as "the state which the soil mass is continuously deforming at constant volume, constant normal effective stress, constant shear stress, and constant velocity. The steady state of deformation is achieved only after all particle orientation has reached a statistically steady state condition and after all particle breakage, if any, is complete so that the shear stress needed to continue deformation and the velocity of deformation remains constant."

Poorooshasb (1989) discussed that the "steady state of deformation" and the "critical state" both are in fact identical and represent a state of a sample, which it may attain ultimately. He noted that the definition of steady state adds the additional requirement of a state of continuous deformation. Zero velocity is also a constant

velocity, which can not be excluded from consideration. Thus Poulos's condition regarding zero velocity can not be met with. Also as pointed out by Been et al. (1991), this definition of the steady state does not state that velocity should be constant (i.e., is it constant shear strain rate?) or what the value of velocity is. Available data suggest that the velocity of deformation has no effect on steady state conditions (McRoberts and Sladen, 1992). To avoid all confusion it is proposed to use the term the ultimate (critical) state for the simple reason that if all samples were distorted far enough they would tend towards the ultimate state (Poorooshasb, 1989).

It is worthy of emphasizing that what Poulos refers to as the "state" is not the same context as it was used by Poorooshasb (1961): it doesn't refer to the "state of the sample." In this regard, Poorooshasb (1989, 1991) defined the state of a sample of a cohesionless granular medium by the entire set of its pertinent state parameters. Any quantity that is directly measurable at the moment of examination without reference to the previous history of the sample is a state parameter. The importance of the combined influence of the void ratio and confining stress as state parameters on the sand behavior was indicated by Roscoe and Poorooshasb (1963) in conjunction with the planning of model tests reproducing the prototype behavior in the laboratory.

Based on the above discussion, it is justifiable to use a single term, "the critical state," for both the critical and the steady state of sands in the remainder of this study.

3.2.3 The Critical State Line

The locus of all critical state points from drained and undrained tests lie on a unique line, called the critical state line. A unique critical state or steady state line does

exist for a given sand independent of stress path, drainage condition, testing method (e.g. stress controlled versus strain controlled), initial density, and sample preparation method. Castro and Poulos (1977) state that the position of the critical state line is a fundamental soil property. Poulos et al. (1988) investigated the behavior of very uniform, fine, angular, quartz sand composed of tailing from tar-sand operations. All samples were tested under isotropic and anisotropic consolidation conditions, strain-controlled as well as load-controlled and both drained and undrained tests. The experiments demonstrated the existence of a unique critical state line.

Ishihara et al. (1991) established the critical state line of Toyura sand from a series of consolidated undrained triaxial tests. Been et al. (1991) showed the uniqueness of the critical state line for Erkask sand based on a relatively extensive series of laboratory tests. In addition, the effect of stress path, sample preparation and stress-controlled loading were examined for both loose and dense samples under drained and undrained conditions. It was concluded that the critical state line is independent of fabric, stress path and sample preparation method for the range of test conditions and sands examined, implying that the critical state line is unique for a void ratio regardless of whether it is reached by drained or undrained loading. Moreover, experimental results reported by Ishihara (1993) have shown that the critical state line is unaffected by the initial fabric as long as the soil mass is homogeneous.

Kuerbis et al. (1988), Vaid et al. (1990) and Vaid and Thomas (1995) have suggested that there exists a difference between extension and compression critical states due to inherent anisotropy. Alarcon-Guzman et al. (1988) also argue that the initial anisotropy affects the location of the critical state line. Been et al. (1992) discussed that

this proposition can not be extended to imply non-uniqueness of the critical state line. Based on several undrained extension and compression tests, no substantial difference was found (Been et al., 1992). Results indicate that the apparent difference between their results may stem from the quasi-steady state being taken as the critical state (which it is not) and the limitation of the triaxial tests to determine the critical state line for dense sands.

Recently, Zhang (1997) conducted a series of experiments on Unimin sand. Based on experimental evidence, there is no distinct difference between critical state behavior and quasi-steady state behavior. It is shown that an important response in the so-called "quasi-steady state behavior" is the post-phase transformation increase in shear resistance under triaxial undrained loading condition. However, this post-phase transformation in shear stress is not an inherent behavior of sands, but it caused mainly by end-restraint. These studies reveal that the critical state line is unique and independent of stress path, fabric, confining stress level, etc (Zhang and Garga, 1997).

Castro et al. (1992) investigated hydraulic fill from the lower San Fernando dam and had testing performed by four independent laboratories. A variety of testing procedures was employed to determine the critical state line for this soil: drained and undrained tests on isotropic and anisotropic consolidation samples, compacted moist samples, pulivated samples, and samples consolidated from slurry. A compilation of the results suggests a unique critical state line.

Sasitharan (1994) studied the behavior of loose reconstituted samples of Fraser River delta sand. The results of his studies on isotropically consolidated monotonic

undrained and drained triaxial compression tests show that the critical state line in the stress state plane is a straight line passing through origin.

The undrained behavior of Fraser River and Syncrude sands under multi-axial loading conditions has been investigated by Uthayakumar (1996) utilizing hollow cylinder torsion device. The specimens were reconstituted by water pluviation. The effective stress conditions at critical state have shown to lie on unique straight line, which pass through origin, regardless of the direction of major principal stress, intermediate principal stress level and the consolidation history, hydrostatic or non-hydrostatic. It is also unaffected by the rotation of principal stress.

Verdugo and Ishihara (1996) also conducted a series of triaxial tests carried out under both undrained and drained conditions on the standard Japanese Toyoura sand. It was shown that the locus of critical state achieved through drained conditions of loading to be coincident with the critical state line evaluated by means of undrained tests. The experimental results strongly indicated that the initial confining pressure does not affect the critical state or ultimate condition.

The conclusion is that a unique critical state line exists which is independent of the methods of sample preparation, drainage conditions, or stress path. Although, before the ultimate (critical) state is reached, the soil behavior is strongly dependent on several factors such as stress path, drainage conditions, initial state parameter and initial fabric. The conflicting experimental evidence is due to different initial fabrics that affect the tests in an unknown manner (Been et al., 1991). Therefore, it is required to develop a unique experimental method in order to produce the field fabric and loading path in the

laboratory. However, at present, this is not possible to quantify initial fabric or inherent anisotropy of sand sample because of unknown the laboratory and field fabrics.

3.3 OBJECTIVE OF THIS STUDY

More than half of the Canadian population is exposed to a significant seismic hazard. Both the eastern and western regions of Canada have active seismic zones and face the risk of major losses due to earthquakes (Finn, 1997). This potential seismic risk has motivated Canadian engineers and scientists to engage in earthquake engineering research. Damage patterns from major earthquakes in Canada, such as 1924 La Malbaie (M = 6.5) reported by Hodgson (1945), 1925 St. Lawrence reported by Hodgson (1950), 1988 Saguenay, 1989 Ungara (M = 6.3) and more recently 1997 Quebec city (M = 5.2) in Quebec (among others of eastern earthquakes) show that there is a continuing need for sustained research in earthquake engineering, especially to understand the cyclic behavior of the cohesionless soil subjected to dynamic loading.

Although in the past few decades, extensive research efforts have been made to describe the conditions causing the development of liquefaction in cohesionless granular media, only a few comprehensive models have been developed that can be used in the analysis of geotechnical structures under seismic loading. This is partly due to the fact that the behavior of cohesionless saturated soils subjected to cyclic loading is much more complex than that of monotonic loading. Therefore it was felt necessary to base the studies on the more fundamental characteristics of soil deformations, i.e. elastic and plastic strains, in order to understand the mechanism by which liquefaction is induced.

The so-called critical void ratio line plotted in the e vs. ln p space shown in Figure 3.1. The symbol e represents the void ratio of the sample while p is the mean effective stress. This concept, discovered by Casagrande (1936, 1975), for many years played a very important role in the field of earthquake engineering and soil liquefaction.

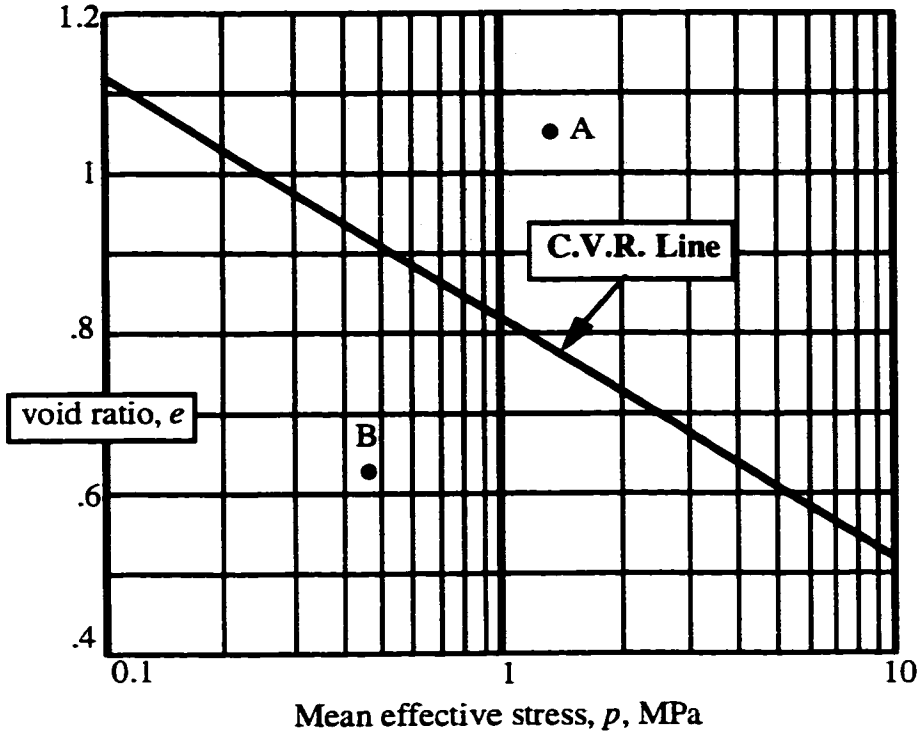

Figure 3.1 Casagrande C.V.R. line for Sacramento River Sand (After Lee [1965], as reported in Holtz and Kovacs [1981])

It had been proposed that if the natural void ratio of a specimen at a depth below grade, where the mean effective stress was p, produced a point to the right of the C.V.R. line, e.g., point A in Figure 3.1, then liquefaction would be imminent in the event of an earthquake. However, if the values of e and p were such that they were represented by a point to the left of the C.V.R. line, e.g., point B, then the soil would have to dilate upon shearing, producing negative pore pressure in the event of an earthquake which would lead to a momentary strengthening of the sample. Liquefaction would, therefore, be

prevented. This is the aim of the present study: to shed some light on the validity of the above proposal. This is done with the aid of a new concept called the "compact state", which was conceived after recalling the results of some experiments by Wroth (1958) and using the so-called one gravity similarity laws.

The remaining portion of this chapter is written in the following sequence. First, a brief discussion of similarity law is presented. Then, a historical review of the CANAsand model as a constitutive model for cohesionless granular media is described. After that the concept of compact state is given, followed by a mathematical formulation of the compact state, recently proposed by Poorooshasb and Noorzad (1996), Noorzad and Poorooshasb (1997). In subsequent sections, a qualitative description of the usefulness of the compact state will be illustrated. The behavior of a cohesionless granular subjected to a cyclic simple shear loading process, together with some numerical examples will be discussed. In analyzing these examples, the development is very simple and straightforward.

3.4 LAWS OF SIMILITUDE

For materials such as soils for which the stress-strain behavior is not fully understood, an attempt is often made to obtain approximate solutions to problems connected with the stability and deformations of the media by carrying out full scale or model tests. Usually cost restricts the investigation to testing on the model scale and many solutions to soil mechanics problems have been, and still are, derived from this procedure. It is therefore surprising that little work has been done to establish any fundamental rules or laws that must be obeyed before the model test results can be

extended to the prototype. Without such laws, the use of model test results to determine the behavior of the prototype may be seriously misleading on a qualitative, much less a quantitative, basis. However, when applying the results of a small-scale model test to predict the behavior of a prototype structure, simply scaling the test results to the ratio of geometric size is not sufficient.

On the basis of both theoretical and experimental consideration, Roscoe and Poorooshasb (1963) proposed one such principle some thirty years ago; they used the piece wise linear theory for soil deformation. Although that mode of description of soil behavior has been overshadowed by the more sophisticated description of theory of plasticity, their conclusions appear to have stood the test of time. They applied critical state principles to tests on remolded clays and artificial soils made up of steel balls and indicated by means of a formula that the effective void ratio (denoted $e^{\cdot}$) to the critical state line at the initial mean stresses must be the same for the model and the prototype. In other words, they concluded that any two samples of a given soil when subjected to geometrically similar stress paths will have the same strains, provided that the difference between the initial void ratio and the void ratio at the critical state at the same normal stress is the same for each sample. This similarity principle has been shown to be valid for many real and artificial soils and forms the basis of a widely used method of normalizing test data which has been described in detail in the textbook by Atkinson and Bransby (1978). Roscoe and Poorooshasb (1963) also wrote, "it is believed this theory (similarity principle) can be extended to apply to cohesionless soils." Recently, Poorooshasb (1989, 1995) has provided a rigorous demonstration of this law within the context of plasticity theory.

Scott (1989) discussed the results of centrifuge testing and examined concepts and scaling relations for $1g$ and higher with respect to the applicability of the model in order to assess prototype behavior. Scott used the same approach as Roscoe and Poorooshasb (1963), but exchanged the void ratio difference for the density index (relative density). Casagrande (1975) showed that for a given sand, the shear strength at critical state is only the function of void ratio. Therefore, the critical state strength of the sand can be uniquely determined from its void ratio, regardless of sample preparation methods, loading modes, strain rate and stress path (Poulos et al., 1985).

However, in agreement with a suggestion of Castro and Poulos (1977), Been and Jefferies (1985) showed that the density index is not a constructive parameter for evaluating soil behavior. Instead, the void ratio difference may be "a first order steady state parameter with widespread applicability on the engineering design of sand structures" and that sands "tested under different combinations of void ratio and mean effective stress, behave similarly if test condition assure an equal proximity to the steady state." Ishihara et al. (1991) recognized the importance of the void ratio difference when extrapolating results from shaking table testing to full-scale situations and criticized the use of the density index as a parameter for this purpose.

Altaee and Fellenius (1994) showed the importance of the effective void ratio ($e^{'}$) by the results of tests on sandy samples subjected to identical stress paths. They concluded the principal requirement to have comparative behavior for a model and prototype at different level of stress is that the initial soil states must be at equal proximity to the steady state (critical state) line.

This completes a brief discussion of similarity law, which is used for the first hypothesis of compact state.

3.5 THE CANAsand MODEL

3.5.1 A Historical Background

CANAsand is a constitutive model, which describes the behavior of cohesionless granular media such as sand and grains. It is a constitutive model that for the first time in geomechanics established that the plastic flow of a cohesionless granular medium follows a non-associated rule. Poorooshasb et al. (1966, 1967) advocate the existence of a potential function (the plastic potential) from which the ratio of the components of the plastic strain rate with respect to each other could be evaluated and a yield function which together with a proportionality factor decides the existence, or otherwise, of these strain ratios and their exact magnitude.

Poorooshasb et al. (1966, 1967) showed that the yielding of sand in triaxial compression defines a family of yield loci in the stress space that does not coincide with the surface of equal plastic potential for the same sand. This finding appears to have stood the test of time and is very simple to use.

In order to determine the yield loci, they conducted a series of triaxial drained tests employing different stress paths involving loading, unloading and reloading. It was found that soil samples yielded during the loading path and behaved more or less elastically upon unloading. During reloading, the elastic behavior continued up to a certain level of deviatoric stress and after that yielding started again. Poorooshasb et al. (1967) suggested that in a stress space, one could assume that the point at which yielding

starts during reloading and the point from which soil is unloaded lie on a unique yield loci. Therefore by connecting these points, it is possible to experimentally find the yield loci. An approximate description of the yielding of sand could be obtained by assuming that the yield loci were lines of constant stress ratio (i.e. $f = \eta$ where η is the stress ratio, q/p; p and q are the stress parameters) in view of its consistency with the behavior of an isotropic cohesionless granular medium composed of non-breakable hard particles.

Based on these experimental studies, Poorooshasb (1971) later suggested the yield function for sands as $f = \eta + m \ln p$ where m is a constant for a particular sand. Note that if $m = 0$, this equation becomes identical to the previously proposed equation, in view of its simplicity. He also showed that the above equation closely reproduced the yield loci of the specific sand he tested irrespective of the density and stress path.

Poorooshasb and Pietruszczak (1985, 1986) presented an extension to the original CANAsand model to account the cyclic behavior of sand. They proposed a two-surface model in which a cone type yield surface was considered to move within the domain enclosed by a geometrically similar bounding surface (Krieg, 1975; Dafalias and Popov, 1975; Mroz et al., 1978; Mroz and Pietruszczak, 1983). A purely kinematic hardening for the yield surface and an isotropic hardening for the bounding surface were considered in the model applicable to both monotonic (virgin) and cyclic (non-virgin) loading conditions. The formulation was based on the theory of plasticity incorporating a non-associated flow rule and the concept of reflected plastic potential (Pande and Pietruszczak, 1982). The direction of plastic strain vector during virgin loading was defined by a global and a local plastic potential, respectively. As long as the loading process does not experience a stress reversal, the bounding surface expands until a

limiting state (failure) is reached. Upon stress reversal, however, the behavior of the material is predominantly governed by yield surface, which is enclosed, and indeed guided, by the bounding surface. If the stress reversal continues until the stress point is once again on the bounding surface and tends to move outside it, the entire stress reversal history is erased from the material memory. It should be emphasized that even during stress reversal programs, the size of bounding surface does not remain constant. It can expand or shrink depending on the mode and a variation of the plastic strain. A comparison of the predicted behavior and observed responses for a number of undrained loading programs carried out on a typical cohessionless granular medium. It was shown that the model performance was in agreement with the experimental data.

The original CANAsand model suffered from major shortcomings; it lacked generality. It could only simulate simple loading path such as monotonically increasing stress paths. It was virtually impossible to make realistic predictions of the behavior of the medium during a cyclic loading program. Through modifications over the years it can now simulate very complicated stress paths such as stress reversal and account for what is known as the "static liquefaction." It is now a unified model that includes such concepts as the "critical state," the "state boundary surface" and "the compact state."

3.5.2 Notations and Definitions

The central issue in CANAsand model is that the flow of material must be described in terms of state parameters; the effective stress and the void ratio of the sand element. The state of a sample of a cohesionless granular medium is defined by the entire set of its pertinent state parameter. Any quantity that is directly measurable at the

moment of examination is a state parameter. If it is judged to be a player in the particular constitutive law under investigation, then it is called a pertinent state parameter (Poorooshasb, 1991). Stated otherwise, a state parameter is any quantity associated with the sample that can be measured without reference to the previous history of the sample.

Stress tensor is measured in terms of its effective components given by:

$$\sigma_{ij} = \sigma_{ij}^{Total} - u\delta_{ij} \tag{3.1}$$

where u is the pore water pressure and δ_{ij} is the Kronecker delta. The state of the sample is represented by a set of four quantities which consist of e, the void ratio, and three parameters related to the invariant of the stress (or its deviation) tensor. From the first invariant of stress tensor I_1 and the second and third invariant of the stress deviation tensor J_2 and J_3, the quantities p (hydrostatic component), q (deviator component) and θ may be defined as follows:

$$p = I_1 / \sqrt{3}\ ;\ I_1 = \sigma_{ii} \tag{3.2}$$

and

$$q = J_2 / \sqrt{2}\ ;\ J_2 = (s_{ij}s_{ij})^{1/2} \tag{3.3}$$

$$\theta = \frac{1}{3}\sin^{-1}\left(\frac{-3\sqrt{3}J_3}{2q^3}\right)\ ;\ J_3 = (s_{ij}s_{jk}s_{ki})^{1/3} \tag{3.4}$$

where s_{ij} is the stress deviation tensor defined as:

$$s_{ij} = \sigma_{ij} - \frac{1}{3}\sigma_{kk}\delta_{ij}$$

The angle θ is analogous to Lode's angle and its range is from $-\pi/6$ to $\pi/6$.

Thus the state space in its simplest form is four-dimensional with the axis representing the set of quantities (e, p, q, θ).

3.5.3 The Ultimate State Surface

Another fundamental concept, which plays an important role in the development of CANAsand model, is the ultimate state concept. It is emphasized that the ultimate state surface is nothing but the generalization of the critical state line as defined originally. In a four dimensional state space of (p, q, θ, e) the "line" would conceivably transform into a "surface." The main reason for the change of the name of this particular surface from critical state to ultimate state is that the use of term "critical" was more than anything else, a historical accident. There is absolutely nothing "critical" about it.

The concept of the ultimate state, which also known as the critical state, postulates the existence, in the four dimensional state space, of a surface for which unlimited distortion of the sample may take place without any change in the state parameters. This surface is referred to as the ultimate state surface. Stated analytically, there exists a surface:

$$p = p\,(e, q, \theta) \tag{3.5}$$

such that for all states on this surface:

$$\frac{\partial p}{\partial \varepsilon} = \frac{\partial q}{\partial \varepsilon} = \frac{\partial \theta}{\partial \varepsilon} = \frac{\partial e}{\partial \varepsilon} = 0 \tag{3.6}$$

where parameter ε, which is not a state parameter, represents the distortion of the sample and is derived from the second invariant of the strain deviation tensor. There exists an abundance of experimental evidence to suggest that at least under uncomplicated testing conditions (e.g. triaxial or simple shear testing) the hypothesis regarding the existence of the ultimate state surface, as described by Equation 3.6, is not irrational.

Graphical representation of the ultimate state surface (Equation 3.5) in a two dimensional space of a sheet of paper is virtually impossible. Nevertheless, if a relationship can be found between two of the parameters, then one of the state parameters appearing in Equation 3.5 may be eliminated and the results are expressed, for example, by the equation:

$$e = e(q,\theta) \tag{3.7}$$

Equation 3.7 is the equation of the ultimate state surface. It is possible to construct contours of equal e in the stress space as a graphical representation of the ultimate state surface. The ultimate state refers to a state of the sample at which unbounded non-reversible distortion can take place in the sample without any change of state. Conceptually all samples, if sheared far enough, would ultimately attain this state. It has the advantage that it can be represented in a two dimensional space by an isometric image as will be seen later. It is also emphasized that it holds true if a one to one relation can be found between two of the state parameters at the ultimate state.

One such relationship is the Casagrande equation that has been shown graphically in Figure 3.1 and can be expressed by the following function:

$$e = e_h - \lambda . \ln(p) \tag{3.8}$$

where e_h is the value of e corresponding to a p = 1 kPa; λ represents the slope of the line shown in Figure 3.1. In other words, it is postulated that, at the ultimate state, a unique relationship exists between the parameter void ratio, e, and the mean stress component, p, and that this relationship is governed by Casagrande's equation. Note that if the slope of the Casagrande "critical void ratio" line in the e-ln (p) space, the coefficient λ, is zero then the model is reduced to the original CANAsand model.

3.5.4 The Compact State Surface

Wroth (1958) conducted a series of experiments on samples of a cohesionless granular medium composed of one-mm diameter steel balls. The samples were tested in the simple shear apparatus and subjected to a large number of stress reversals. Wroth observed that as the loading proceeded, the sample became denser, and after a number of cycles, the steel balls, which had been placed in the apparatus in a random pattern, rearranged themselves in an absolutely regular triangular pattern. A regular triangular pattern is equivalent to the most compact form of assemblage of spherical particles. This observation, which is the basis of the thoughts presented in this study, was only reported in Wroth's thesis and did not attract the attention it deserved.

Granular media are not, in general, composed of equal diameter spherical particles and hence, can not form a regular pattern. Nevertheless they can rearrange themselves in such a way as to lead to a more compact state.

There is no doubt about the fact that the compact state exists. However, to make it a useful concept in analysis the following two hypotheses are made.

1. The compact state traces a line in the Casagrande space of e vs. ln p parallel to the C.V.R. line. This hypothesis is necessary if certain laws of similarity which have been proposed and tested (see e.g., Roscoe and Poorooshasb [1963], Scott [1988]) are to be obeyed.

2. At the compact state, the response of the granular sample to a stress change is reversible. That is, it behaves as an elastic material. At the compact state, the interlocking between the particles is so strong that slippage does not take place. Consequently, plastic deformation, which is the result of particle slippage, does not occur.

In view of the first hypothesis stated above, a close tie exists between the ultimate (critical) state and the compact state. Consequently, the relationship between the void ratio and p at the compact state may also be written in the form of:

$$e = e_c - \lambda . \ln(p) \tag{3.9}$$

where $e_c = e_h - c$ and c is a constant value representing the vertical distance between the compact void ratio line and the C.V.R. line as shown in Figure 3.2.

Figure 3.3 shows the isometric representation of the ultimate (critical) state surface in the (q, θ, e) as determined by Poorooshasb (1989). Poorooshasb and Noorzad (1996) postulated that the compact state also lie on a surface in the state space and this surface is parallel to the ultimate state surface. Also shown in this figure is the isometric view of the compact state surface that is similar in shape to the former surface. This is a direct consequence of the first hypothesis and conforms to the law of similarity for a cohesionless granular material when subjected to the range of loads likely to be encountered in soil mechanics.

The usefulness of the concept of compact state will become apparent in the next section, which discusses the behavior of a cohesionless granular media subjected to a cyclic simple shear loading process. The reason for choosing a simple shear loading process is that the formulation of the constitution law in the general stress space is rather

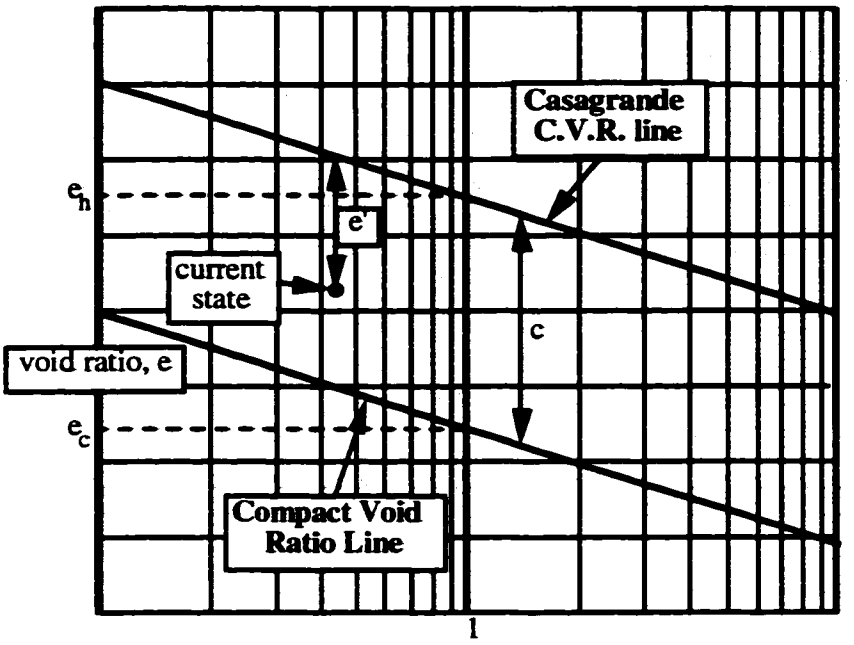

Mean effective stress, p, MPa

Figure 3.2 Casagrande C.V.R. and the compact void ratio lines

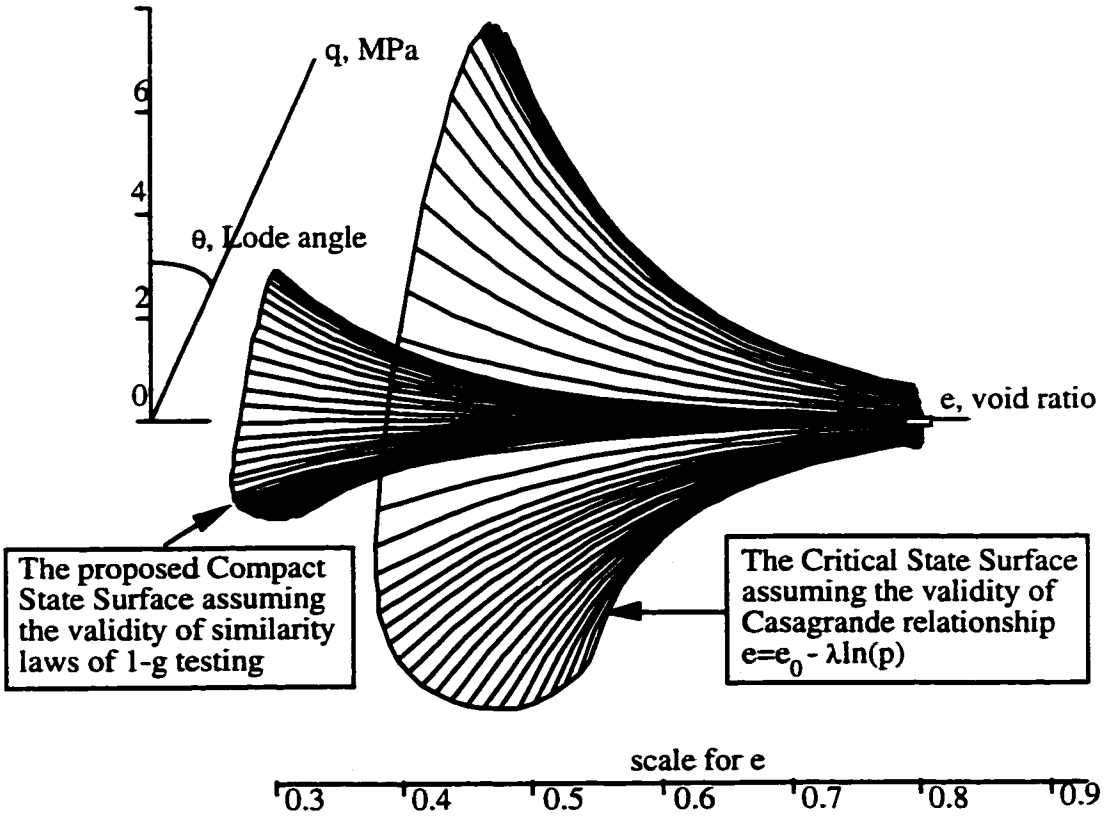

Figure 3.3 Isometric view of the ultimate (critical) and proposed compact state surfaces

complicated. Arguments can be presented more clearly in the stress space associated with simple shear.

3.5.5 The State Boundary Surface

All possible states that an element may assume are enclosed within a boundary called the "state boundary." Obviously such states can be represented by a surface in the state space which is called the state boundary surface (SBS). Note that all the states that can be assumed by a sample are contained within the state boundary surface by definition (Poorooshasb, 1961).

It is emphasized that not all points of the state space "enclosed" by the state boundary surface are accessible by a sample; rather, those points, which are not enclosed, are inaccessible. Thus during a loading process the sample may follow a path on, or within the volume bounded by the state boundary surface or ride it. It may not, however, cross it. This surface is very useful in describing the strain softening in conjunction with the ultimate state surface can provide a framework within which a unified constitutive law may be formulated.

Figure 3.4 shows the state boundary surface plotted in the (p, q, e) domain; i.e. for an e = constant situation. As shown the ultimate state and the compact state trace a curve on the state boundary surface.

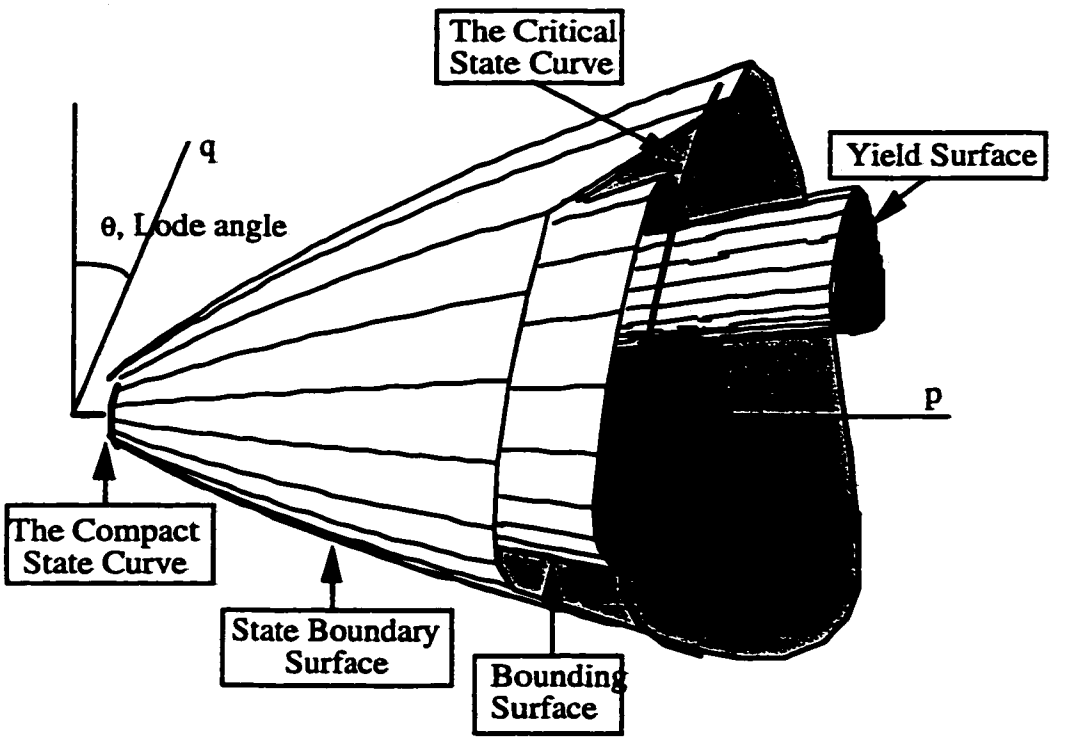

Figure 3.4 Trace of the ultimate and the compact state surfaces on the state boundary surface

3.6 MODELING THE NON-LINEAR SOIL BEHAVIOR

3.6.1 Preliminaries

There is an interest in developing even more reliable and comprehensive but conceptually simple and computationally efficient constitutive models for soil to solve geomechanics problems. The aim of this section is to present a simple but realistic mathematical formulation for sands. It is demonstrated that the proposed model can lead to acceptable results over a wide range of void ratios. This section also contains a comprehensive series of simulations covering the behavior of very loose to very dense sands over a wide range of void ratios under cyclic loading.

3.6.2. Constitutive Formulation for Cyclic Simple Shear of Sand

The stress space associated with the simple shear has two components, which are denoted by σ (equivalent to p) and τ (equivalent to q) Roscoe et al. (1958). Thus, the state space has (σ, τ, e') as its reference axes. The parameter e' deserve some attention. It is called the effective void ratio and is measure of "compaction" of the sample. Roscoe and Poorooshasb (1963) demonstrated that the difference between the initial void ratio and void ratio at the critical state at the same mean stress level could be used as a scaling factor in model testing. Soils with similar values for this difference (effective void ratio) can be expected to behave in a similar manner. This difference has been termed state parameter by Been and Jefferies (1985), who also presented empirical data that support the validity of Roscoe and Poorooshasb' concept.

Poorooshasb (1989) suggested the use of the term, "effective void ratio," e' as;

$$e' = e_{Cas} - e = e_{\lambda} - \lambda . \ln(\sigma) - e \qquad (3.10)$$

where $e_{Cas.}$ is the void ratio on the Casagrande C.V.R. line at equal (σ) value. Figure 3.2 shows a graphical representation of the effective void ratio.

In the (σ, τ, e') space, the state boundary surface assumes the form shown in Figure 3.5. In this figure, two angles are shown which represent two fundamental constants for the material. The first is the angle of friction associated with the ultimate state and is denoted by $tan^{-1}\mu$. The second is an angle associated with the degree of interlocking of the particles and is denoted by $tan^{-1}\delta$.

Based on a series of tests on 1-mm diameter steel balls tested in simple shear apparatus, Poorooshasb (1961) noted a fairly simple relation for state boundary surface,

which can be expressed in terms of state parameters. Thus, the state boundary surface may be expressed analytically by the following equation:

$$\tau = (\mu + \delta.e')\sigma \tag{3.11}$$

Note that at states "looser" than the ultimate state, e' is negative and the value of $\tau/\sigma < \mu$. This factor plays a very important role in the deformation response of the medium as will be seen later on.

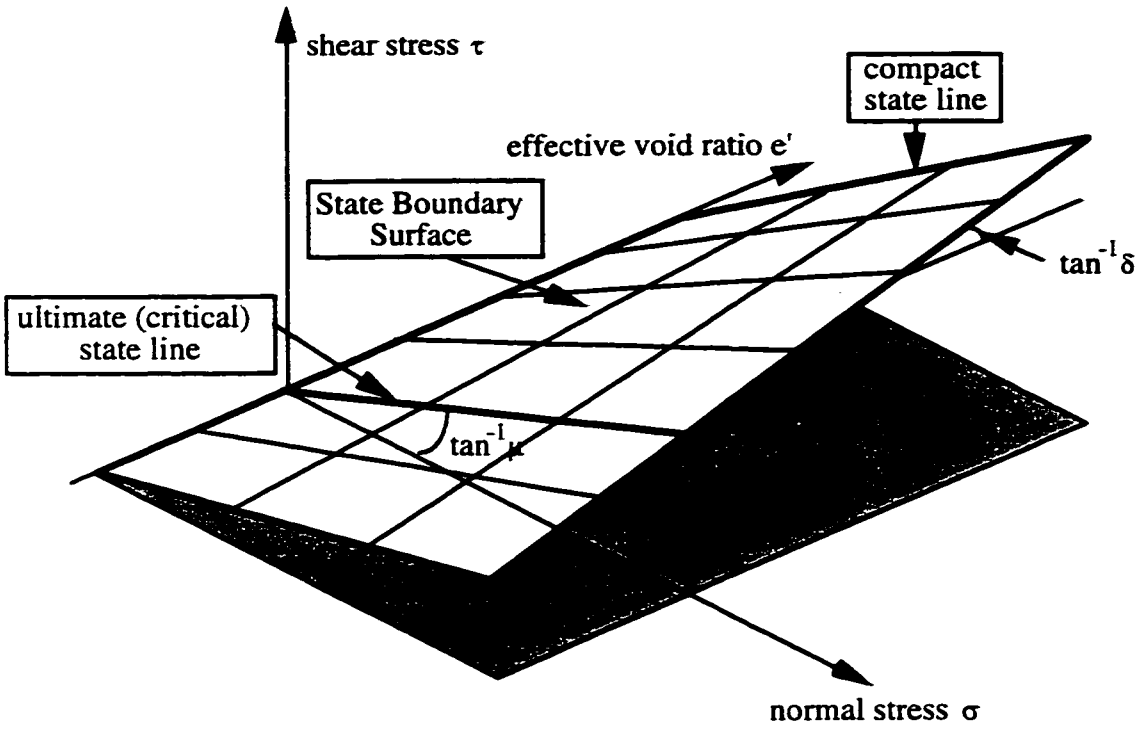

Figure 3.5 State boundary surface in the (σ, τ, e') space

The strain increment components, associated with τ and σ, are denoted by $d\varepsilon$ and dv and represent respectively the shear strain increment and the volumetric strain increment. Each component is, in turn, composed of an elastic (reversible) and a plastic (non-reversible) part, i.e.:

$$d\varepsilon = d\varepsilon^e + d\varepsilon^p, \quad dv = dv^e + dv^p \tag{3.12}$$

The elastic parts are related to the stress increment via moduli G (shear modulus) and K (the bulk modulus). In a first (virgin) loading of a specimen, the plastic strain increments are given by the following relations:

$$d\varepsilon^p = h\frac{\partial \Psi}{\partial \tau}\left(\frac{\partial f}{\partial \tau}d\tau + \frac{\partial f}{\partial \sigma}d\sigma\right),$$

$$dv^p = h\frac{\partial \Psi}{\partial \tau}\left(\frac{\partial f}{\partial \tau}d\tau + \frac{\partial f}{\partial \sigma}d\sigma\right) \tag{3.13}$$

where h is a function of state, Ψ is the so-called plastic potential and $f\,(=\tau/\sigma)$ is the yield function. Within the yield surface the material behaves as an elastic material; once the stress point approaches the surface and tends to move outside, the material behave as an elastic-plastic material. The stress ratio τ/σ occurs several times in what follows and therefore it is denoted by the symbol η.

This formulation carries an error as it ignores the curvature of the yield surface, i.e. it is not composed of rays with slight curvature emitted from the origin of the state space shown in Figure 3.4. This is in variance to what was proposed in the original CANAsand model although Poorooshasb (1971) did report the curvature of the yield surface. The magnitude of the error is very small, however, and the convenience it affords in the computational phase is enormous.

The plastic potential function Ψ has a general form:

$$\Psi = \sigma\,\bar{\Psi}(\eta, e^{\cdot}) - \sigma_0 = 0 \tag{3.14}$$

If it is stipulated that $\bar{\Psi}(0, e^{\cdot}) = 1$, then σ_0 represents the abscissa of the point of intersection of a Ψ = constant contour with the σ axis. A particular form of the plastic potential is the expression:

$$\Psi = \sigma.\exp(\eta/\mu) - \sigma_0 = 0 \tag{3.15}$$

which is independent of e'. Its use is very common at present and, in view of its simplicity, it will be used in the examples given below.

This completes a description of the response of the soil during the virgin loading of the sample. To deal with stress reversal, two additional concepts are employed. The first is the concept of "reflected plastic potential" and the second that of the bounding surface (Dafalias and Popov, 1975) which distinguishes between virgin loading and secondary loading (such as stress reversals and cyclic loading). The behavior of the soil within the bounding surface is guided by the properties of a point on the bounding surface. During virgin loading the bounding surface moves (expands) as the stress point traces a curve in the stress space. During a stress reversal the yield surface moves within the bounding surface and its kinematic is guided by two particular stress vectors known as the conjugate and datum stress vectors located on the bounding surface respectively. The intersection of these stress vectors and the π plane passing through the current stress points are known as the conjugate and datum stress points.

Referring to Figure 3.6, let AB represent a portion of the plastic potential contour passing through the current stress point. Then by definition, the reflected plastic potential is the contour A'B' which is the mirror image of AB about the line passing through the origin of the stress space. Thus, in a stress reversal process, the plastic strain increment vector is given by:

$$d\varepsilon^p = h_r \frac{\partial \Psi_r}{\partial \tau}\left(\frac{\partial f}{\partial \tau} d\tau + \frac{\partial f}{\partial \sigma} d\sigma\right),$$

$$dv^p = h_r \frac{\partial \Psi_r}{\partial \tau}\left(\frac{\partial f}{\partial \tau} d\tau + \frac{\partial f}{\partial \sigma} d\sigma\right) \tag{3.16}$$

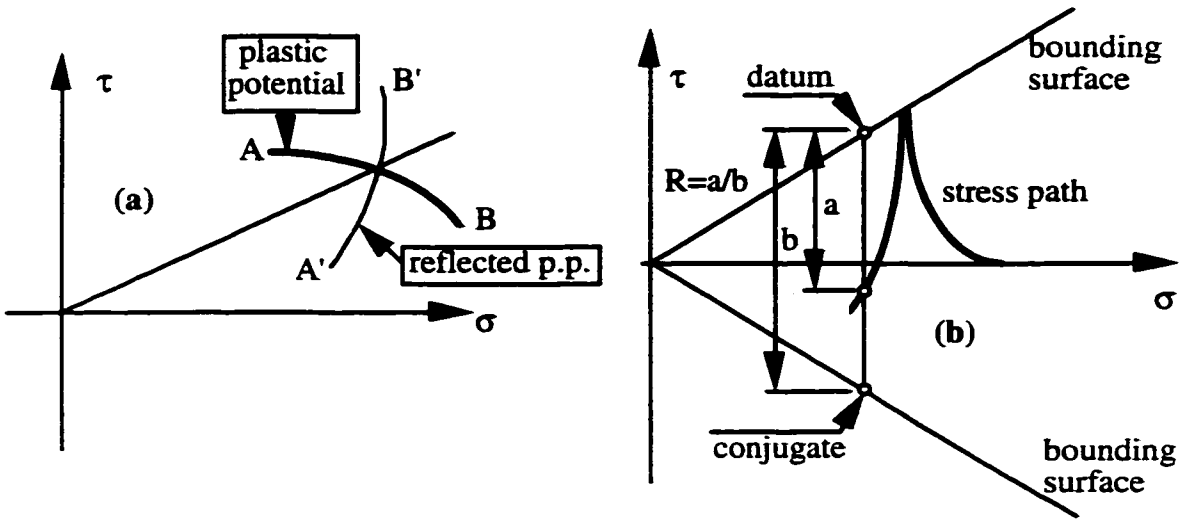

Figure 3.6 a) Reflected plastic potential, b) Bounding surface and the position of the datum and conjugate stress point.

Note that here the loading function h is replaced by h_r to indicate that a stress reversal is in progress. The magnitude of h_r is related to the value of h_c associated with the conjugate stress point on the bounding surface, (see Figure 3.6b) through the equation:

$$h_r = R^n h_c \tag{3.17}$$

where R is defined in Figure 3.6b and n is the coefficient of the interpolation function which must be determined empirically. It is observed that the material response is not particularly sensitive to mild variation of the n parameter.

As mentioned before, the loading factor h is a function of state. To incorporate the second hypothesis given at the beginning of this chapter, i.e., at the compact state the plastic strains are not present, the factor h must satisfy the condition that:

$$e \to e_c, h \to 0 \tag{3.18}$$

Thus, if a new parameter of $e^* = e - e_c$ is defined, then $h = h\ (\tau, \sigma, e^*)$, where $h\ (\tau, \sigma, 0) = 0$ can be accepted as a rational formulation. The simplest form that the function h can have is:

$$h = \frac{ae^*\eta_{SBS}}{(\eta_{SBS} - \eta)^2} \frac{[\Psi_{,\tau}^2 + \Psi_{,\sigma}^2]^{1/2}}{\Psi_{,\tau}} \tag{3.19}$$

where:

$$\Psi_{,\tau} = \frac{\partial \Psi}{\partial \tau}, \qquad \Psi_{,\sigma} = \frac{\partial \Psi}{\partial \sigma}$$

Here a is a constant and η_{SBS} is the stress ratio τ / σ at the state boundary surface. This function clearly satisfies condition 3.18 and in addition follows the so-called hyperbolic form of the deformation response. These types of functions describe the strain-hardening behavior only. This concludes a very brief description of the constitutive law for cohesionless granular media subjected to simple shear loading.

3.7 TYPICAL SIMULATION RESULTS

In this section the results of some simulations are presented. A single set of material constants is considered in simulating the cyclic simple shear behavior of sand in both loose and dense states under a constant cell pressure. In the particular heuristic examples cited in this study, the specific material constants appearing in the equations and used for evaluation are as follows.

Constants associated with the state boundary surface appearing in Equation 3.11 are $\mu = \delta = 0.745$. These values indicate an angle of friction for the medium equal to 36.7^{o} for the ultimate (critical) state and 47^{o} for the compact state. Graphical

representation of the ultimate state line and the compact state line as well as those of plastic potential contours are provided in the upper right hand side of Figure 3.7.

Typical material parameters corresponding to the Casagrande C.V.R. line (Equation 3.8) are $e_h = 1.45$ and $\lambda = 0.13$. Constant c employed in $e_c = e_h - c$ of Equation 3.9 is $c = 0.45$. Furthermore, select constant a in Equation 3.19 equal to 0.05 and constant n in Equation 3.17 equal to 2. It should be noted that for the present choice of parameters, the shear modulus G was assumed to be equal to 50σ.

All the reported "test" results (i.e., computer test results) are under a constant normal stress of 100 kPa, at pressure, which the Casagrande equation provides a void ratio of 0.85.

3.7.1 Drained Response

The result of numerical simulation of a test on an extremely loose sample having an initial void ratio of 1.15 is presented in Figure 3.7. As a matter of fact, this range of void ratio infrequently exists in nature. However, at low pressures, Casagrande C.V.R. line (Figure 3.1) predicts unrealistically high values of void ratio. Therefore, it was chosen to demonstrate the capabilities of the model in verifying the proposed formulation. In this test as in the subsequent ones, the sample was subjected to 25 loading cycles (unless, of course, the sample failed). The most noteworthy feature of Figure 3.7 is the reduction in void ratio of the sample during the first quarter cycle of loading. It appears as if the whole structure of the skeleton of the specimen collapsed. In fact the reduction in the void ratio during the first quarter cycle (about 0.3) is larger than the reduction during the next 24.75 cycles (about 0.25). The result also appears to be

closely comparable with the experimental results performed and reported by Youd (1972). It is observed that after a number of cycles, there was little or no influence on the amount of void ratio reduction.

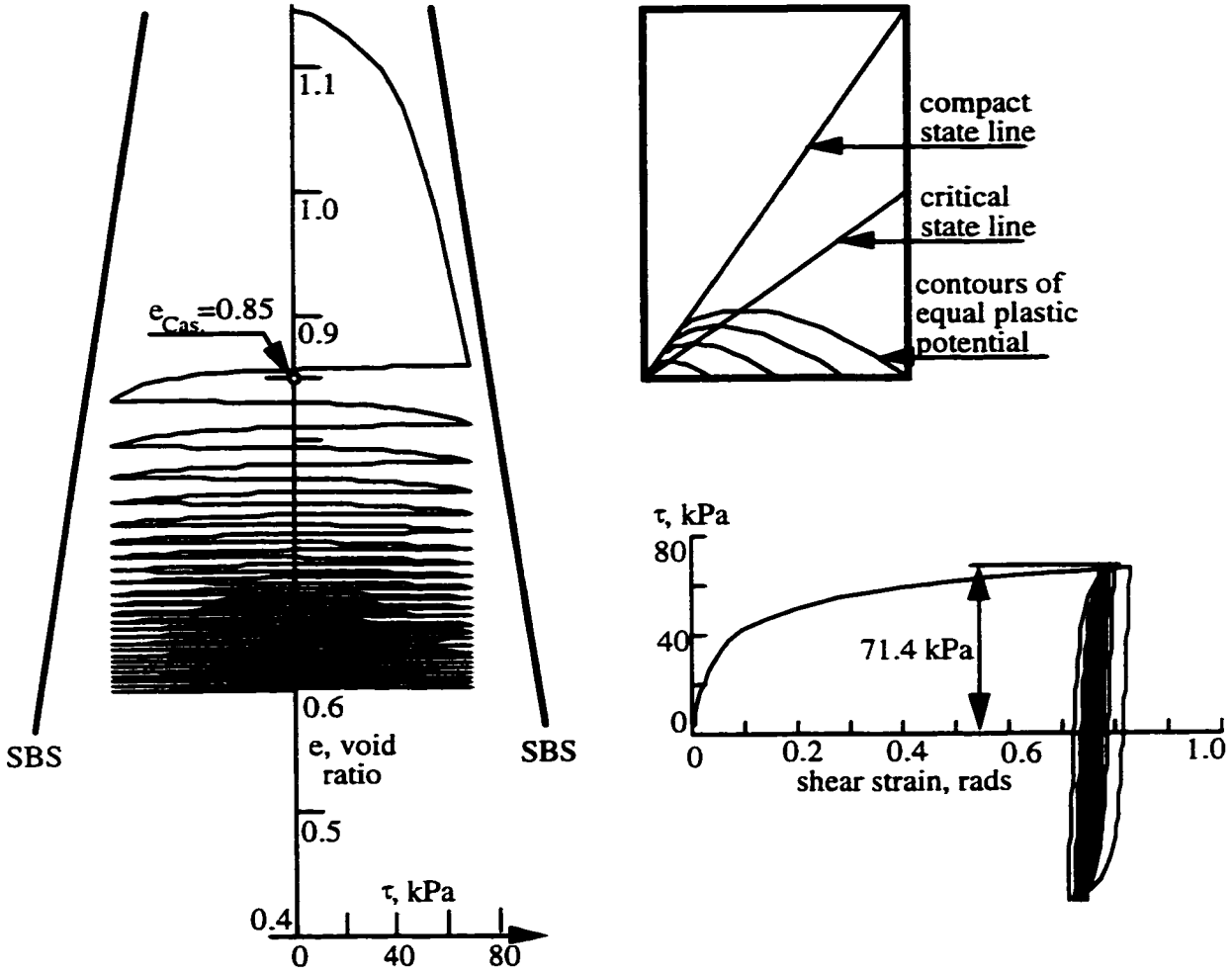

Figure 3.7 Response of a very loose sample (e_0 = 1.15) to cyclic loading

The test was repeated (Figure 3.8) using a denser sample (e_0 = 1.05) which, nevertheless, had an initial void ratio larger than the value given by the Casagrande equation (e = 0.85). Again the reduction in void ratio in the first loading cycle is remarkable. The results obtained herein are in agreement with the conclusion presented by Silver and Seed (1971).

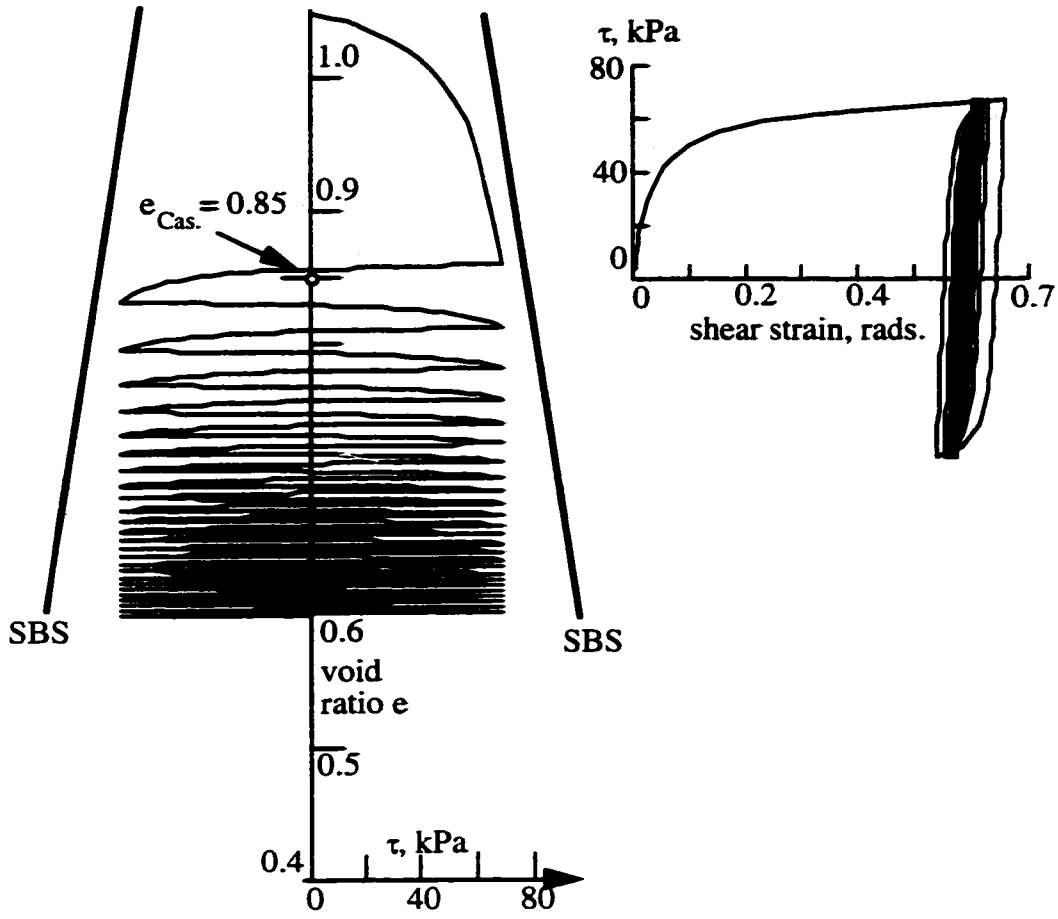

Figure 3.8 Response of a loose sample (e_0 = 1.05) to cyclic loading

In both tests, the amplitude of the loading process (maximum value of shear stress imposed) was rather high, being equal to 71.4 kPa (as compared to 74.5 kPa for the ultimate state). That is why both samples immediately tended to approach the ultimate state upon loading, a fact that has been verified experimentally time and again. Thus, in the next test, the value of the amplitude of the load was reduced to a smaller value of 54 kPa. The results are shown in Figure 3.9. It is seen that now it takes the sample about four cycles to reach the value of the void ratio given by the Casagrande equation. Again as the number of cycles increase, the sample tends to contract reaching the compact state eventually. The final void ratio after 25 cycles of loading (e = 0.65), however, is not

much different from that of previous test (0.6) in spite of the fact that the amplitude of the load is smaller.

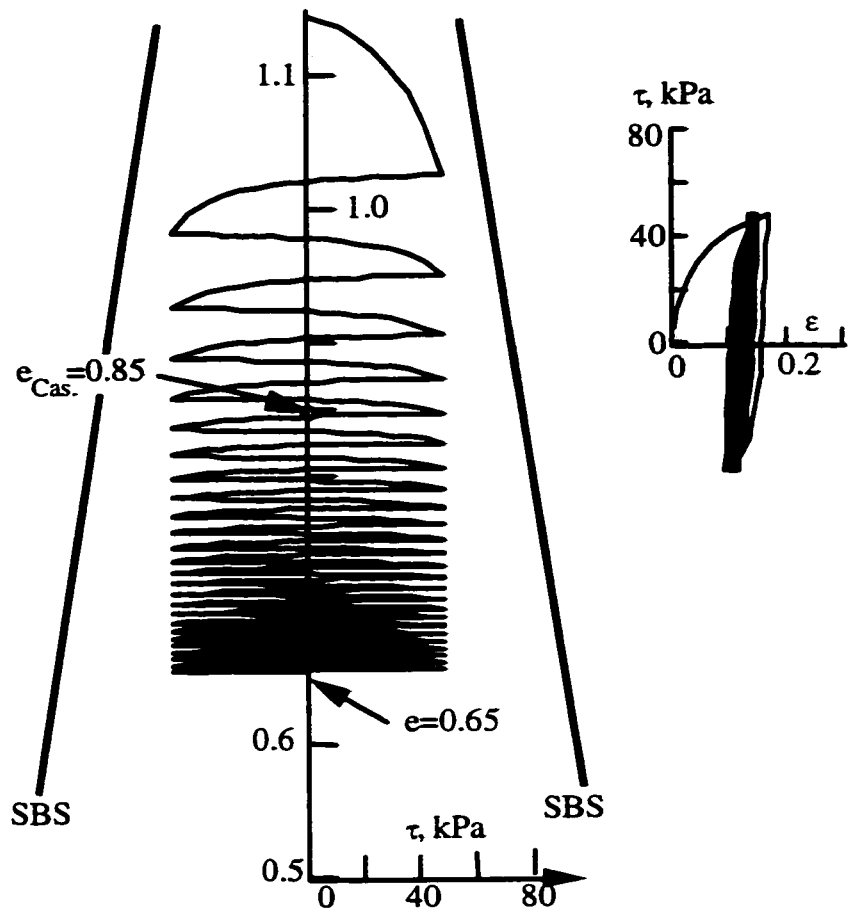

Figure 3.9 Response of a very loose sample (e_0 = 1.15) to cyclic loading (Maximum shear stress, 54 kPa)

All the above tests were conducted on loose samples. Thus, the next computer test was performed on a sample with a void ratio of 0.75, which is denser than $e_{Cas.}$= 0.85. Figure 3.10 shows the predictions corresponding to the e = 0.75. It may be noted that, although the sample still contracts (its void ratio decreases as the number of cycles of loading increases), nevertheless, the degree of contraction is not high. That is, after 25 cycles of loading its void ratio has decreased by 0.16 as compared to the first specimen

(Figure 3.7), which had a reduction in the void ratio of 0.55. This appears to be contrary to a belief that dominated the field of geomechanics for some extended period during which period it was advocated that deposits denser than the Casagrande critical void ratio would not, in the event of an earthquake, liquefy.

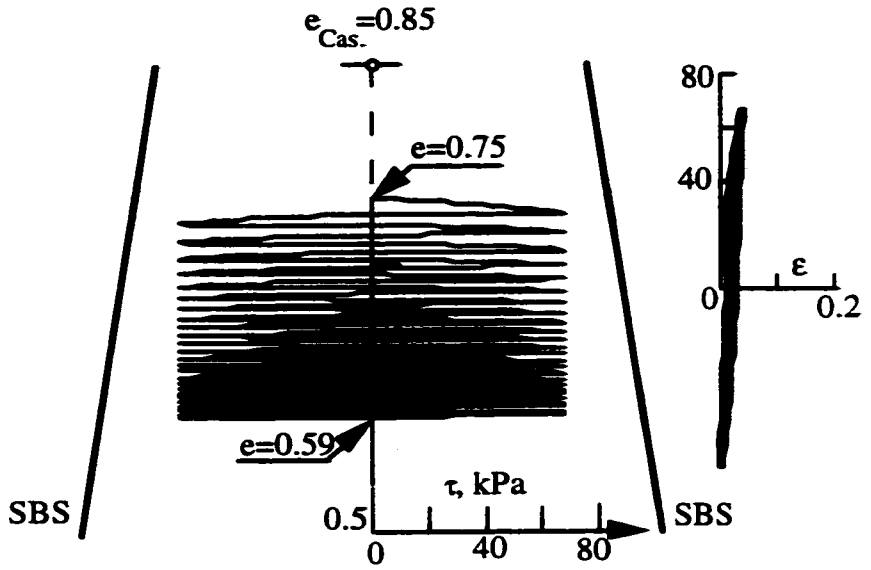

Figure 3.10 Response of a medium dense sample ($e_0 = 0.75$) to cyclic loading (Maximum shear stress, 71.4 kPa)

The question now arises that if even dense samples, such as the one just described, contract during cyclic loading, how is it that Casagrande's criterion survived for as long as it did. That is, do dense samples dilate (increase their void ratio) during cyclic loading under any circumstances? The answer is that they do so provided the amplitude of the loading cycles is large enough. Figure 3.11 clarifies this point.

Consider now a very dense sample (e = 0.65) which is subjected to a high amplitude cyclic load of 85.6 kPa. At the initiation of each cycle, there is a small tendency for the sample to contract. As the magnitude of the imposed stress increases, the sample dilates and the overall effect is an increase in the void ratio of the sample. At

some stage, however, (at a void ratio of 0.73, see Figure 3.11) it reaches the state boundary surface and fails. After this limit if the straining continues, say in a strain-controlled test, the sample would ride on the state boundary surface and behave as a work softening material.

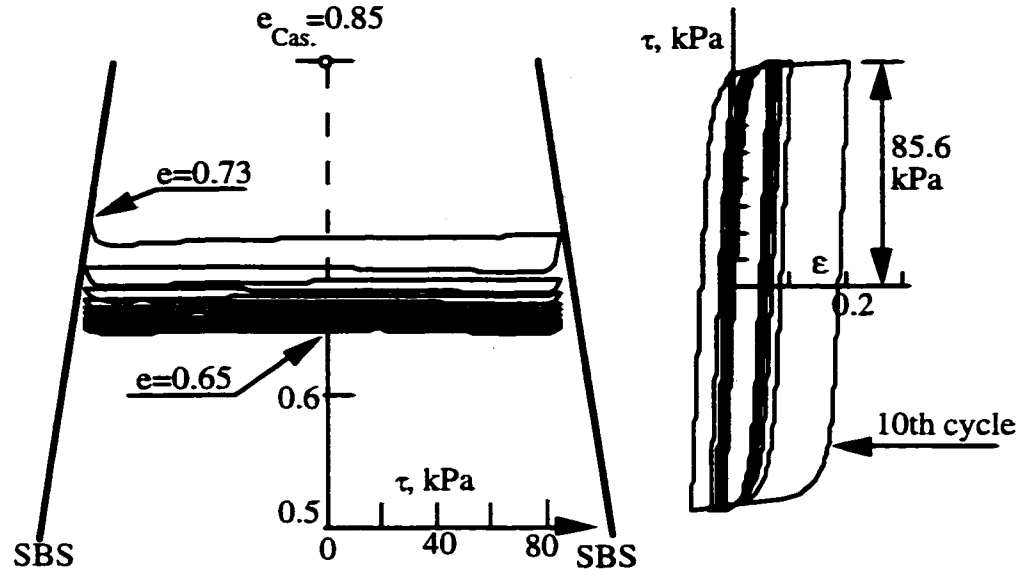

Figure 3.11 Response of a very dense sample (e_0 = 0.65) to cyclic loading (Maximum shear stress, 85.6 kPa).

These results have rather serious implications. Therefore, was Casagrande's criterion, which for so many years dominated the field of geodynamics, correct? The answer is partly. Samples looser than the critical void ratio have a very high potential to collapse upon loading. In the context of foundation engineering, loose sand deposits whose void ratio are higher than the critical void ratio would certainly liquefy if the seepage of water were somehow prevented or slow down.

Deposits denser than the critical void ratio could also liquefy. The tendency to contract exists even in these deposits. Dilatation (increase in volume) manifests itself only if the deposit is subjected to large amplitude cyclic loading. Such high stress

loading cycles are not likely to occur very often in nature. Thus, a complete dynamic analysis must be performed to determine if a particular stratum is likely to liquefy and, if so, would it lead to catastrophic failure.

3.7.2 Undrained Response

Up until now, consideration has been given to the behavior of cohesionless samples in drained tests. To see the effect of cyclic loading on undrained behavior of saturated sands, still another series of tests were conducted whose results are shown as follow.

Since liquefaction takes place under essentially undrained conditions then two more tests were performed under the undrained (constant volume) conditions. The first test, the result of which is shown in Figure 3.12, was performed on a sample looser than the critical void ratio.

The stress path associated with this test shows a peak in the first quarter cycle and under stress reversals develops very large pore water pressure and the sample liquefies after two cycles; that is, the normal effective stress acting on the sample approaches zero.

For the sample denser than the critical state, Figure 3.13, development of the positive pore water pressure is not as pronounced and the sample does not liquefy. Instead it reaches the compact state and behaves as elastic solid. This does not mean that samples denser than the critical void ratio would not liquefy. Rather, that their tendency to liquefy depends on their position in the state space relative to the compact state.

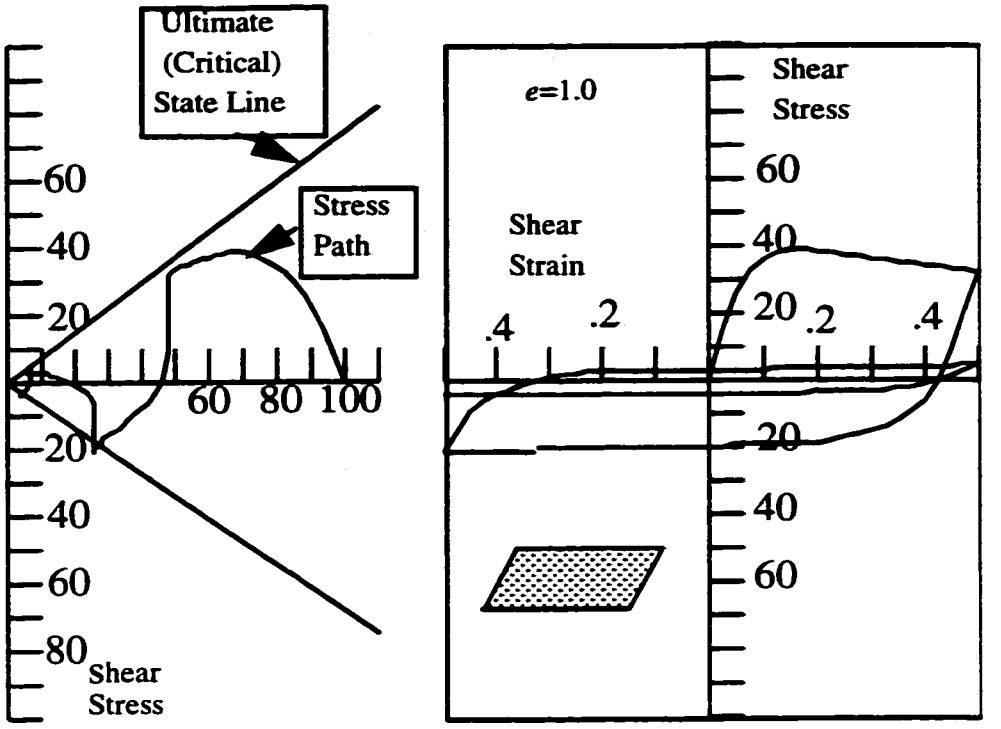

Figure 3.12 Undrained simple shear test on a sand sample looser than the critical void ratio, e =1.0

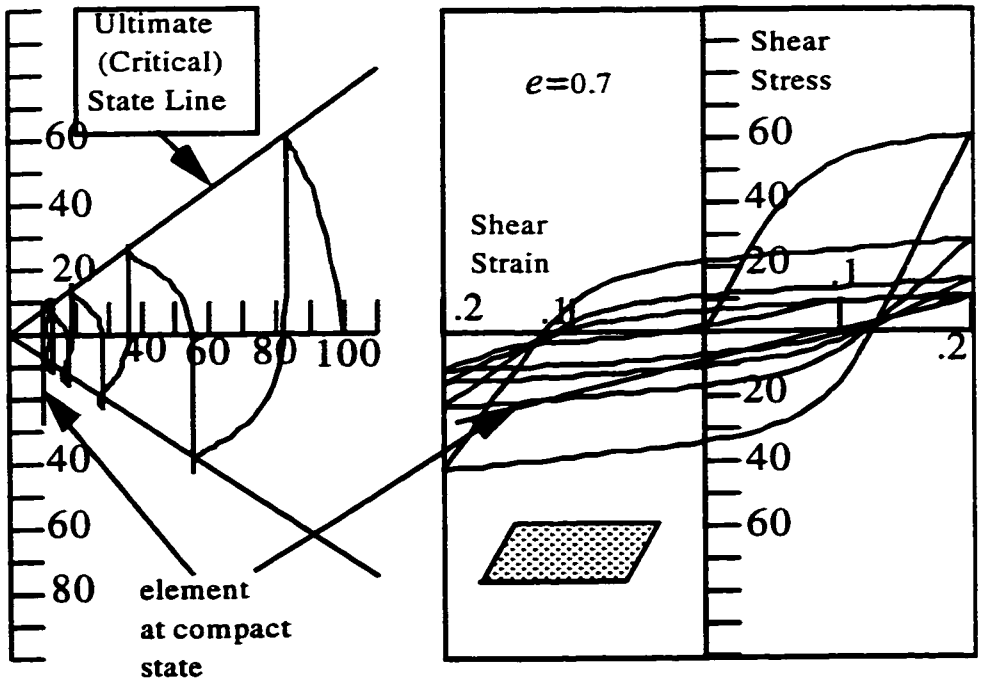

Figure 3.13 Undrained simple shear test on a sand sample denser than the critical void ratio, e=0.7

3.8 CONCLUSION

The concept of compact state postulates the existence of some states at which the element ceases to behave as an elastic-plastic material and would behave as a simple elastic material. At the compact state the particles are so interlocked that under normal loading conditions they would simply behave as a solid. Needless to say that the compact state represents the densest possible state a granular can achieve.

The fact that the "compact state" exists cannot be disputed. However, the properties attributed to it by the two hypotheses stated at this study need to be established experimentally. The available experimental data (similarity principles and increase in sample stiffness with an increase in the degree of compaction) indicate the relative merits of these hypotheses.

The compact state, as qualified above, is a useful concept in deriving the constitutive law of deformation of cohesionless granular media. It is believed that the compact state concept can be very useful in formulating the behavior of the cohesionless granular media when subjected to a stress reversal loading process.

Based on the present study the following conclusion may be drawn. If the representation of the void ratio of a sample from a sand deposit falls above the Casagrande line, then the liquefaction of the deposit, when subjected to dynamic loading, is certain. If, on the other hand, the representation indicates a point below the Casagrande line, it does not mean that the deposit is safe. The safety of the deposit against liquefaction depends how far the state point is from the line presenting the compact state, the magnitude and duration of the earthquake it must withstand.

4

MODELING WAVE-INDUCED LOADING OF A SEABED DEPOSIT

4.1 INTRODUCTION

Shoreline protective structures are subjected to the action of waves that can exert forces of significant magnitude. Stability and deformation of the seabed in response to ocean wave loading is an important consideration in the design of near-shore structures. Water wave propagating over a permeable seabed will induce a cyclic pressure, which may be significant in shallow water. The wave-induced pore water pressures and associated effective stress field in the seabed may be sufficient to cause liquefaction conditions in the soil.

The interaction of ocean and sea floor is a very complex problem and all methods for assessing stability are based on extensive simplifying assumptions. Waves significantly influence the planning and design of shore protection structures and other coastal works. An adequate understanding of the fundamental physical processes of surface wave generation and propagation must precede any attempt to understand the mechanics of wave motion in the nearshore areas.

Water waves propagating on the ocean may be considered to consist of an infinite number of wave trains having a constant amplitude and wave length. Passage of such an array of waves on the sea floor creates harmonic pressure waves on the seabed, increasing the pressure under the crest and reducing it under the trough.

In general, actual water-wave phenomena are complex and difficult to describe mathematically because of non-linearities, three-dimensional characteristics, and apparent random behavior. However, there are two classical theories, one developed by Airy (1845) and other by Stokes (1880), that describe simple waves. The Airy and Stokes theories generally predict wave behavior better where water depth relative to wave length is not too small.

This chapter presents an overview of the previous works related to the analysis of wave-induced loading. It is followed by a brief description of wave characteristics. Then the linear wave theory for determining the wave-induced pressure at sea bottom (mud line) is introduced. Finally, modeling of a seabed deposit subjected to the action of standing waves is presented.

4.2 LITERATURE SURVEY

Many investigators have been attracted to the problem of assessing the transient stress field and the variation of pore water pressure. Some others have considered the development of the progressive pore water pressure caused by the cyclic shear stress. These investigators have made various simplified assumptions in order to study seabed response. In various approaches, the sea floor has been considered as either a one-phase (total stress theory) or a two-phase (effective stress theory) medium by uncoupled or coupled schemes.

The simplest theory for evaluating the transient pore pressure in the seabed due to wave loading was developed by Putnam (1949). He analyzed the flow induced in a rigid and non-deformable saturated porous bed by the pressure field. He assumed incompressible flow with an isotropic permeability, the validity of Darcy's law and

hydraulic isotropy. Under these conditions, he showed that the governing equation for the pore pressure in the soil is the Laplace equation.

The total stress solution in uncoupled analyzes could be determined by elastic theories from Boussinesq's classical solution for a two-dimensional plane strain surface loading. Fung (1965) has given expressions for the amplitudes of the total stresses in a semi-infinite homogeneous isotropic elastic medium similar to Putnam's problem under a static sinusoidal loading.

Henkel (1970) was one of the first to provide the application of limit equilibrium methods to wave-induced instability of marine slopes. He assumed the sea floor to be a one-phase medium and performed the stability analysis along a circular failure plane. His contribution is historically important because he demonstrates conclusively that the pressure changes on the sea floor induced by storm waves could be a significant factor affecting seabed stability. Since this study was concerned with cohesive materials, the stability of the bed could realistically be analyzed based on a total stress analysis. As such, this study did not address the problem of wave-induced flow within the bed.

Sleath (1970) extended the Putnam analysis to include anisotropic permeability. He demonstrated that the theoretically predicted pore pressures induced by water waves over a porous bed compared favorably with results of small scale laboratory experiments. However, Sleath's work was confined to the prediction of pore pressures induced by water waves.

Moshagen and Torum (1975) presented a theoretical model for the bed pressure response assuming a permeably and rigid bed containing a compressible fluid with hydraulic anisotropy. The pore water pressure in this case is governed by the heat

conduction equation. The assumptions of a rigid soil skeleton and compressibility of the fluid together are unrealistic and lead to an excessive rate of pore pressure attenuation with depth, as shown by Prevost et al. (1975). Assuming that the pore water pressure is equal to the change in the octahedral normal stresses in the elastic continuum, Prevost et al. (1975) concluded that the pore water pressure is the same as the one obtained from the Laplace equation and, therefore, is independent of the permeability of the soil. This approach is, however, not physically consistent. Liu (1977) following along the same method investigated the effects of stratified permeabilities.

The above analyses neglect the mechanical properties of the soil, so that there is no coupling between the deformations of the soil skeleton and the pore water pressure response. Such uncoupled analyses contrast with more completed analyses based on Biot's theory of consolidation (1941). Biot (1941) established the mathematical theory governing the behavior of saturated porous media with a single fluid phase for linear elastic materials by a straightforward physical approach.

Pore water flow, volume change, and deformation occur simultaneously in real soil beds. Taking the assumption of deformability of the soil skeleton and the interaction of the solid and fluid phases, different researches have carried out studies by applying the general theory of three dimensional consolidation (Biot, 1941). Yamamoto (1978) used Biot's theory to solve for not only the pore pressure response, but also the effective stresses and their distribution in the seabed due to the passage of waves for a saturated soil bed of both infinite and finite depth with isotropic permeability. Madsen (1978) presented a general theory for the transient pore pressures and effective stresses, using

Biot's equation for a poroelastic two-phase medium of infinite depth with anisotropic permeability.

Yamamoto-Madsen final governing equation was a linear differential equation of the sixth order and did not contain the properties of the sand skeleton, or the water, or the permeability of the sand. Yamamoto (1983) introduced the effects of Coulomb damping and nonlinear shear modulus via the Hardin-Drnevich (1972) formulas using the Biot model and obtained good correlation with experiments.

There is a unique one-to-one relationship between the predicted response and the applied load at any time. Therefore, the design storm wave condition in the coupled effective stress analysis is specified in terms of a single wave with the largest amplitude.

A computer program was developed by Siddharthan and Finn (1979) for the analysis of transient pore water pressures and effective stress due to wave loading. It is also based on Biot's equations and extends the capacity for analysis to layered soils with hydraulic anisotropy and variable depth. The program evaluates the stability of the sea floor under the wave-induced effective stress system using the Mohr-Coulomb failure criterion.

Mei and Foda (1981) modified the mass and momentum conservation equations of the solid skeleton and the pore water by using several assumptions. They modeled the seabed response to waves as a superposition of an elastic response of one-phase medium and a seepage flow near the bed surface. The seepage flow is appreciable only in a thin layer, namely boundary layer, near the bed surface. Solutions for both regions were obtained, and the final solution was given as a sum of both solutions.

An analytical solution for the problem of cyclic pore pressures caused by sea waves in a poro-elastic half-plane was proposed by Verruijt (1982). He defined a characteristic wave parameter in terms of the wave length, the wave period, and the coefficient of consolidation to identify long and short waves. It has been shown that the phenomenon of consolidation due to surface wave on a porous bed is determined mainly by this parameter.

Finn et al. (1983) have shown analytically the ocean wave propagation induces oscillatory shear stresses in the seabed. They have concluded that in a finite layer, there is a difference between the results of coupled and uncoupled solutions near the lower boundary, with the coupled solution showing increases in pore pressure and shear stress in that region. Also, the finite layer solution is dependent on the permeability, even in the case of hydraulic isotropy. Hydraulic anisotropy appears to have little effect on the shear stress distribution with depth. They proposed the uncoupled analyses are desirable for compact fine sands; however, for many other cases, the transient pore pressures and effective stresses can be determined from the simpler uncoupled analyses.

For short-period waves, Tsui and Helfrich (1983) have suggested that the Stokes' second-order theory gives a closer prediction of bottom pressures on the surface of sand layer. In practice, the general uncertainties with geometrical and soil parameters are such that it appears adequate to use the simple linear wave theory to predict bottom pressures due to waves.

Okusa (1985) has developed the same simple analytical solution as Madsen and Yamamoto (1978) in which the governing equation was reduced to a linear differential equation of the fourth order in terms of the stress and pore pressure components. Using

his solution, he discussed the effects of harmonic ocean waves on unsaturated sediments in horizontal seabeds. Later, Okusa and Yoshimura (1987) carried out a stability analysis of a very gently sloped plannar sea floor. The general solution of the problem of flow through poro-elastic media and their deformation is presented by a linear combination of the solution of the Fourier's equation and the diffusion (consolidation) equation. A possible failure mechanism is assumed to be a circular arc slip failure. They showed that the harmonically varying stress field on the sea floor induced by a plane traveling surface wave loading may be enough to cause sea floor slides.

Gatmiri (1990) developed the linear elastic analysis of the coupled effective stress and pore pressure to a submarine sediment with sloping surface. He also considered the response of an inhomogeneous seabed to wave loadings and showed that the effect of a soft layer near the sea-soil interface is very important. Later, Gatmiri (1991, 1992, 1994) has extended the non-linear behavior of a saturated permeable seabed under transient loading by applying the finite element idealization. He considered the effect of the stress level and induced deformation on the soil stiffness by introducing the hyperbolic Hardin and Drnevich (1972) behavior model in the field equation.

However, none of the above-mentioned response analysis accounts for the residual pore water pressure and permanent deformation. The residual pore pressures are induced by the cyclic shear stresses generated by the differential loading of the seabed by the bottom pressure varying harmonically in time and space. The wave-induced progressive pore water pressure has been subject of many studies. In the case of cyclic loading applied to a seabed by waves, a proper analysis of the effects of these pore pressures on the

stability of the sea floor requires account to be taken of the simultaneous generation and dissipation of these residual excess pore pressures.

Seed and Rahman (1977) have proposed a method for estimating the magnitude of the residual pore water pressures. They represent the complex pattern of storm waves by packets of uniform harmonic waves, with the height, period, and length of the wave being specified for each packet. The shear stresses generated by each wave type are computed assuming elastic behavior. Later, El-Zahaby and Rahman (1993) presented a general semi-analytical method for the analysis of seabed response under two-dimensional progressive, standing and short-crested wave. The seabed is idealized as poroelastic medium of finite thickness filled with a single compressible fluid with anisotropic flow. The coupled process of fluid flow and deformation of soil skeleton is formulated in the framework of Biot's theory.

The wave-induced liquefaction of seabed has recently received attention of the marine geotechnical engineers. It may occur in sand or silt deposits, thereby exerting damaging influences on the nearshore structures. The term "liquefaction" refers to the possibility of a soil undergoing continued deformation due to the build-up and maintenance of high pore water pressure as the cyclic axial stress is applied and eventually approaches to a value equal to the initially applied confining pressure (Seed and Lee, 1966) or producing an axial strain of about 5% in double amplitude (Ishihara, 1983, 1993). The common procedure to evaluate the resistance of soil to liquefaction is to test soil specimens by means of the cyclic triaxial test apparatus.

Christian et al. (1974) presented an analysis for the evaluation of liquefaction in soils subjected to the direct action of waves. They showed that liquefaction can result in

the flotation of pipelines. The observed failure was due to the liquefaction of the backfill material, which was in very loose condition.

Lee and Focht (1975) have presented simplified analyses for evaluating the pore pressure response in connection with the studies of the Ekofisk oil tank. In their analysis the effect of pore pressure dissipation is considered in an approximate way. Their work was probably the first to investigate the problem of ocean wave-induced liquefaction utilizing the principle established for the solution of seismic liquefaction problems.

Seed and Rahman (1978) developed a methodology in which generation and contemporaneous dissipation of excess pore water pressure during strong wave loadings can be evaluated. An uncoupled scheme was adopted. This was accomplished by solving the usual continuity equation of flow in conjunction with a pore water pressure generation model proposed by Seed et al. (1976). The effective stress was computed assuming elastic behavior. The residual pore water pressure is not uniquely related to the instantaneous values of wave-induced stresses, but depends on the intensity and duration of the storm and on the drainage characteristics of the sea floor. Under these circumstances, the design storm wave condition in Seed's liquefaction analysis is specified in terms of the wave height, number of waves and duration.

A computer program which has been developed by Siddharthan and Finn (1979) is a generalization of the Seed and Rahman method and includes the effect of increasing pore water pressures during a storm on the shear and bulk moduli. Later, Finn et al. (1983) extended this approach to stability analyzes of the seabed deposit on the basis of the effective stress principle.

Nataraja and Gill (1983) developed a simplified procedure for ocean wave-induced liquefaction analysis and examined a few case histories for evaluation of their procedure. In this procedure, the existing solutions from the theory of elasticity are used to estimate the cyclic shear stress distribution resulting from the passage of a wave train. The existing data on cyclic shear strength of liquefaction under seismic loadings are modified and extended to estimate the cyclic shear strength of liquefaction under wave loading conditions. It can serve as a first step in determining whether a sophisticated analysis is required.

The effects of the principal stress axis rotation on the response of a clean sand have been extensively investigated by Arthur et al. (1980) by means of a specially designed flexible boundary shear apparatus. It was shown by Ishihara and Towhata (1983) that the change in shear stress induced in the sea floor deposits by waves traveling overhead involves a continuous rotation of the principal stress axes. Later, Ishihara (1983), Ishihara and Yamazaki (1984) have indicated that the principal stress axes rotation could be an important factor influencing the pore water pressure build up during cyclic loading.

Ishihara and Yamazaki (1984) developed useful charts to evaluate wave-induced liquefaction but didn't include the contemporaneous dissipation effects by assuming the seabed deposit to be a homogeneous elastic half-space. They also demonstrated that cyclic change of shear stress included in an elastic half space by a harmonic load moving on its surface is characterized by continuos rotation of the principal stress direction, with the deviator stress remaining constant. This contrasts with other time dependent stresses caused by earthquakes.

Rahman and Jaber (1986) developed a drained analysis for the wave-induced liquefaction showing that the effect of dissipation may be quite significant and should not be ignored.

Siddharthan (1987) outlined an approach to compute the sea floor response to a storm wave group. The sea floor soil was modeled as a nonlinear porous effective stress dependent material. Dynamic effects such as inertia and damping are included in the approach. A computer program was developed to analyze the sea floor response. The approach includes the effects of the residual pore water pressure when the largest wave in the storm applies loading on the sea floor. The procedure adopted to compute residual pore water pressure is based on the Seed-Rahman (1978) in which contemporaneous generation and dissipation of residual porewater pressure is considered. He also showed that the inclusion of damping, inertia and anisotropic permeabilities is not important relative to ocean sands.

In an attempt to analyze the liquefaction susceptibility of the sea floor deposits under wave action, Poorooshasb et al. (1987) have carried out the finite element nonlinear coupled analysis for standing wave loading in which the sea floor was assumed to be a saturated porous medium simulated by a two-surface plastic model (Poorooshasb and Pietruszczak, 1985) for the solid phase. It was probably the first time that the wave-induced seabed response was investigated by elasto-plastic effective stress analysis step by step following the wave loading history. Later, Poorooshasb et al. (1990) extended a simultaneous solution (direct integration) scheme for analysis of the seabed deposit subjected to standing wave action by finite element method in which the two surface

plastic constitutive model is adopted. Results from the coupled nonlinear analysis predict that liquefaction may indeed occur for certain loose deposits.

Yang (1990) predicted the susceptibility of liquefaction of the sea floor under storm waves at a pipeline site in Lake Ontario and Ekofisk tank in the North Sea using a simple constitutive model based on the generalized plasticity-bounding surface formulation. The model is capable of simulating both loose and dense sand behavior under monotonic and cyclic loading, drained and undrained conditions.

Zen and Yamazaki (1990 a) presented a liquefaction criterion in which the dominant factors on the liquefaction are the wave-associated bottom pressure, the oscillatory pore pressure in the seabed and the vertical effective stress at calm. In a companion paper, Zen and Yamazaki (1990 b) studied the wave-induced oscillatory pore pressure experimentally and proposed an elementary analysis to evaluate the wave-induced liquefaction in partly saturated sediments. Zen and Yamazaki (1990) also suggested that the one-dimensional uncoupled analysis is applicable to the estimation of liquefaction potential when the wave length is large enough compared with the thickness of permeable seabed. Zen et al. (1991) observed that scouring near the edge of the breakwater is associated with the wave-induced liquefaction in partly saturated sediment due to oscillatory pore pressure. Later, Zen and Yamazaki (1991) observed wave pressure and pore water pressures at the surface and pore water pressures in the subsoil in both a one-dimensional model ground and the field. Their record manifests a delayed response of subsurface pore water pressure after the loading of surface wave pressure. The important feature in these approaches is the degree of saturation of the soil. If the soil is completely saturated, no phase lag in the pore pressure response and amplitude decay of oscillatory

pore pressure at different depths, relative to the pressure fluctuation above the seabed are anticipated.

Rahman (1991, 1992) formulated the conditions necessary for wave-induced instability through simplified analyses. He showed that a fully saturated seabed with cohesionless sediments may experience liquefaction associated with progressive buildup of pore pressure in the region of vulnerable water, and also, a partly saturated seabed may also experience liquefaction associated with oscillatory pore pressure. The liquefaction potential increases with the decrease in degree of saturation and with the increase in wave period.

Nago et al. (1993) investigated the dynamic behavior of loosely sand bed under wave motion experimentally. They observed two types of liquefaction in their experiment, namely, the sustained liquefaction due to the build up of excess pore pressure and the cyclic transient liquefaction due to the damping of amplitude and phase lag in the pore water pressure. The surface layer of sand layer is densified through these two types of liquefaction and reaches a stable state.

An elasto-plastic constitutive model was used by Oka et al. (1993). This model incorporates both the transient and progressive pore water pressure for an effective stress analysis of the wave-induced liquefaction of the seabed. The governing equations are obtained through an application of the two-phase mixture theory by Biot (1941) using a U-P formulation (Zienkiewicz and Bettess 1982). An elasto-plastic constitutive model along with the concept of nonlinear kinematic hardening rule is formulated to describe the stress-strain behavior of granular materials under cyclic loading. It was found that the

seabed liquefies more quickly in two than in one-dimensional case, presumably, due to the rotation of the principal stress axis.

Recently, Yang et al. (1994) have presented an elasto-plastic constitutive model for the traveling wave-induced response of sea floor deposits. An artificial boundary is suggested to deal with the unbounded domain problems. It has been used for the analysis of seabed response to traveling wave with success.

Almost all of the literature cited above recognizes the wave-induced liquefaction phenomena. However, little work has been done towards using the elasto-plastic effective stress analysis along the concept of bounding surface plasticity. An attempt is made to incorporate the non-linearities of soil behavior as described by the extended CANAsand model (including the compact state concept) in forthcoming sections.

4.3 WAVE CHARACTERISTICS

Any adequate physical description of a water wave involves both its surface form and the fluid motion beneath the wave. A wave that can be described in simple mathematical terms is called a simple wave. Sinusoidal or simple harmonic waves are examples of simple wave since their surface profile can be described by a single sine or cosine function. A wave is periodic if its motion and surface profile recur in equal interval of time. A progressive wave, as the name implies, progresses across the ocean, so that successive crests pass a fixed station. Two progressive waves of equal period and height which are propagating in exactly opposite direction is defined as standing wave. Water waves are considered oscillatory if the water particle is described by orbits that are closed or nearly closed for each wave period.

The most fundamental description of a simple sinusoidal oscillatory wave is by its length L (the horizontal distance between corresponding points on two successive waves), height H (the vertical distance to its crest from the preceding trough), period T (the time for two successive crests to pass a given point), and depth d (the distance from the bed to the stillwater level) as shown in Fig. 4.1.

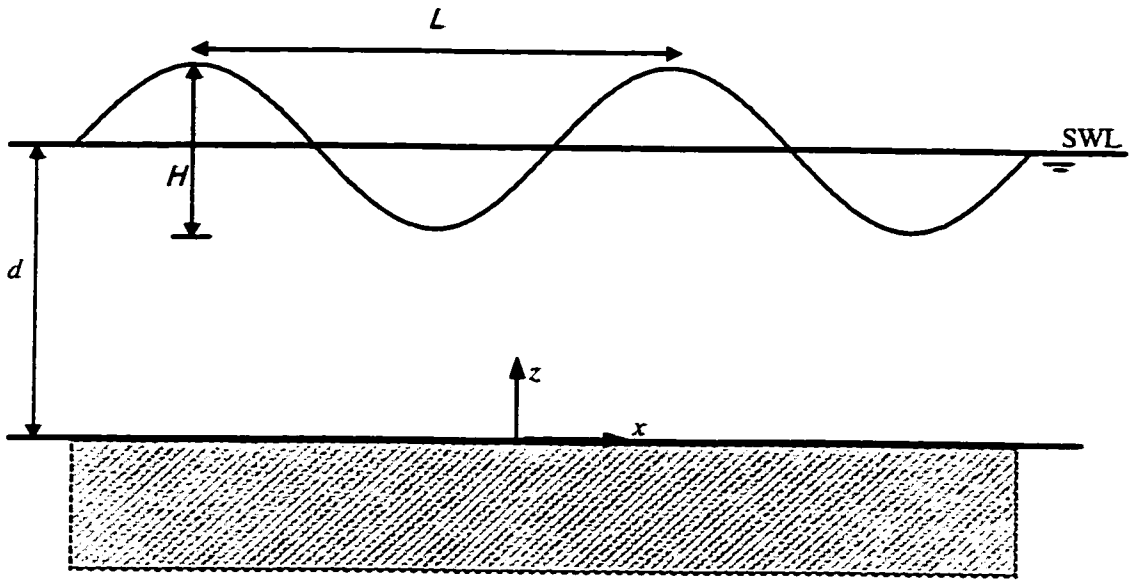

Figure 4.1 Definition sketch for a progressive wave

The water surface profile ζ was given as a function of position and time by

$$\zeta = \frac{H}{2} Cos\left[2\pi\left(\frac{x}{L} - \frac{t}{T}\right)\right] = \frac{H}{2} Cos(Nx - \omega t) \tag{4.1}$$

where N and ω denote the wave number and wave angular frequency respectively.

The wave speed or celerity C is the speed of the wave traveling through the fluid $(C=L/T)$. It is convenient to work with the wave angular frequency $\omega = 2\pi/T$, wave number $N=2\pi/L$ and thus $(C=\omega/N)$ too.

4.3.1 Linear Wave Theory

The most elementary progressive wave theory, referred to as linear wave theory (Stokes of first approximation), was developed by Airy (1845). This wave theory is of fundamental importance since it is not only easy to apply, but also reliable over a large segment of the whole wave regime. Mathematically, the Airy theory can be considered as a first approximation of a complete theoretical description of wave behavior.

Linear wave theory can be developed by the introduction of a velocity potential $\varphi(x, z, t)$. Horizontal and vertical components of the water particle velocities are defined at a point (x, z) in the fluid as $U=\partial\varphi/\partial x$ and $W=\partial\varphi/\partial z$. The velocity potential, Laplace's equation and Bernoulli's dynamic equation together with the appropriate boundary conditions provides the necessary information to derive the linear wave theory formulas.

Two serious difficulties arise in the attempt to obtain an exact solution for a two-dimensional wave train. The first is that the free-surface boundary conditions are nonlinear and the second is that these conditions are prescribed at the free surface $z = \zeta$ which is initially unknown. The simplest and most fundamental approach is to seek a linear solution of the problem by taking the wave height H to be very much smaller than both the wave length L and the still water depth d, i.e. $H<<d$. The wave theory, which results from this assumption, is referred to alternatively as small amplitude wave theory, linear wave theory or Airy wave theory.

According to this theory, the pressure at any point within the body of the water may be given by the equation;

$$P=\rho_w g(z-d)+\rho_w g\frac{H}{2}\frac{\cosh[N(z+d)]}{\cosh(Nd)}\sin(Nx-\omega t) \tag{4.2}$$

where ρ_w is the unit mass of the water and g is the acceleration of gravity. In the above formula, the first term is hydrostatic pressure and the second term is the hydrodynamic

pressure due to particle acceleration. The values of N and ω in equation (4.2) can not be arbitrarily chosen, but are derived, as follows, from the basic solution of the small - amplitude wave theory (dispersion relationship);

$$\omega^2=gN\tanh(Nd) \tag{4.3}$$

in which $N = 2\pi/L$, $\omega = 2\pi/T$. The above equation can also be written in the following form;

$$L=\frac{gT^2}{2\pi}\tanh\left(\frac{2\pi d}{L}\right) \tag{4.4}$$

4.3.2 Wave-induced Pressure at Sea Bottom

At the seabed elevation, $z = 0$, the exerted water pressure (i.e. the pressure exerted due to wave action alone) is given by;

$$P=\gamma_w d+\gamma_w \frac{H}{2}\frac{1}{Cosh(Nd)}Cos(Nx-\omega t) \tag{4.5}$$

where γ_w is the unit weight of the sea water. The amplitude of pressure exerted on the sea bottom due to the traveling wave is given by

$$P_o =\rho_w g \frac{H}{2}\frac{1}{Cosh(Nd)} \tag{4.6}$$

The above equation relates sea floor pressures to wave characteristics for a wave traveling at speed of $C=L/T$. In the case of standing waves which are the combination of two traveling in opposite directions, the corresponding hydrodynamic equation is;

$$P=\rho_w g \frac{H}{2}\frac{\cos(Nx)}{\cosh(Nd)}Sin(\omega t) = P_0\cos(Nx)\sin(\omega t) \tag{4.7}$$

Such a situation is observed in front of seawalls. It is emphasized that for the shallow water wave the magnitude of $2\pi d/L$ is less than ¼ whereas for the deep water waves its

value is greater than π. Equations 4.5 and 4.7 are sufficiently accurate to be used as the loading boundary conditions imposed on the surface of the seabed.

4.4 AVAILABLE APPROACH TO ANALYSIS OF WAVE FORCES

With the objective of developing simplified analysis for the wave-induced liquefaction of the seabed, the Ishihara's method, which is most popular and reliable for obtaining such soil responses, is briefly presented. Ishihara (1983), Ishihara and Towhata (1983), and Ishihara and Yamazaki (1984) proposed an analysis which, while somewhat elementary, it is possibly the only method that can conveniently be handled by a practicing engineer.

Consider water waves propagating over a seabed. At the instant when the crest of a wave is positioned directly above the soil element being considered in the sea bottom, a positive vertical pressure will be exerted, but when the trough is located above the soil element, the resulting stress will be a negative vertical pressure. Consequently, there occurs a cyclic excursion of the vertical stress during wave propagation through a distance of one wavelength. In the intermediate instant when the point of zero wave height comes right above the soil element, it will be subjected to a horizontal shear stress. This horizontal shear stress also changes its direction back and forth in the course of the wave propagation, inducing another cyclic alteration of shear stress in the soil deposit.

The most fundamental assumption in Ishihara's analysis is that boundary loads are transmitted to the seabed surface in total, i.e., not as a pore water pressure on the surface. Stated otherwise in this analysis it is assumed that an infinitely flexible and completely

impermeable sheet covers the seabed surface. Thus the exerted water pressures are treated as ordinary loads acting through an impermeable boundary as shown in Figure 4.2.

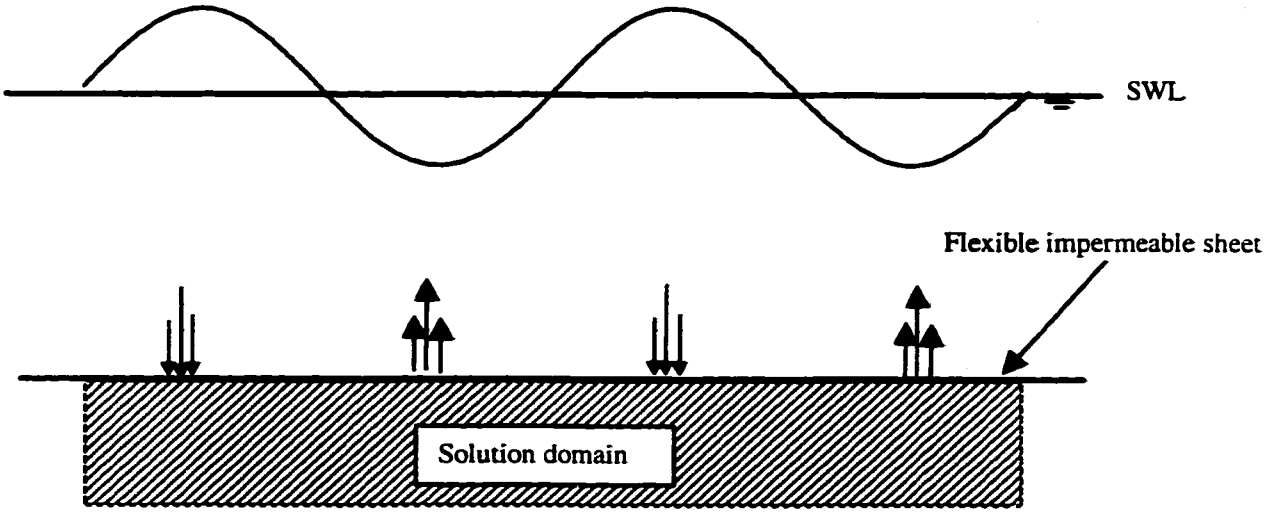

Fig. 4.2 Graphical representation of the fundamental assumption in Ishihara's analysis

The solution domain itself is treated as a homogeneous elastic material and the Airy stress function $(\varphi = Ar\theta\sin\theta)$ is used to evaluate the stress components at a given point at a given instant of time. Assume that a harmonic load

$$P(x) = P_o\cos\left(\frac{2\pi}{L}d - \frac{2\pi}{T}t\right) \tag{4.8}$$

is distributed on the surface of an elastic half-space, where P_o is the amplitude of the load. The vertical normal stress, σ_v, horizontal normal stress, σ_h, and shear stress, τ_{vh}, induced in the half-space by this load are determined according to Yamamoto et al. (1978) and Madsen (1978) as

$$\begin{aligned}
\sigma_v &= P_o(1+Nz)\exp(-Nz)\cdot\cos(Nx-\omega t)\\
\sigma_h &= P_o(1-Nz)\exp(-Nz)\cdot\cos(Nx-\omega t)\\
\tau_{vh} &= P_o(Nz)\exp(-Nz)\cdot\sin(Nx-\omega t)
\end{aligned} \tag{4.9}$$

assuming the origin of the coordinate system on the sea floor and the z ordinate pointing downwards into the solution domain.

Ishihara's analysis is not exact for three reasons. First, his analysis does not include the contemporaneous dissipation effects. In other words, the stress components (Eq. 4.9) are total stress components. Also note that these components do not contain terms involving the elastic parameters such as E, the Young's modulus and v, the Poisson's ratio, a situation common to plane strain problems of linear elasticity.

Second, Ishihara's approach is only statically admissible. That is, the total stress field expressed by Equation 4.9 satisfies only the boundary conditions of the problem and the incremental equations of the equilibrium;

$$\frac{\partial \sigma_{xx}}{\partial x} + \frac{\partial \tau_{xz}}{\partial z} = 0 \qquad (4.10)$$

$$\frac{\partial \tau_{xz}}{\partial x} + \frac{\partial \sigma_{zz}}{\partial z} = 0$$

The displacement field obtained from this stress field (Eq. 4.9) is unlikely to satisfy the kinematic constraints. Third, Ishihara did not consider initial in-situ stresses.

4.5 MODELING SEABED DEPOSIT SUBJECTED TO STANDING WAVES

Standing waves may be formed easily when a train of progressive waves is reflected by an impervious vertical wall and the reflected waves are superimposed on the incoming waves. This situation occurs often in front of the ocean side of composite breakwaters. The shearing resistance of cohesionless seabeds, being frictional in nature, may be reduced to zero due to progressive build-up of pore water pressure. The pore

water pressure may become high enough to reduce the effective normal stress to zero. This phenomenon, implying a total loss of strength, has been termed liquefaction. The behavior of cohesionless seabeds under standing waves has therefore received serious attention related to the stability of near-shore structures that might be easily affected by liquefaction phenomena. The purpose of this study is to represent a theoretical framework for analyzing liquefaction of loosely deposited soils under the action of standing waves.

The present section is organized into four separate parts. First the general equations for determining of cyclic stresses due to wave loading are derived. This is followed by mathematical formulation of the model to describe the stress-strain behavior of granular materials under cycle loading. Then the governing equation of seabed deposits subjected to standing waves is presented. Finally, the applicability of the proposed model is examined by some numerical examples. In what follows, compressive stresses and compressive strains are taken as positive.

4.5.1 Development of Cyclic Stresses under Seabed due to Wave Loading

The computation of actual cyclic stresses developed under the seafloor as a result of a passage of a wave train is a complex task. The resulting pressure distribution on the seabed will also be in the form of a cosine/sine wave. This loading can be reasonably approximated by plane strain conditions. Existing solutions from the theory of elasticity can be suitably modified to estimate the cyclic stresses under wave loading. The stress components in Cartesian coordinates, at a point x, z, in an elastic half space due to a vertical line load of intensity P is given by the following equations;

$$\sigma_{zz} = \frac{2P}{\pi r}\cos^3\alpha \tag{4.11}$$

$$\sigma_{xx} = \frac{2P}{\pi r}\cos\alpha\sin^2\alpha \tag{4.12}$$

Consider an element, $d\xi$, at a distance, ξ, from the middle of a wave loading as illustrated in Figure 4.3.

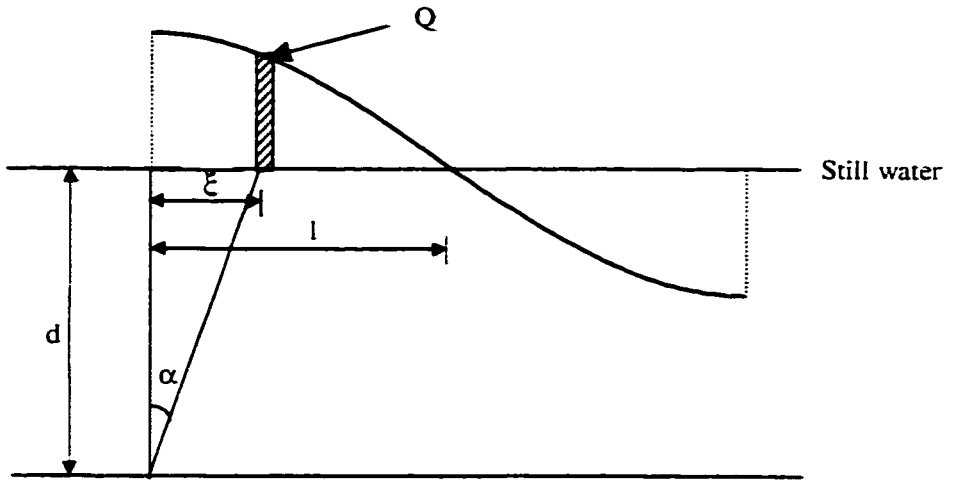

Figure 4.3. Cyclic stresses due to wave loading on seabed

Load density, Q, at any point on the wave can be expressed as follows:

$$Q = P_o \cos\left(\frac{\pi\xi}{2l}\right) \tag{4.13}$$

where $\xi = d\tan\alpha$ and $d\xi = \frac{d}{\cos^2\alpha}d\alpha$. Using $r = \frac{d}{\cos\alpha}$, Equations 4.11 and 4.12 may be rewritten as:

$$\sigma_{zz} = \frac{2P}{\pi d}\cos^4\alpha \tag{4.14}$$

$$\sigma_{xx} = \frac{2P}{\pi d}\cos^2\alpha\sin^2\alpha \tag{4.15}$$

where d is the depth of water and α is the angle between r and the z-axis.

Substituting $P = Qd\xi$ for P in Equations 4.14 and 4.15, the following equations are set up for the stress components at a point, x, z, under the wave loading:

$$P = \frac{Qd}{\cos^2\alpha}d\alpha = P_o d\cos\left(\frac{\pi\xi}{2l}\right)\frac{d\alpha}{\cos^2\alpha} \tag{4.16}$$

$$d\sigma_{zz} = \frac{2P_0}{\pi}\cos\left(\frac{\pi\xi}{2l}\right)\cos^2\alpha\, d\alpha$$

$$\sigma_{zz} = \frac{2P_0}{\pi}\int_o^{\pi/2}\cos\left(\frac{\pi d}{2l}\tan\alpha\right)\cos^2\alpha\, d\alpha \tag{4.17}$$

In a similar way it may be shown that:

$$\sigma_{xx} = \frac{2P_0}{\pi}\int_o^{\pi/2}\cos\left(\frac{\pi d}{2l}\tan\alpha\right)\sin^2\alpha\, d\alpha \tag{4.18}$$

These equations can be evaluated for various values of α as a function of r. Usually principal stresses have been written with subscripts 1, 2, and 3 specifying the major, intermediate, and minor principal stresses. Then in the remaining part of the present chapter the subscripts 1 and 3 will be used for the σ_{zz} and σ_{xx}, respectively.

4.5.2 Constitutive Modeling of Soil with Cyclic Plasticity

To describe the characteristics of the cohesionless seabed deposit, constitutive equations are derived within the framework of bounding surface plasticity theory along with the concept of compact state. In accordance with the concept of two surface plasticity, the proposed model consists of an inner (yield) surface and outer (bounding) surface. The bounding surface serves as envelop of many possible positions which the

yield surface may reach during the process of deformation. The yield surface undergoes a combination of isotropic and kinematic hardening while the bounding surface expands until a limiting state indicating possible states of failure in the material is reached. A non-associated flow rule is used in the derivation of the equations.

The state of stress is given by the two parameters as:

$$p = (\sigma_1 + 2\sigma_3)/\sqrt{3} \tag{4.19}$$

and

$$q = \sqrt{2/3}(\sigma_1 - \sigma_3) \tag{4.20}$$

In what follows, the term stress stands for effective stress unless otherwise noted. In the effective stress theory proposed by Terzaghi (1943), the deformational behavior and failure conditions of the solid matrix is only dependent on the effective stress. This assumption is generally valid for saturated soils.

An increment of strain is represented by the set of quantities of $\dot{\varepsilon}_{ij}$, and it is assumed to be the additive decomposition of an elastic strain increment and a plastic strain increment part. In the absence of rate-dependent behavior, the strain rates can equivalently be used instead of strain increments, i.e.;

$$\dot{\varepsilon}_{ij} = \dot{\varepsilon}_{ij}^{e} + \dot{\varepsilon}_{ij}^{p} \tag{4.21}$$

The upper indexes e and p refer to the elastic and plastic strains respectively. The upper dot denotes the rate. The elastic strain rate for an isotropic body is assumed to be completely described within the framework of the generalized Hooke's law where two material parameters such as Young's modulus E which is a function of p, e and a Poisson's ratio, ν, which is a constant:

$$\dot{\varepsilon}_{ij}^{e} = \frac{1+\nu}{E}\dot{\sigma}_{ij} - \frac{\nu}{E}\delta_{ij}\dot{\sigma}_{kk} \tag{4.22}$$

where δ_{ij} denotes the identity tensor of order two, i.e., the Kronecker delta. The summation convention applies to the repeated suffices. The plastic part of the rate of deformation tensor is defined as:

$$\dot{\varepsilon}_{ij}^{P} = <\dot{\lambda}> \frac{\partial \psi}{\partial \sigma_{ij}} \tag{4.23}$$

where ψ is the so-called plastic potential and $\dot{\lambda}$ is an incremental quantity. It is sometimes called the loading index or the plastic loading function. The magnitude of the parameter $\dot{\lambda}$ depends on whether the sample is experiencing loading, unloading or a neutral loading. The symbol < > stands for the Macauley bracket, i.e., $<\dot{\lambda}> = \dot{\lambda}$ if $\dot{\lambda} \geq 0$ and $<\dot{\lambda}> = 0$ if $\dot{\lambda} < 0$. The value of $\dot{\lambda}$ can be obtained from the so-called consistency condition. The loading index, $\dot{\lambda}$, is expressed by the following equation:

$$\dot{\lambda} = h(\partial f / \partial \sigma_{mn})\dot{\sigma}_{mn} \tag{4.24}$$

where h is a strain-hardening parameter and f is the yield function. In its simplest form, the yield locus is a straight ray passing through the origin of the stress space. The yield function is given by the simple expression:

$$f = \eta = q / p \tag{4.25}$$

If the plastic potential is taken as a function of the stress tensor and is assumed to be smooth anywhere in the stress space, then the Equation 4.23 specifies a unique direction for the plastic strain increment in whatever direction the stress increment is

applied. This is indeed observed experimentally. This observation is the permit to use ψ in the constitutive equation that is expressed as

$$\psi = p\exp(\eta/\eta_c) \tag{4.26}$$

where $\eta_c = 2\sqrt{2}\sin\varphi_c/(3-\sin\varphi_c)$, φ_c being the angle of the friction associated with the critical state of the medium. The critical state is a state of (σ_{ij}, e) where continuous flow can take place without any change in the state of the medium.

The strain parameters compatible with stress parameters p and q are:

$$\dot{v} = (\dot{\varepsilon}_1 + 2\dot{\varepsilon}_3)/\sqrt{3} \tag{4.27}$$

$$\dot{\varepsilon} = \sqrt{2/3}(\dot{\varepsilon}_1 - \dot{\varepsilon}_3)$$

where $\dot{v}$ is related to the volumetric strain rate as is $\dot{\varepsilon}$ to the shear strain rate.

Note that the rate at which work is performed is $p\dot{v} + q\dot{\varepsilon} = \sigma_1\dot{\varepsilon}_1 + 2\sigma_3\dot{\varepsilon}_3$. The plastic volumetric train rate and the plastic distortion during virgin loading are expressed as:

$$\dot{v}^p = \dot{\lambda}[1-\eta/\eta_c]\exp(\eta/\eta_c)/M \tag{4.28}$$

$$\dot{\varepsilon}^p = \dot{\lambda}[1/\eta_c]\exp(\eta/\eta_c)/M$$

where $M = \left[(\psi_{,\sigma_1})^2 + (\psi_{,\sigma_3})^2\right]^{1/2}$. The factor M is used to normalize the gradients of ψ. The comma denotes the partial differentiation with respect to the suffix following. Having defined the plastic potential, it is required to determine the factor $\dot{\lambda}$ for loading increments. To this end, it is postulated that the magnitude of $\dot{\lambda}$ is in direct proportion to the yielding rate $\dot{f}$, which is equal to $\dot{\eta}$ from Equation 4.25, i.e.,

$$\dot{\lambda} = h\dot{\eta} \tag{4.29}$$

where h is a strain hardening parameter with a magnitude depending on the stress level. To evaluate the value of h it is necessary to establish, experimentally, the form of a plastic base curve relating the parameter ε^p to η. A simple conventional compression test is sufficient for this purpose. For loose sands, this curve can be approximated by the so-called hyperbolic relation which has the form $\varepsilon^p = a\eta/(\eta_f - \eta)$ where a is a constant to be determined experimentally and η_f will be defined later. From this equation, the plastic distortion rate is obtained as:

$$\dot{\varepsilon}_1^p = \left[a\eta_f/(\eta_f - \eta)^2\right]\dot{\eta}$$

But $\dot{\varepsilon}^p = \dot{\lambda}[1/\eta_c]\exp(\eta/\eta_c)/M = h\exp(\eta/\eta_c)\dot{\eta}/\eta_c M$. Equating these two values of $\dot{\varepsilon}^p$, the magnitude of h is evaluated as:

$$h = \frac{a\eta_c\eta_f M}{(\eta_f - \eta)^2}\exp(-\eta/\eta_c) \tag{4.30}$$

Note that as η tends toward η_f then h tends to infinity indicating the sample has reached its failure stage. Using these equations, the plastic strain components are calculated and added to the total elastic strains in order to obtain the strain path.

During the passage of waves, an element of soil in the seabed would be subjected to a number of stress reversals. Considering the stress reversal process, the plastic flow is described by evolution of the yield surface, which is created inside the boundary surface. Upon stress reversal, the yield surface is initially tangential to the boundary surface at the stress point. For subsequent loading, if the stress remains inside the yield surface, the

response of the material is elastic. Beyond this range, irreversible deformation takes place and the yield surface moves within the domain enclosed by the bounding surface.

To account the behavior of medium under such loading conditions, it is therefore necessary to modify the set of Equations 4.23, 4.26, 4.29 and 4.30 with the two additional concepts. The first is the concept of the bounding surface. To express this idea mathematically, let us introduce an interpolation function relating h to h_c where h_c is the value of h at the conjugate stress point which is on the bounding surface and a datum stress which is also located on the bounding surface. The datum stress point is "opposite" to the conjugate stress point and is the intersection of the line joining the conjugate stress point, a point on the axis of the bounding surface with the mean stress equal to that of the conjugate stress, and the yield surface on the opposite side.

A number of extrapolation functions are currently used. The one used in this study is expressed as

$$h = h_c\left(\delta/\delta_o\right)^n \tag{4.31}$$

where δ is the distance between the datum and the stress point and δ_o is the spatial distance between the conjugate stress and the datum stress. n is a positive constant and it is considered to be 7 in this study. Note that when the stress point is at the beginning of the stress reversal process, $\delta = 0$ and hence $h = 0$. When it approaches its conjugate $h \Rightarrow h_c$ the material behaves, once again, as a virgin soil. Let η_m be the highest level of η experienced during the loading process. Then the conjugate of the stress point with coordinates (q, p) located on the stress path is a point with coordinates $(-q', p)$ where;

$$q' = p\eta_m \frac{3-\sin\varphi_c}{3+\sin\varphi_c} \tag{4.32}$$

φ being the angle of friction of the soil. The inclusion of factor $(3-\sin\varphi_c)/(3+\sin\varphi_c)$ is to ensure that the conjugate of the stress point is contained within the envelope prescribed by the Mohr-Coulomb failure criterion. The datum stress point which is located on the η_m ray is with coordinates (q^*, p) where $q^* = \eta_m \cdot p$.

The second is the concept of reflected plastic potential which is the reflection of the virgin curve about the η constant line passing through the current stress path. The components of the unit vector normal to the reflected curve are obtained using simple coordinate transformations.

Realizing that h is a function depending on the state of the sample and considering the effect of the compact state in which there are not plastic strains at the compact state, the following condition must be met for the factor h;

$$e \to e_{comp},\ h \to 0 \tag{4.33}$$

where e is the void ratio of the soil and e_{comp} is the void ratio at the compact state.

In order to choose a suitable and simple form for the h, it is considered in the present model to be of the following form:

$$h = \frac{a(e-e_{comp})\eta_f}{(\eta_f-\eta)^2 M} \tag{4.34}$$

where a is a constant, η_f is the stress ratio at the state boundary surface and is defined as:

$$\eta_f = \eta_c + (\eta_{comp}-\eta_c)(e_c-e_o)/(e_c-e_{comp}) \tag{4.35}$$

η_{comp} is the stress ratio at the compact state and is written

$$\eta_{comp} = \frac{2\sqrt{2}\sin\varphi_{comp}}{3-\sin\varphi_{comp}} \tag{4.36}$$

where φ_{comp} is the angle of friction at the compact state, e is the initial void ratio and e_c is the critical void ratio which is given by

$$e_c = e_h - \lambda\log(p) \tag{4.37}$$

Obviously the value of M in the Equation 4.34 is evaluated at the conjugate stress. Here it should be noted that the role of $e-e_{comp}$ in Equation 4.34 is to satisfy the condition defined in Equation 4.33 and in addition follows the hyperbolic form of the deformation response.

4.5.3 Governing Equation of Poro-Elastoplastic Beds to Standing Waves

The load exerted on the seabed surface due to the action of standing waves would be a sinusoidal nature of fairly long periods of action and may be expressed as $P = P_a \cos Nx \sin \omega t$. Thus, it is rational to omit the dynamic terms from the equations of equilibrium. Considering the medium is to be isotropic and homogeneous and the flow to be governed by Darcy's law, the equation governing the flow can be written as;

$$\frac{k}{\gamma_w}\frac{\partial^2 U}{\partial z^2} = -\dot{\varepsilon}_{ii} \tag{4.38}$$

where k is the coefficient of permeability of the soil, γ_w is the unit weight of water, U is the pore water pressure and $\dot{\varepsilon}_{ii}$ is the volumetric strain rate.

The stress-strain relationship for the elasto-plastic skeleton is written as;

$$\dot{\varepsilon}_{ii} = h\left[\psi_{,\sigma_1} + 2\psi_{,\sigma_3}\right]\dot{\eta} + \frac{1-2\nu}{E}\left[\dot{\sigma}_1 + 2\dot{\sigma}_3\right] - \frac{3(1-2\nu)}{E}\dot{U} \tag{4.39}$$

The stress-strain characteristics of the seabed sand has to be incorporated in the equation of continuity. Substituting the above constitutive equation into Equation 4.38 leads to the following:

$$\frac{\partial U}{\partial t} = A\frac{\partial^2 U}{\partial z^2} + B \tag{4.40}$$

where $A = \frac{k}{\gamma_w}\left[\frac{E}{3(1-2\nu)} + \frac{\sigma_3}{(1-\eta)h}\cdot\frac{1}{(\psi_{,\sigma_1} + 2\psi_{,\sigma_3})}\right]$,

and $B = \frac{h(\psi_{,\sigma_1} + 2\psi_{,\sigma_3})(\dot{\sigma}_1 - \eta\dot{\sigma}_3)/\sigma_3 + (1-2\nu)(\dot{\sigma}_1 + 2\dot{\sigma}_3)/E}{h(1-\eta)[(\psi_{,\sigma_1} + 2\psi_{,\sigma_3})/\sigma_3] + 3(1-2\nu)/E}$

An elasto-plastic body must obey the equilibrium equation,

$$\dot{\sigma}_{ij},_j = 0$$

For this problem, the above equation may be written in the form:

$$\begin{aligned}\sigma_1 &= \gamma' z + \frac{2\gamma_w H}{\pi}\left(\int_o^{\frac{\pi}{2}} \cos\left[\frac{\pi z}{2L}\tan\alpha\right]\cos^2\alpha d\alpha\right)\sin\omega t - U \\ \sigma_3 &= k_o\gamma' z + \frac{2\gamma_w H}{\pi}\left(\int_o^{\frac{\pi}{2}} \cos\left[\frac{\pi z}{2L}\tan\alpha\right]\sin^2\alpha d\alpha\right)\sin\omega t - U\end{aligned} \tag{4.41}$$

where γ' is the effective unit weight, k_o is the coefficient of earth pressure at rest and has been chosen equal to $1-\sin\varphi_c$.

Since the process is assumed to be constant volume then $\dot{\gamma} = 0$. After differentiating Equation 4.41 with respect to time, the above relations take the form

$$\begin{aligned}\dot{\sigma}_1 &= \frac{2\gamma_w H\omega}{\pi}\left(\int_o^{\frac{\pi}{2}} \cos\left[\frac{\pi z}{2L}\tan\alpha\right]\cos^2\alpha d\alpha\right)\cos\omega t - \dot{U} \\ \dot{\sigma}_3 &= \frac{2\gamma_w H\omega}{\pi}\left(\int_o^{\frac{\pi}{2}} \cos\left[\frac{\pi z}{2L}\tan\alpha\right]\sin^2\alpha d\alpha\right)\cos\omega t - \dot{U}\end{aligned} \tag{4.42}$$

The Equation 4.40 is the governing equation for the response of a shallow depth seabed sand stratum subjected to the action of standing surface waves. Boundary and initial conditions have to be taken into account for solving the governing equation. The initial condition can be given as;

$U(z,0) = \gamma_w(d+z), \sigma_1 = \gamma' z,\ \sigma_{33} = k_o\sigma_1$

The boundary conditions to be satisfied by a solution to the governing equation are written

Upper B.C. @ z=0 $\quad U = \gamma_w d + \frac{\gamma_w H}{2}\sin\omega t$

Lower B.C. @ z=z $\quad \partial U/\partial z = 0$

The governing equation together with the initial and boundary conditions may be solved using the finite-difference (FD) method. Finite difference method is one of numerical techniques, which is a common procedure employed in geotechnical engineering. Thus, the governing equation will be discretized spatially with the forward finite difference method. An accurate and stable solution can always be expected if the time steps are made sufficiently small. Therefore in this approach a time interval of 0.02 sec is applied to ensure that the stability condition of $0 < \Delta t/(\Delta z)^2 < 1/2$ is met. This method provides a small truncation error throughout the solution domain.

4.6 FD SIMULATED RESULTS AND DISCUSSION

In this section typical plane strain finite difference model simulations of a seabed deposit subjected to the action of standing waves are presented. In a parametric study, a homogeneous, isotropic soil is assumed. The thickness of seabed is set to 10 m and the

water dept at 10 m. The base is considered rough, rigid and impermeable. Drainage is only allowed from the seabed surface. The assumed parameters of the wave are T = 10 sec, L = 10 or 20 m and H = 2, 4 and 5 m. Material parameters for the proposed constitutive model are:

$$\nu = 0.2,\ \gamma_w = 9.8kN/m^3,\ k = 10^{-4} - 10^{-1} cm/\sec,\ G_s = 2.70,$$
$$a = 0.05,\ \varphi_c = 30^o,\ \varphi_{comp} = 45^o, \lambda = 0.3,\ e_h = 1.4$$

Different void ratios are employed varying in the range of 0.6-0.9. The value of $c = e_c - e_{comp} = 0.4$ is chosen.

It may be noted that, in contrast to some metal elasticity, the elastic moduli are not constants for soils. In most cases they are pressure sensitive and in this study the variation of the Young's modulus is assumed to be E= 10p. The simple dependence of the E to the mean effective stress satisfactory accounts for more realistic behavior of sand.

To illustrate the basic feature of the proposed model, several computer tests on saturated sandy soils with a wide variety of void ratios have been performed under wave loading. Note that all "tests" start from the hydrostatic axis, i.e., q =0. In this study, although the wave length is assumed to be 10 m or 20 m, a relatively wide range of the void ratio is used to investigate the effect of loose to dense sands subjected to the action of standing waves.

The result of a typical dense sand with a void ratio of 0.6 is depicted in Figure 4.4. For this test, the amplitude of wave loading is equal to 2m and the wave length is 10m. Wave characteristic is represented in the upper left part of this figure. Figure 4.4a is a plot of the effective stress path at three different depths at 1m, 6m and 10m. Also in this figure the trace of state boundary surface at the critical state and at the compact state as well as

those of k_o line and hydrostatic line are shown. The evolution of the deviator stress with respect to the axial strain for the corresponding depths is illustrated in Figure 4.4b. Figure 4.4c shows the change in mean effective stress against the void ratio of elements at various depths in the seabed.

It is observed that the element at 1m behaves more like an elastic continuum. The behavior can be explained in considering that it characterizes the passage from the elasto-plastic behavior to the elastic one. The behavior may be observed on the stress path as well on the *e-p* state path.

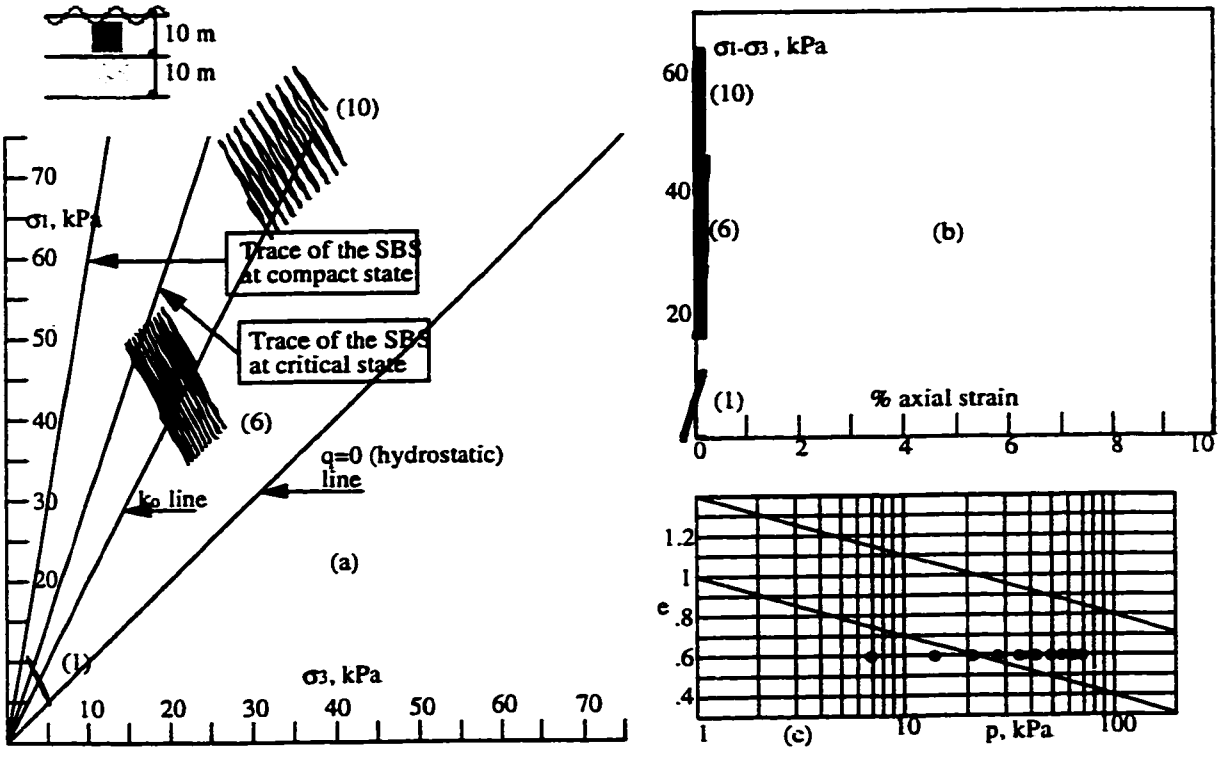

Figure 4.4 The response of a dense sand bed
(a) the effective stress path at different depths, (b) the corresponding stress-strain curves, (c) the *e*-log *p* graph and the position of the elements during cyclic loading.

This observation is the result of the second hypothesis of the compact state concerning the elastic behavior at this state. As shown in Figure 4.4b after about 10

cycles of loading the axial strain did not exceed 0.5%, even for the elements at 6m and 10m. The axial strains are very small: they fall within the axial strain range of –0.5% and +0.5%.

The wave conditions used in the first example are for a wave length of 10m and a wave amplitude of 2m. In the second example the wave length was increased to 20m without changing other parameters. The effect of the wave length on the response of dense sand bed can be viewed in Figure 4.5 for the same sand bed. Comparing Figure 4.4 with Figure 4.5, it is found that there is no significant effect by increasing the wave length to 20m.

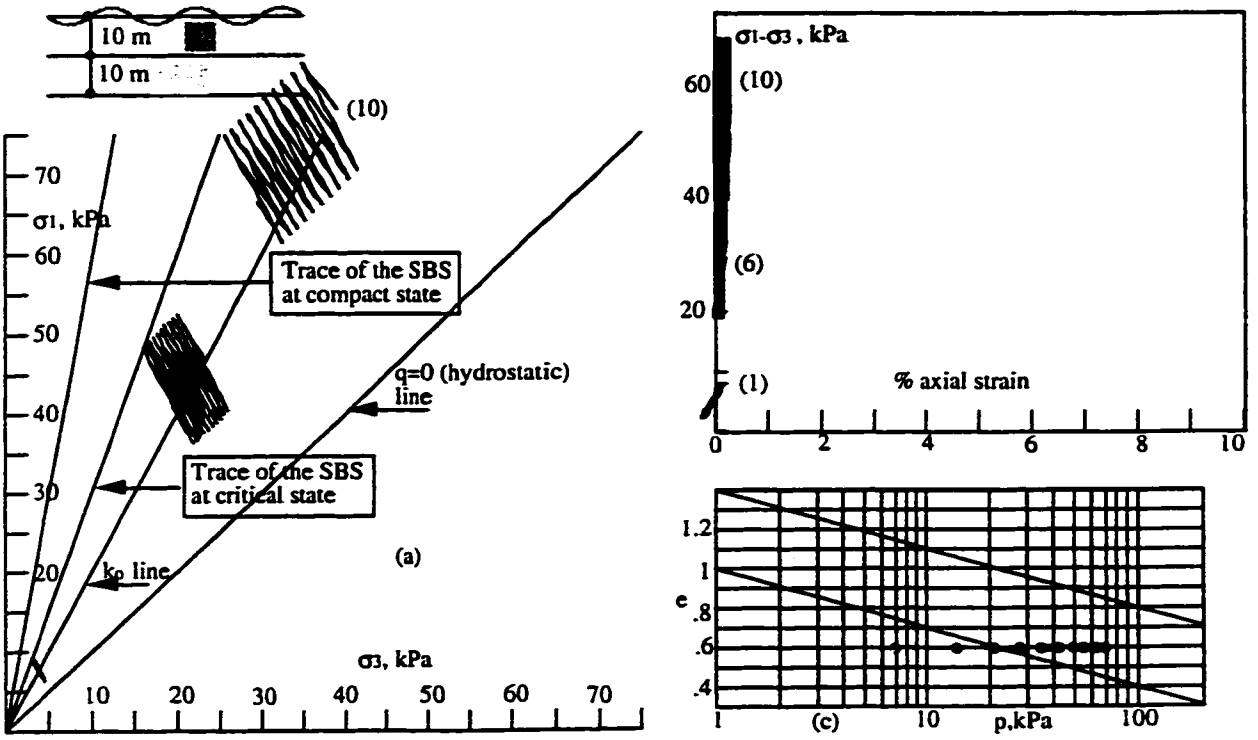

Figure 4.5 The response of a dense sand deposit for the L=20m
(a) effective stress paths, (b) stress-strain curves, (c) the *e*-log *p* graph.

The next computer test was performed for a loose sand with a void ratio of 0.8. Figure 4.6 shows the response of loose sand utilizing the same wave conditions of the first

example. The element at 10m approaches the state of instability, which is associated with large strains.

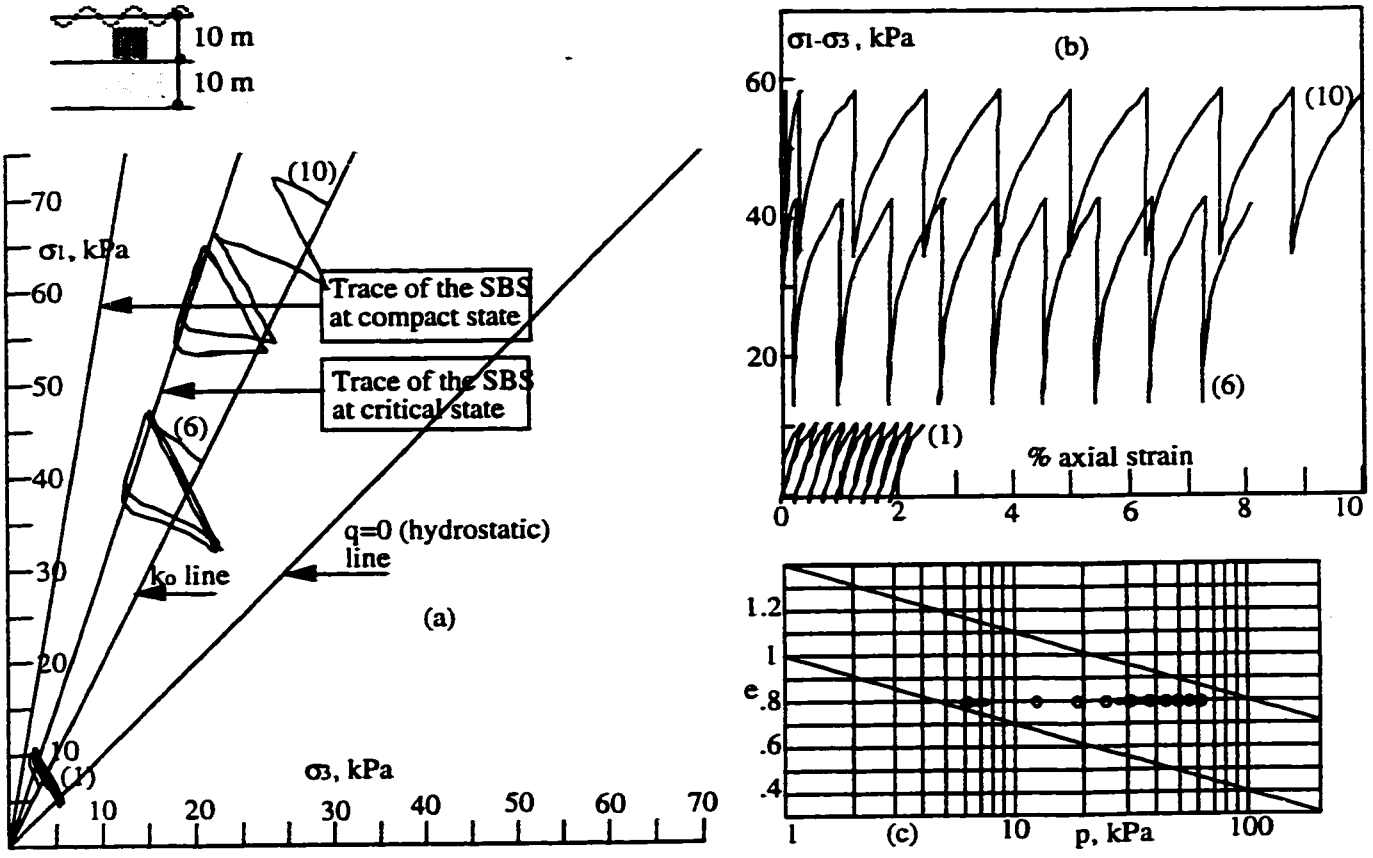

Figure 4.6 Behavior of a loose sand on the wave-induced response (L=10m)
(a) effective stress paths, (b) stress- strain curves, (c) the *e*-log *p* graph

For the next test, the wave and soil conditions employed in the third example were kept the same, except for a new wave length of L=20m. As shown in Figure 4.7, again it can be observed that the wave length does not affect the response of loose sand significantly except for the sample at 1m.

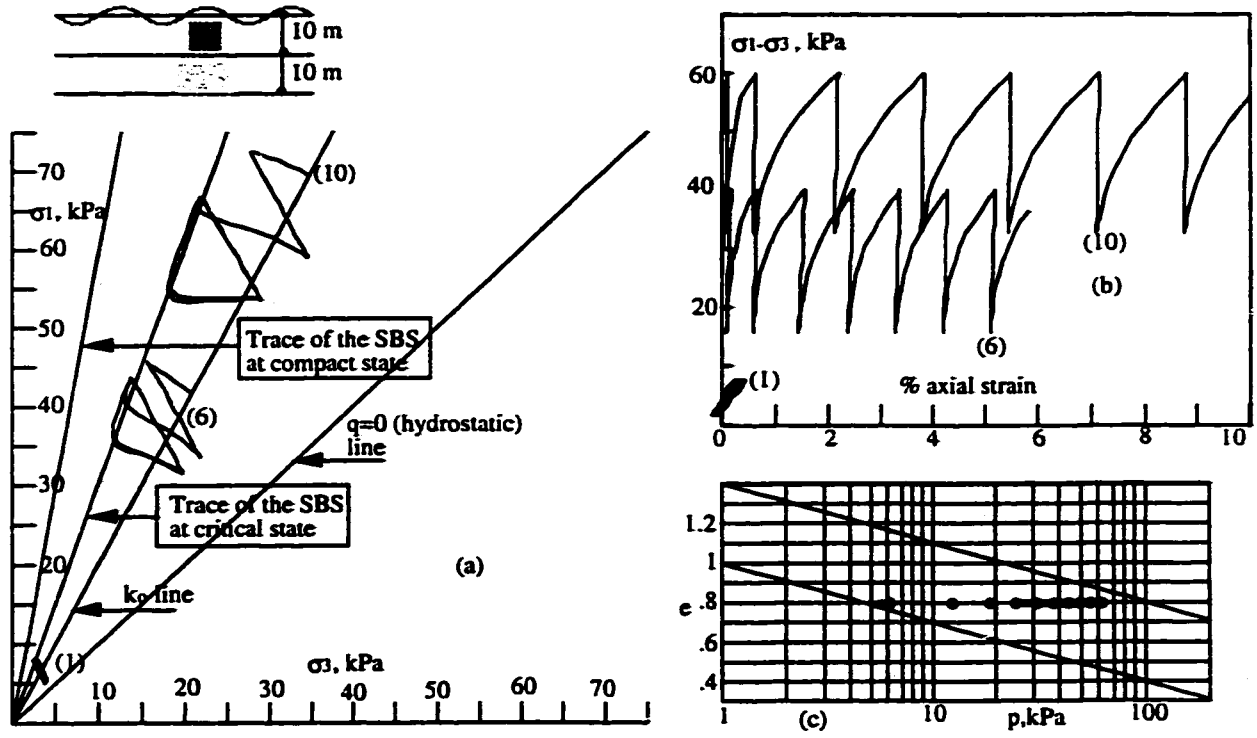

Figure 4.7 Behavior of a loose sand on the wave induced response (L=20m)
(a) effective stress paths, (b) stress- strain curves, (c) the *e*-log *p* graph

In order to investigate the effect of the wave amplitude on the response of loose sand, two more tests were performed with wave amplitude of 4m and 5m. Using the same wave and soil conditions shown in Figure 4.5, the effect of the wave amplitude is considered with the elasto-plastic model. The stress paths for elements at various depths, 1m, 6m and 10m, and the corresponding stress-strain behavior for the same elements are plotted in Figure 4.8 and 4.9. It is interesting to note that the seabed experiences large distortions more quickly in the second (with the wave amplitude of 5m) than in the first case (with a wave amplitude of 4m), due to higher value of the wave amplitude. This has a distinctive difference on the behavior of loose sand when compared with the results of previous example. It can be concluded that the passage of large amplitude waves on the

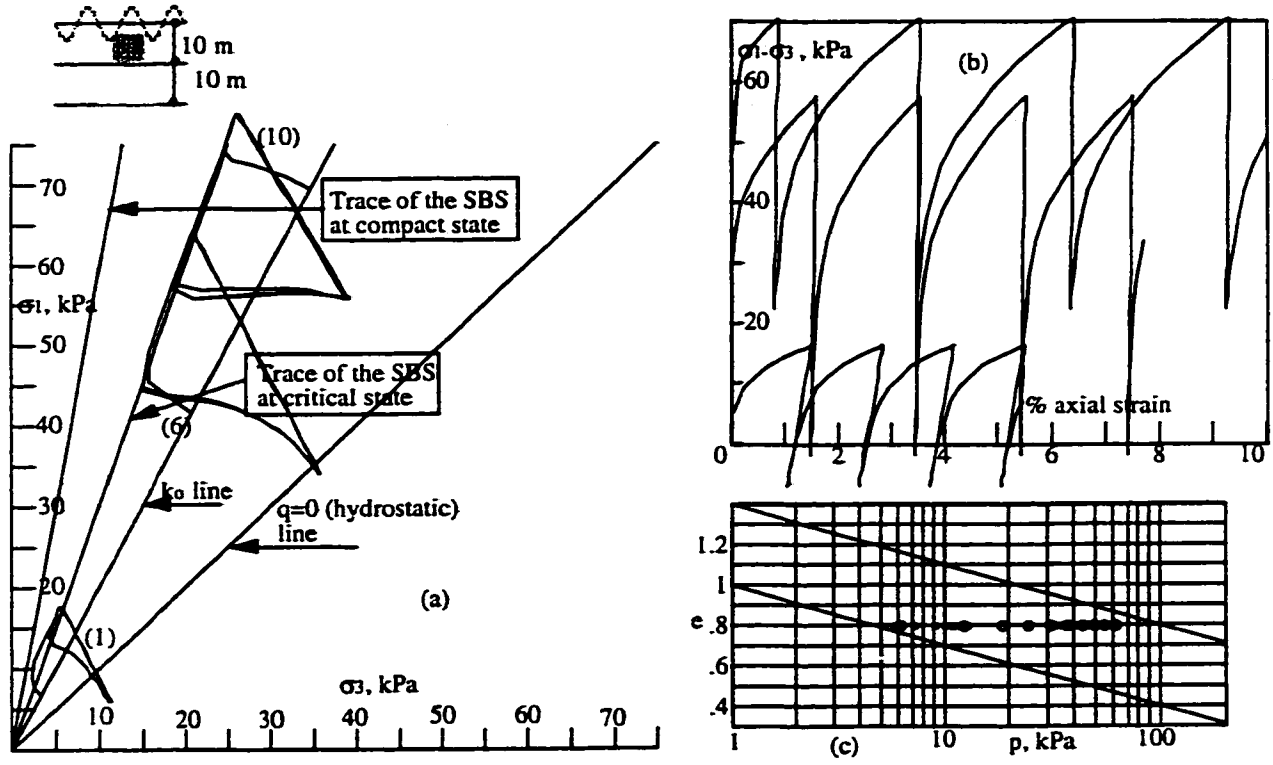

Figure 4.8 Response of a loose sand with wave length of 10m and wave amplitude of 4m (a) effective stress paths, (b) stress-strain curves, (c) the *e*-log *p* graph

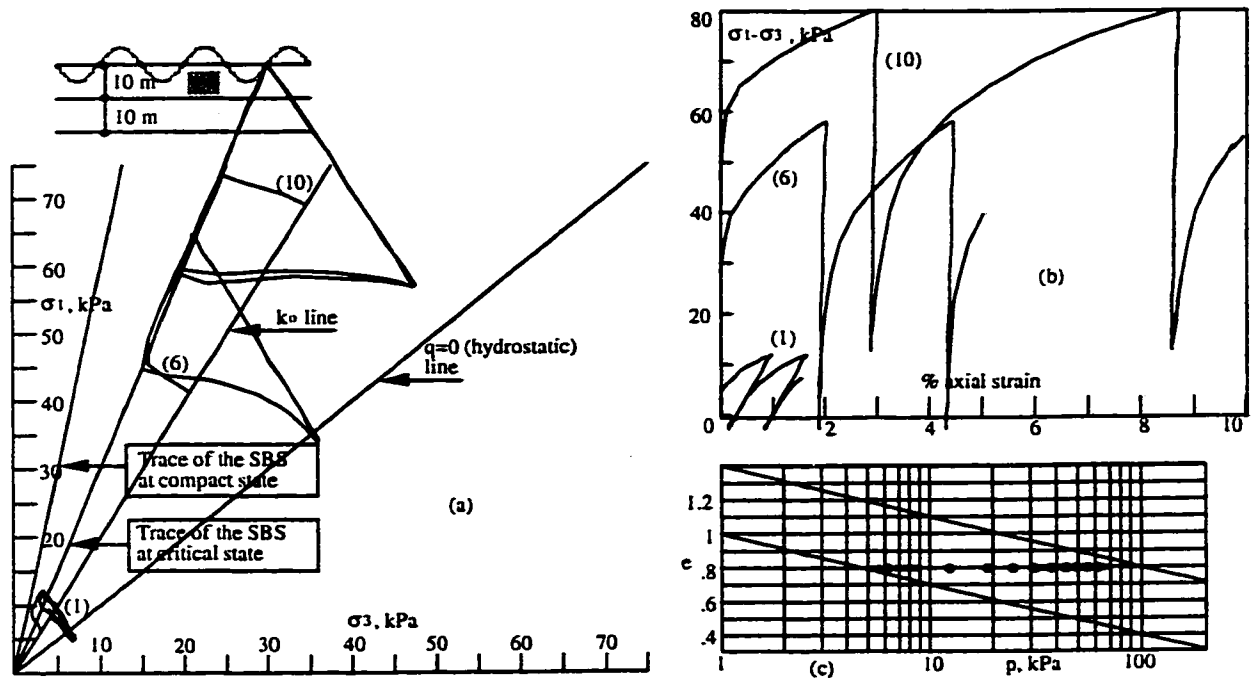

Figure 4.9 Response of a loose sand with wave length of 20m and wave amplitude of 5m (a) effective stress paths, (b) stress-strain curves, (c) the *e*-log *p* graph

surface of the sea may also produce relatively large displacements of soil on the sea bottom. It should be noted here that although the wave length in the second case is increased to 20m, the wave amplitude has the dominant effect on the seabed response.

Another test was performed for the same wave and soil conditions employed in producing Figure 4.6, except now for a very loose sand with a void ratio of 0.9 in order to evaluate the seabed response to the various void ratio. The result is illustrated in Figure 4.10. After one cycle of loading, the soil tends to be unstable and experiences large distortions. The test was repeated for the very loose sand with the same values of wave and soil parameters except the wave length, which is again set equal to 20m. The result is shown in Figure 4.11.

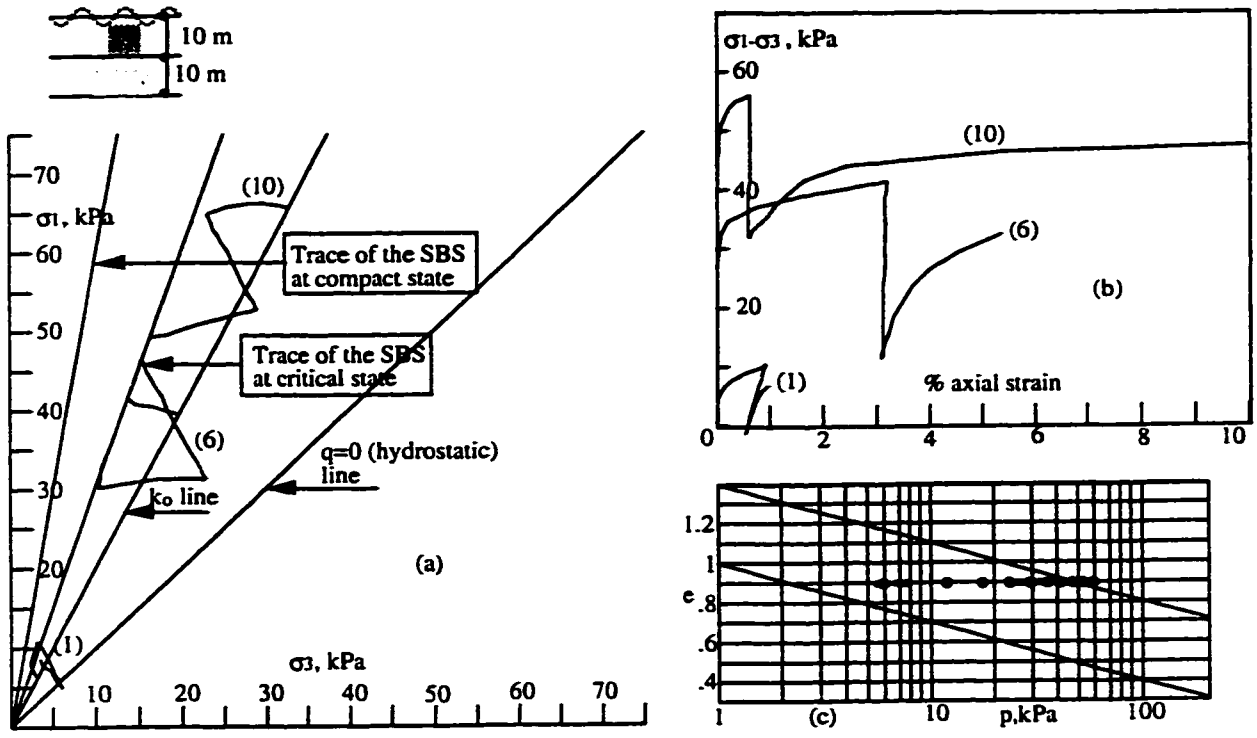

Figure 4.10 Behavior of a sand in very loose state (e=0.9) with L=10m
(a) effective stress paths, (b) stress-strain curves, (c) the e-log p graph

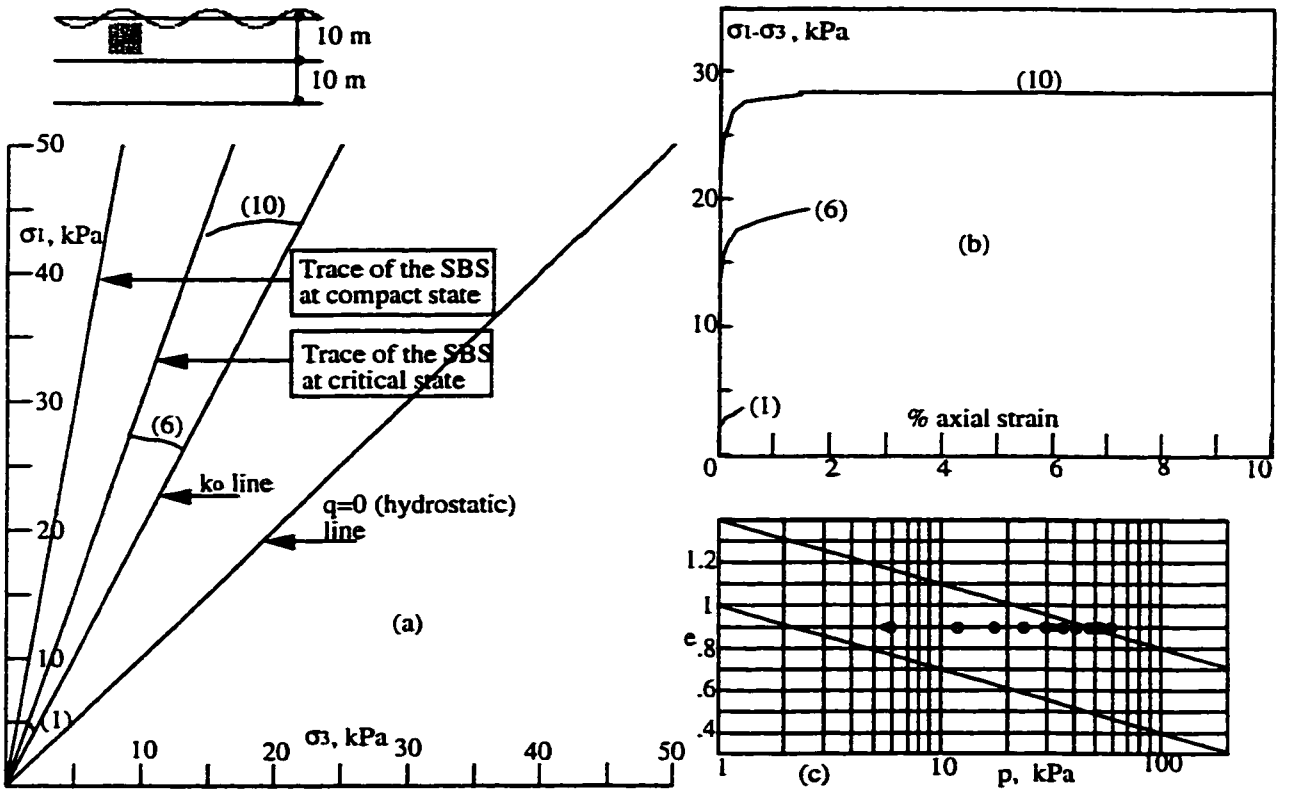

Figure 4.11 Behavior of a sand in very loose state (e=0.9) with L=20m
(a) effective stress paths, (b) stress-strain curves, (c) the e-log p graph

Upon comparing Figure 4.10 with Figure 4.11, it is found that the wave length does affect the response significantly and the soil experiences a total failure at about one half cycle of wave loading. The importance of the wave length in affecting the soil behavior can thus become apparent.

The analytical procedure presented in this study provides a means for evaluating stability of sea deposits against wave-induced instability. There is no doubt that the proposed model possesses several drawbacks and limitations. For example, it does not take into account the kinematic constraints. However, the main advantage of the model seems to be its simplicity that can conveniently handle different conditions, which may be observed in practice. It also overcomes the deficiencies of Ishihara's method in

considering elasto-plastic behavior of soil and initial in-situ stresses. It is also found from the examples given in this study that loose sands have been shown to respond differently from dense sands to the same wave input. For the two different sands the nature of the solution clearly exhibits the expected feature that effects of void ratio are more pronounced for the very loose sand. The solutions are the free field solutions, since inclusion of structures in the analysis would make the problem much more complicated. A free field solution can provide a valuable information for geotechnical considerations in the offshore structure design. Hence, engineering judgment should be exercised in assessing the seafloor response and its effects on the structural response.

5

NONLINEAR DYNAMIC ANALYSIS OF A UNIFORM SAND LAYER

5.1 INTRODUCTION

The behavior of cohesionless granular media under dynamic loading is one of the most important problems facing geotechnical engineers. The effect of earthquake shaking for soils is primarily the development of volume changes that lead to settlements. These occur as a result of the pore pressure build up at some depth. If the upward gradient is large enough, the following water will buoy up the soil particles. It is more likely, however, that the flow will break through to the surface in places where the topmost stratum is especially thin or where there are cracks or other weaknesses in the superficial soil. The water, which may flow violently, usually brings considerable sand particles with the water creating a pile of sand around the vent, referred to as a sand volcano.

Earthquake-induced settlement could develop as a result of water migration to a zone of soil, which becomes looser than prior to earthquake and then causes, the failure. Migration of water could occur through short distances as a film of water just underneath the impermeable top layer so that only thin layers could loosen.

This chapter is written in the following sequential sections. The first section of the present study summarizes the past work on the sand blow phenomenon. Then, a brief description of the ID (Integro-Differential) technique that is used to analyze the problem is presented. It is followed by derivation of the governing equation of the problem. Finally, the simulation results of the proposed model are illustrated. In this section the distortion of the shape of the soil layer as a function of time and the stress-strain behavior of soil at

different depth are demonstrated. Numerical simulations have been carried out to identify the typical trends in the response of cohesionless soil in a broad range of void ratio subjected to dynamic loading.

5.2 REVIEW OF PAST WORK

The high incidence of liquefaction during earthquakes, together with its potential for damage, has made the phenomenon a prime subject of concern in earthquake engineering. Due to its complexity, the mechanism of the liquefaction phenomenon is not yet completely understood and a large amount of research is still being done.

In the last few years, two aspects of the liquefaction problem have generated a great deal of discussion and motivated significant research. The first aspect relates to the conditions necessary to produce unlimited flow of the liquefied soil in the field under the action of gravity loads such as those occurring in a slope or beneath a structure. The second aspect of the problem relates to the developments of sand blows (also referred to as sand volcanoes) due to eruption of water through cracks, holes, etc. which carries with it fine sand particles. Water flow existing locally at the ground surface transports considerable suspended sediments that settle and form a conical sand deposit. In extreme cases, water has been observed to spout out to heights of 1.2-1.5m above ground, and the sand volcanoes can be as large as few meters in diameter.

Sand blows are a well-known phenomenon in geotechnical engineering. However, only a few attempts have been made to extract information from sand blows left behind by liquefaction. The first plausible basic mechanism underlying the development of sand spouts is that presented by Housner (1958). He suggested that an earthquake liquefies the underlying soils, which thereafter consolidate as does a compressible soil under an applied load. Analyzing the resulting process by Terzaghi's consolidation theory, Housner (1958) calculated the quantity and flow rate of water that would emerge at the ground surface.

He also demonstrated that the large gradients needed to cause sand blows when a deep layer of soil develops high pore pressure in a uniform soil deposit. This theory was followed and elaborated on by Florin and Ivanov (1961). They developed a model that predicts the upward movement of the lower boundary of the soil with zero effective stress, which they referred to as the "compaction front".

Based on laboratory experiments, Scott and Zuckerman (1973) showed how the excess water produced by liquefaction makes its way to the surface by an unstable process of cavity formation and then of channel formation in the upper layers. Lenses of water may develop near the bottom of an overlying cohesive layer. If the cavity approaches the ground surface, the pressured, soil-laden water in the cavity may break through almost explosively to form a waterspout or sand volcano, bringing sand with it from the liquefied zone. Scott and Zuckerman (1973) also showed that the presence of a finer-grained layer of soils overlying the liquefiable zone is necessary for the formation of sand blows.

In the same line of thought, Muir and Scott (1981) analyzed the patterns of the sand blows during the 1971 San Fernando, California earthquake and 1979 Imperial Valley, California earthquake. They observed that the greater the thickness of the layer overlying the liquefied soils, the fewer and larger the blows because the break through of the first vents inhibits the concurrent development of cavities. In a thick layer, fewer cavities reach the surface. Venting of the liquefied soil may be influenced by the presence of animal holes, burrows, or man-made openings such as trenches, ditches and water wells. The path of the surface is generally not vertical, but complicated, depending on the nonuniformity or anisotropy of the soil.

In order to establish a framework within which one can understand the soil response during earthquakes, Castro (1987) proposed a classification of the types of soil behavior on the presence of "driving" shear stresses in the soil from static loading existing prior to the earthquake. The term "driving" refers to those shear stresses that are required for static equilibrium. He concluded that sand blows occur under zero driving shear stress

and are more likely to be observed in soils with low blow counts, i.e., looser soils in which higher pore pressures would develop for a given earthquake and also would compress more and thus release more water during densification.

It should be noted that sand blows and associated sand volcanoes are also observed at the bottom of excavations in sandy soils below the groundwater level, downstream of dams and other water retaining structures. Piping of the sand under large upward exit gradients creates the sand blows. The physical mechanism of the formation of sand volcanoes in these cases is similar to the one that occurs during and after earthquakes, except that the source of the hydraulic gradients is different.

5.3 INTEGRO-DIFFERENTIAL (ID) TECHNIQUE

An important class of problems in the field of geotechnical engineering may be analyzed with the aid of a simple integro-differential (ID) equation by Poorooshasb et al. (1996 a, b and c). The ID technique is a simple analytical tool that can be utilized in the evaluating and solving a certain type of situation encountered in geomechanics. It is called the ID technique because it involves the evaluation of an integro-differential equation depending on the type of problem.

The technique is recently developed for the first time in solving some geotechnical problems and applied to the examination of the performance of a system of vertical piles. The other applications of this method have been made to axisymmetric problems, e.g. analysis of piled-raft foundation (Poorooshasb et al., 1995), design of inclined piles (Poorooshasb et al., 1998), and also plane strain problems (e.g. Poorooshasb et al., 1997).

The calibration of the ID technique was carried out against some other numerical techniques, e.g. CRISP Program (Britto and Gunn, 1987). The agreement between the results from the ID technique and those obtained from CRISP Program, which uses finite element method is considered satisfactory.

The ID technique is simple to understand and straight forward to apply. The requirements of computational facilities in applying the ID technique are minimal in comparison to other numerical methods. The general validity and the effectiveness of the ID technique, applicable to different geotechnical problems have been established.

5.4 MATHEMATICAL FORMULATION OF THE PROBLEM

Sand blows have occurred in many locations during earthquakes. Different mechanisms have been suggested to account for the behavior of sand spouts. Several different theories have been advanced on the analysis of sand blows, however, there are few studies in modeling this phenomenon in order to mitigate the severe damage caused to structures. It appeared, therefore, that a necessary to develop a model of the soil behavior during earthquakes loading.

Let u be the displacement of a typical point and τ the shearing stress. From the dynamic incremental equation of equilibrium, the following equation is shown to be hold,

$$\frac{\partial \tau}{\partial z} = \frac{\gamma}{g} \frac{\partial^2 u}{\partial t^2} \tag{5.1}$$

where γ is the unit weight of the soil and g is the gravity. z and t are the space and time variable. Differentiating both sides of Equation 5.1 with respect to time results in

$$\frac{\partial \dot{\tau}}{\partial z} = \frac{\gamma}{g} \frac{\partial^2 \dot{u}}{\partial t^2} \tag{5.2}$$

Noting that $\dot{\gamma}$ is too small and for small strain theory it can be neglected. Now integrating the right hand side of Equation (5.2) with regard to z yields;

$$\dot{\tau} = \frac{\gamma}{g}\int_o^z \frac{\partial^2 \dot{u}(\xi,t)}{\partial t^2} d\xi \tag{5.3}$$

where ξ is a dummy space variable. The relation between the shear stress rate and strain component can be expressible in the form

$$\dot{\tau} = G_{ep}\ \dot{\varepsilon} = G_{ep}\ \frac{\partial \dot{u}}{\partial z} \tag{5.4}$$

where G_{ep} is the elastic-plastic shear modulus. G_{ep} is not to be treated as a constant: it is a variable, which may be a function of space parameter z. In general it can also be a function of time and the stress level. This type of non-linearity will not, however, be dealt with here.

Upon substituting Equation 5.4 into Equation 5.3 yield the required relation viz.,

$$\frac{\partial \dot{u}}{\partial z} = \alpha(z)\int_o^z \frac{\partial^2 \dot{u}(\xi,t)}{\partial t^2} d\xi \tag{5.5}$$

where $\alpha(z) = \gamma / g G_{ep}(z)$. The developed formulation is intended to serve as the basis of numerical procedure proposed in the next section for the analysis of sand blows. Note that the governing equation (Equation 5.5) must be solved with the appropriate initial boundary conditions, which are explained later.

The governing equations developed here along with the boundary conditions are not sufficient to solve the problem in soil dynamics. Thus constitutive equations are necessary to make the problem well posed. Constitutive equations have significant impact on the solution of any boundary value problem in soil mechanics and must present a realistic modeling of the soil behavior.

Constitutive models based on plasticity formulation have contributed significantly to the development of analytical procedures. However, several important aspects of dynamic soil behavior are not yet incorporated into these models, including sand blows. There is a need to investigate the effect of sand blows on the response of system subjected

to ground motion. The CANAsand model, which is based on the boundary surface plasticity incorporating a non-associated flow rule, has been shown in recent studies to be capable of modeling the response characteristics of sandy soils subjected to monotonic and cyclic loading (Poorooshasb, 1994). The model proves applicable for both loose and dense sands. In the present work, the CANAsand constitutive model developed in chapter 3 is used to represent the stress-strain behavior of granular cohesionless media under dynamic loading.

5.5 THE NUMERICAL SCHEME

Equation 5.5 may be written in its finite difference form as

$$\frac{\dot{u}(i+1,j)-\dot{u}(i,j)}{\Delta z}=\alpha(z)\sum\frac{\dot{u}(i,j-1)-2\dot{u}(i,j)+\dot{u}(i,j+1)}{(\Delta t)^2}\Delta\xi \tag{5.6}$$

The numerical scheme employed to evaluate the governing equation is simple and will be demonstrated briefly here. In this scheme the solution domain is covered by a finite difference mesh, which is shown in Fig. 5.1.

Referring to Fig. 5.1, it is assumed that the mesh has j_{max} columns, spaced regularly at Δt intervals, and i_{max} rows, spaced regularly at Δz intervals. Let Δz be kept constant thus $\Delta\xi=\Delta z$. It is the object of the analysis to evaluate the magnitude of $\dot{u}$ at each and every point of the mesh. This is done by first deriving the coefficients of a set of linear simultaneous equations for $\dot{u}(1),\dot{u}(2),...\dot{u}(n_{max})$, where n_{max} = $(i_{max}$ -1) * j_{max} +j_{max} =i_{max}* j_{max} is the total unknown to be determined.

Consider the situation at node *(i, j)* with a node identification n= $(i$-1$)\,j_{max}$+ j. The objective is to find the values of constants *a (n, 1), a (n, 2)...a (n, n)...a (n,* n_{max}+ *1)* so that one of the equations of the set corresponding to the node n may be found as;

$$a(n,1)\dot{u}(1)+a(n,2)\dot{u}(2)+...\alpha(n,n)\dot{u}(n)+a(n,n+1)\dot{u}(n+1)+...=a(n,n_{max}+1) \tag{5.7}$$

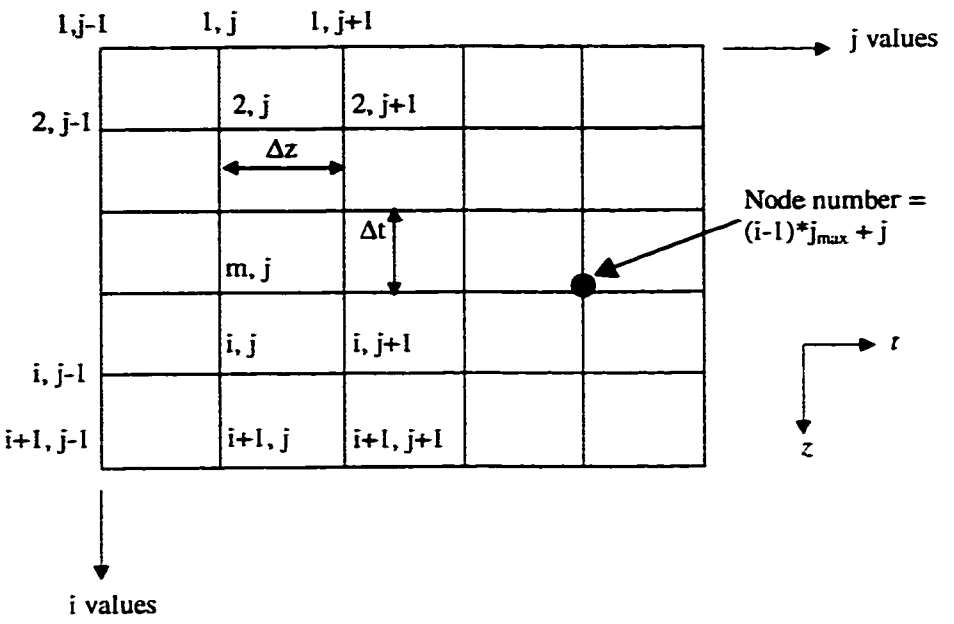

Figure 5.1 Finite Difference (FD) mesh

With the aid of the last results and recalling Equation 5.6 one can write

$$\dot{u}(i+1, j) - \dot{u}(i, j) = \sum_{m=1}^{j} \alpha(m, j)\left[\dot{u}(m, j-1) - 2\dot{u}(m, j) + \dot{u}(m, j+1)\right] \qquad (5.8)$$

where $\alpha(m, j) = \alpha(z)\dfrac{(m-1)(\Delta Z)^2}{(\Delta t)^2} = \dfrac{\gamma(m-1)(\Delta Z)^2}{gG_{ep}(z)(\Delta t)^2}$ and the nodal number assigned to the point *(m, j)* is $s = (m\text{-}1)j_{max} + j$. The node directly below the *(m, j)* will have a nodal number of $r = m\, j_{max} + j$. It remains to express Equation 5.8 in a form suitable for coding. That is, to reduce it to a number of simultaneous algebraic equations. Thus Equation 5.8 can be rewritten as;

$$\dot{u}(r) - \dot{u}(n) = \sum_{s=1}^{n} \alpha(s)\left[\dot{u}(s-1) - 2\dot{u}(s) + \dot{u}(s+1)\right] \qquad (5.9)$$

The scheme is fully explicit. In the present study it is considered as *T*/32 in order to get an accurate picture of the situation, where *T* is the period.

Equation 5.9 must be solved subject to the following initial and boundary condition

$@\, t = o \quad \dot{u} = o, \sigma = \gamma z$

$@\, z = o \quad \dot{u} = o$ (*the surface is assumed free of shearing stress*)

$@\, z = z \quad \dot{u} = a_0 \omega \cos \omega t$

where a_o is the amplitude of the wave of periodic sine function and ω is the angular wave frequency (radians/sec).

5.6 SIMULATION OF EARTHQUAKE INDUCED SETTLEMENT

Due to the lack of experimental data necessary for a calibration of the constitutive equations, the model parameters can be considered as follows. The elasto-plastic shear modulus G_{ep} characterizes the elastic-plastic response of the material and is assumed to be a function of the current state of effective stress and some index parameters identifying the current state of the sand such as void ratio. In the present model, the relationship is chosen to characterize the variation of this moduli, namely

$$G_{ep} = 1 / \left[\frac{1}{G_e} + \frac{a\eta_f}{(\eta_f - \eta)^2} \right] \tag{5.10}$$

where $\eta = \tau / \sigma$ and G_e is the elastic shear modulus. The variation of G_e with σ and void ratio can be estimated by the following equation.

$$G_e = 20\sigma \left(1 - \frac{e - e_{comp}}{e_o - e_{comp}} \right) \tag{5.11}$$

where e is the void ratio and e_{comp} is the void ratio at compact state. e_o is defined as the limit of the state boundary surface and is given by

$$e_o = e_{comp} - \frac{c\eta_{comp}}{\eta_c - \eta_{comp}} \tag{5.12}$$

where η_c and η_{comp} are related to the φ_c and φ_{comp} which are respectively assumed to be 30° and 45°. c is the vertical distance between e_c and e_{comp} in *e-log p* graph and in this study may be chosen as 0.4. The value of η_f is expressed as

$$\eta_f = \eta_c + \frac{e_c - e}{c}(\eta_{comp} - \eta_c) \tag{5.13}$$

where e_c is the void ratio at critical state and is written as $e_c = e_h - \lambda \log\sigma$. The value of e_h and λ are considered 0.95 and 0.1 (in log base 10) respectively.

There are two parameters in the model formulation which describe the hardening law for plastic moduli, a, n. These parameters should be found by trial and error procedure in order to achieve the best results of drained tests. Based on the second hypothesis of compact state ensuring non plastic behavior at compact state the value of a is determined.

$$a = 0.1(e - e_{comp}) \tag{5.14}$$

The plastic hardening exponent, n is considered to be of the following form:

$$n = 12 - \frac{4(e - e_{comp})}{c} \tag{5.15}$$

In the present research, the numerical simulations are restricted to dry sand or saturated sand deposits with very high coefficient of permeability. The simulations correspond to the dynamic response of the sand layer with a thickness of 10m under a sinusoidal loading of the natural frequency of 2 cycles/sec. and the amplitude of 0.02. Duration of strong motion is considered 8 seconds (16 cycles) with a maximum acceleration of 33% applied at the base in plane strain loading condition.

5.7 RESULTS OF NUMERICAL SIMULATIONS

Earthquake vibrations may induce settlements in non-cohesive soils. The amount of these settlements can be estimated using the proposed model. In order to evaluate the performance of the model the sandy soil is considered with a wide range of void ratio varying 0.46 - 0.9 from very loose to very dense sand. The first simulation is related to a very dense sand with a void ratio of 0.46. Figure 5.2 shows the evolution of settlement during the strong earthquake. The stress-strain behavior of the soil at depths 3 m and 8 m are illustrated in Figure 5.2a and b. The variation of the void ratio against depth is given

in Figure 5.2c. The solid circles indicate the initial void ratio and the open circles designate the conditions after cyclic loading. Also shown the critical state line and compact state line in this figure. The soil displacement pattern is plotted in Figure 5.2d. This figure shows the distorted shape of the sand layer at various times.

It can be seen that after 16 cycles, the soil had a settlement of 5.8 cm. It is important to note that because the void ratio of the soil was close to the void ratio at the compact state, therefore the soil behavior is elastic as shown in Figure 5.2a and b. This is consistent with the second hypothesis reported in Chapter 3.

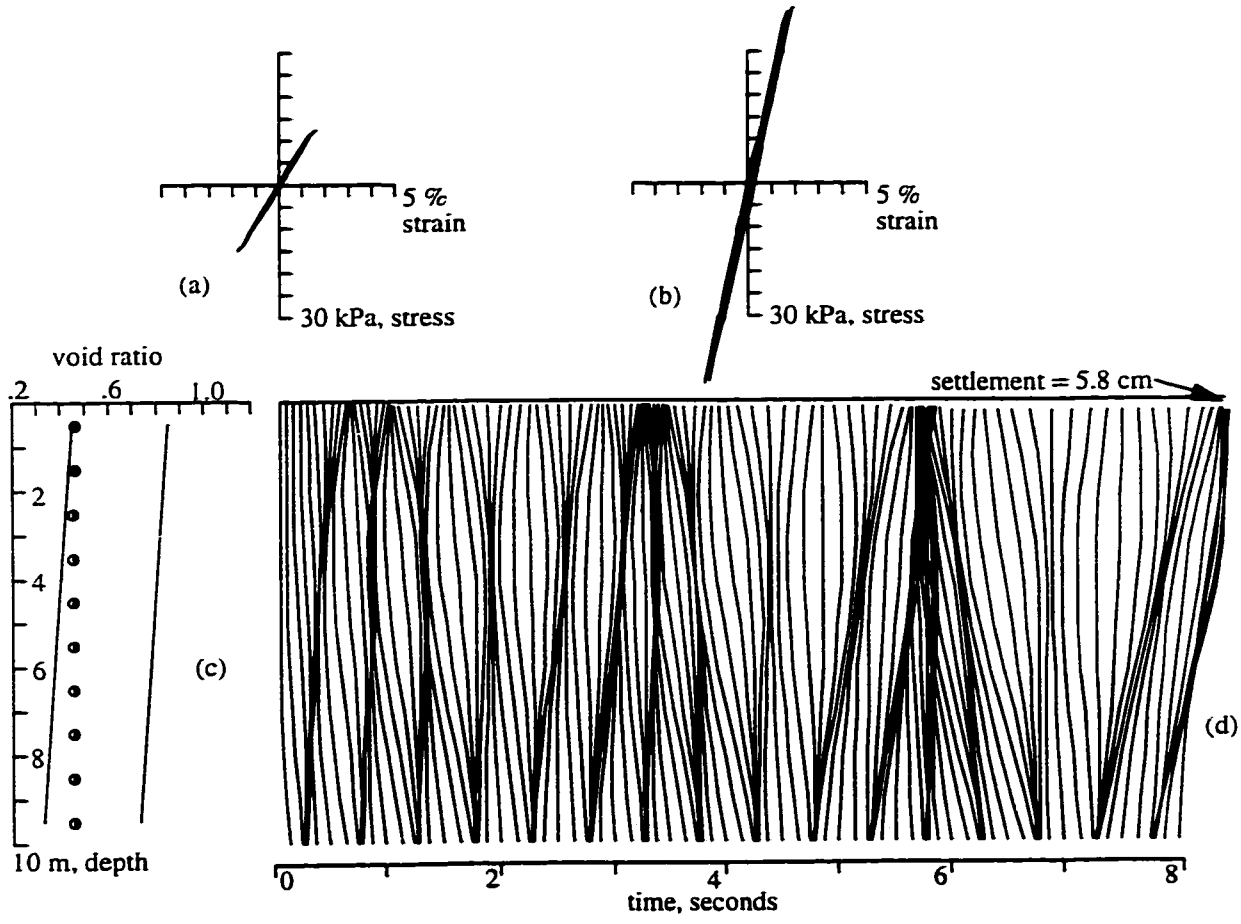

Figure 5.2 Model simulation of a very dense sand
a) stress-strain at 3m, b) stress-strain at 8 m, c) void ratio versus depth,
d) soil displacement pattern.

For the next computer test the value of void ratio is increased to 0.5. Again the soil behavior seems to be elastic but there is some plastic strain at 8 m, although the soil tends toward the compact state line. Since the sand is looser than the previous one, the settlement is increased about 40%, that is 8.1 cm as shown in Figure 5.3.

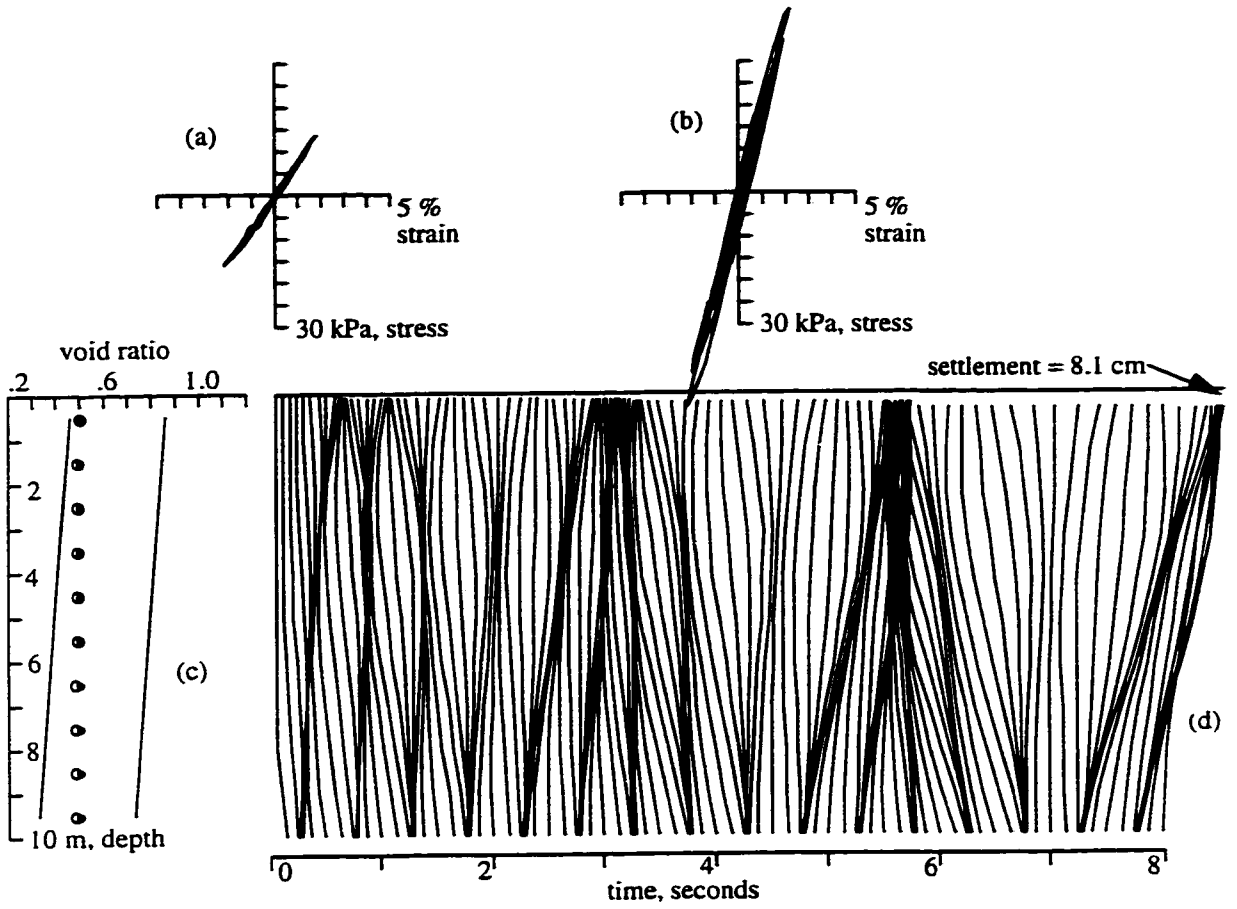

Figure 5.3 Model simulation of a dense sand
a)stress-strain at 3 m, b)stress-strain at 8m, c) void ratio versus depth,
d) soil displacement pattern.

The result of the test on medium sand (e = 0.6) is presented in Figure 5.4. It is evident that as the void ratio is increased the soil behaves elasto-plastic rather than elastic behavior. In this case, the settlement becomes 16.9 cm, i.e. about 100% more than the case for e=0.50.

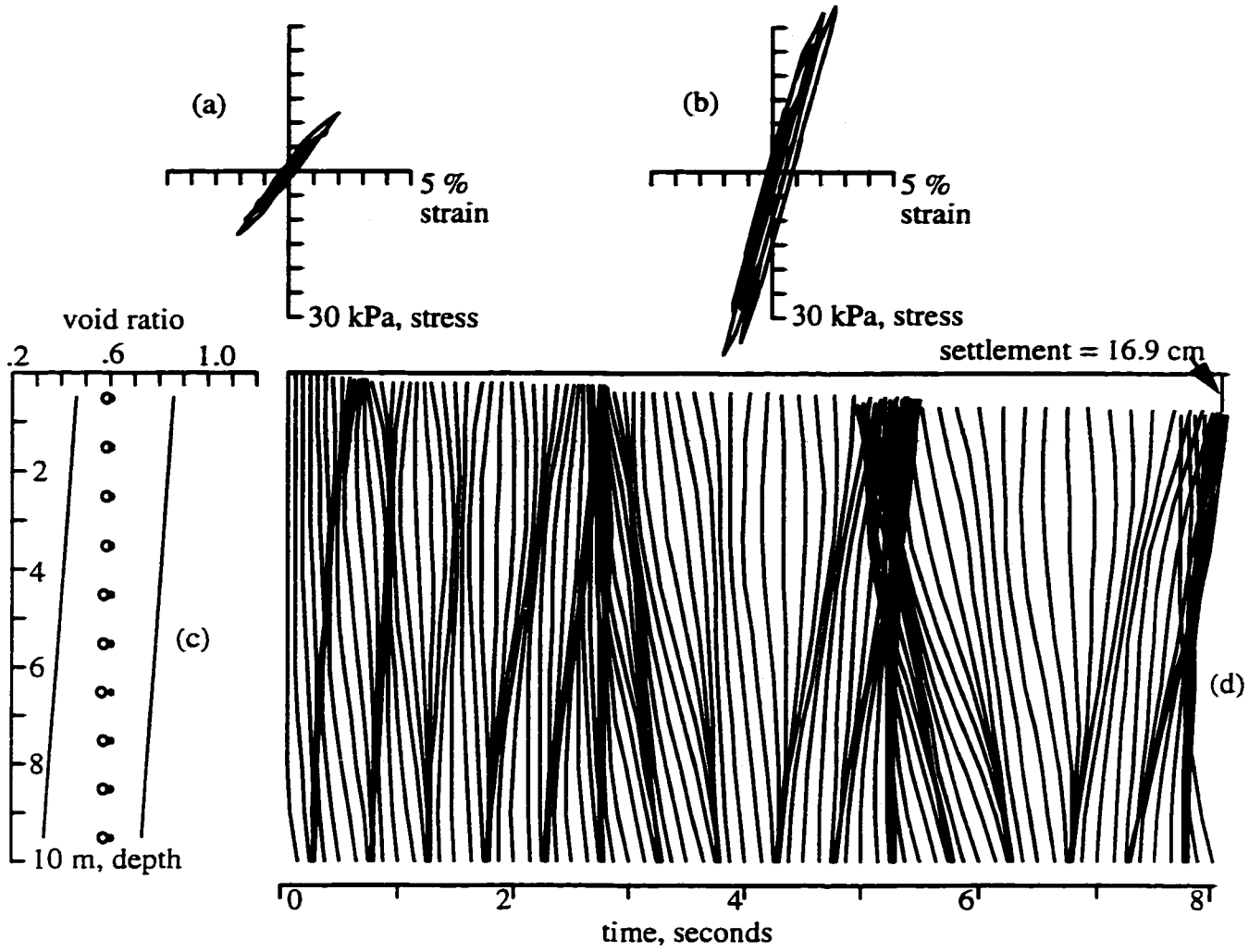

Figure 5.4 Model simulation of a medium sand
a)stress-strain at 3 m, b)stress-strain at 8m, c) void ratio versus depth,
d) soil displacement pattern.

The response of the loose sand with void ratio of 0.7 is shown in Figure 5.5. The settlement progressively increases until it reaches 25.8 after 16 cycles of earthquake loading. As expected by increasing the void ratio the settlement of the soil layer increases too.

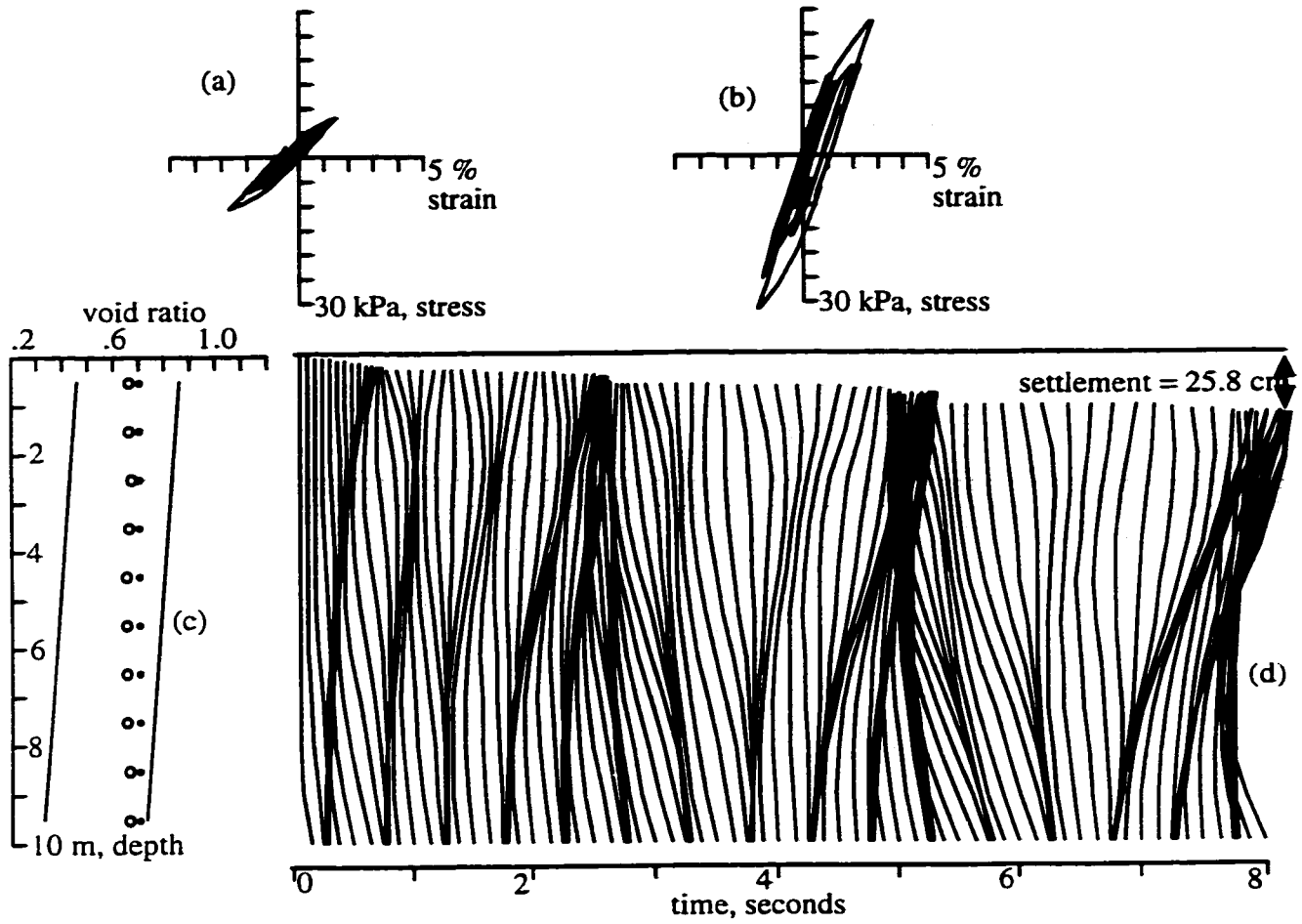

Figure 5.5 Model simulation of a loose sand
a)stress-strain at 3 m, b)stress-strain at 8m, c) void ratio versus depth,
d) soil displacement pattern.

In the test carried out on the loose to very loose sand (e=0.8), the response under the strong shaking with a maximum acceleration of 0.33g is similar to that of loose sand. In particular, the settlement increases up to 40.6 cm and the maximum stress reaches 15 kpa at 2% of strain. This is due to the fact that the void ratio is close to the critical state line as shown in Figure 5.6c.

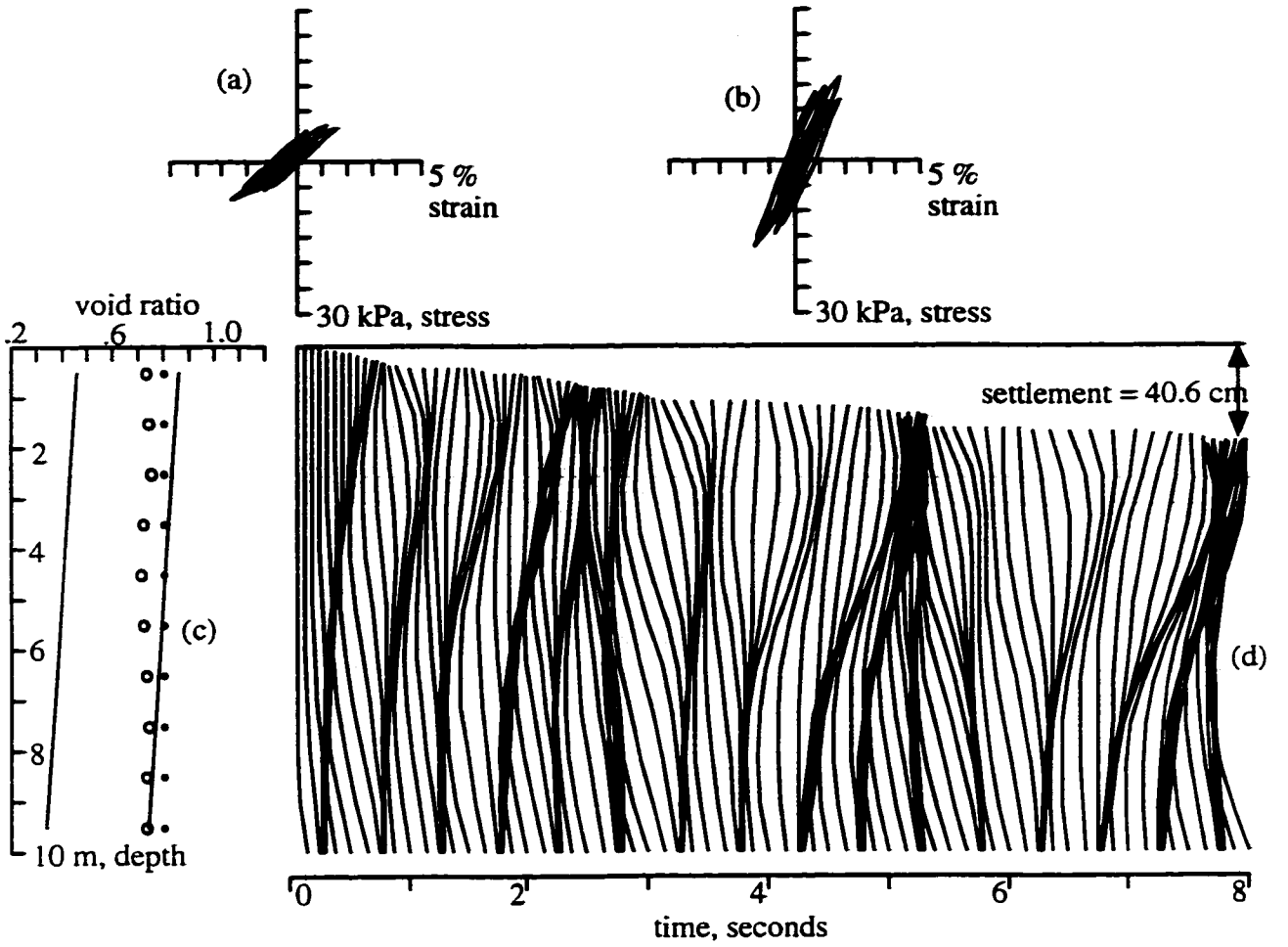

Figure 5.6 Model simulation of a loose to very loose sand
a)stress-strain at 3 m, b)stress-strain at 8m, c) void ratio versus depth,
d) soil displacement pattern.

The last test was performed on a very loose sand with a void ratio of 0.9. The distorted shape of the sand layer at various times is illustrated in Figure 5.7d. The result corresponds to the most critical points in the layer. This is quite reasonable, as the void ratio of the soil is larger than the critical void ratio.

5.8 FINAL REMARKS

It was shown that the simple plasticity model developed in this chapter is capable of replicating most of the important features of the behavior of cohesionless soils.

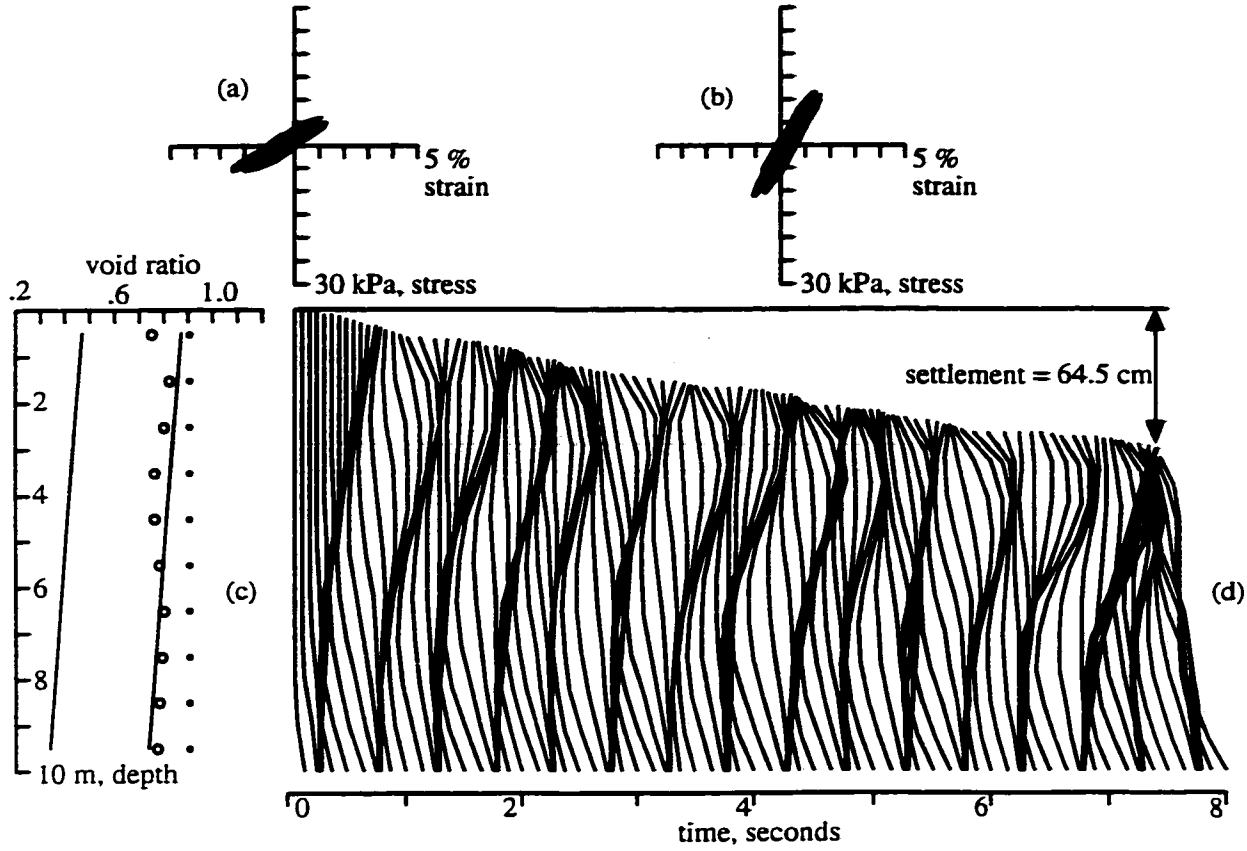

Figure 5.7 Model simulation of a very loose sand
a)stress-strain at 3 m, b)stress-strain at 8m, c) void ratio versus depth,
d) soil displacement pattern.

The results illustrate the importance of the effect of void ratio characteristics in the dynamic behavior of granular media when the influence of earthquake loading is taken into consideration. Small settling is associated with lower void ratio whereas large settling is associated with high void ratio leading to instability of the system. It was found that the settlements for loose to very loose sands were in the range of 0.2 - 0.65 m. These values appear to have the right magnitude. For example the Kobe earthquake of Japan (Bardet et al., 1997) recorded subsidence in the range of 0.2 – 0.7m. It may cause cracks or differential displacements in structures and paved surfaces as observed in many sites subjected to earthquake loading.

6

CONCLUSION

6.1 CONCLUDING REMARKS

Analysis of soil liquefaction is one of the major problems that geotechnical engineers have been facing during the last few decades. The stability of the geotechnical structures containing cohesionless granular media can not easily be modeled with the current concept of soil plasticity and flow. The major difficulty arises from the peculiar behavior of sands in a cyclic loading. For this reason the concept of the compact state, defined as the state that all granular will eventually assume when subjected to large number of stress cycles, is postulated.

It is believed that the compact state concept proposed in the present study provide a useful approach in modeling soil behavior under monotonic and cyclic loading. The proposed material constitutive model, based on the bounding surface plasticity along with the critical state and the compact state, was developed that can be used for the analysis of soil behavior under cyclic loading. The model is capable of simulating both loose and dense sands behavior.

The two hypotheses of the compact state are based on the current knowledge regarding similarity of soil behavior and the performance of the sample at very dense levels.

Based on the studies presented in this thesis an important conclusion can be drawn: If the representation of the void ratio of a sample from a sand deposit falls above the Casagrande line, then the liquefaction of the deposit, when subjected to dynamic loading is certain. If, on the other hand, the representation indicates a point below the Casagrande line, it does not mean that the deposit is safe. The safety of the deposit against liquefaction depends on how far the start point is from the line representing the compact state.

Realizing the versatility and effectiveness of the modified CANAsand model incorporating the compact state concept, a simple model was developed for the analysis of wave-induced instability problems. Since the dynamic effect has been found to be negligible, a quasi-static analysis is adopted in this phase of the work. To assess the quasi-static response of seabed sand deposit the model in conjunction with the finite difference method is used. The response of sand to the standing wave loading is determined for a broad range of void ratio, different wave amplitude and wave length.

From the numerical simulations it is found that loose sands have been shown to respond differently from dense sands to the same wave input. For the same sands it is observed that the wave amplitude has the dominant effect on the seabed response. Although the wave length does affect the response significantly in case of very loose sand resulting a total failure at about one half cycle of wave loading.

The model also overcomes the deficiencies of Ishihara's method by considering elasto-plastic behavior of soil and initial in-situ stresses.

In the present research it was also attempted to formulate the dynamics of sandy soils. In a real soil profile of two layers, liquefaction may be caused by creating a film of

water between the sand deposit and the impervious layer. Subsequently it causes a collapse in the support layer. The mixture of sand and water then may vent through fractures to the surface, often violently, where it forms "sand blow" deposits. Sand blows are considered diagnostic evidence of severe liquefaction. A plane strain analysis is employed in derivation of the governing equation of the problem. A numerical process known as the ID technique is used.

The parameters characterizing the phenomena are principally the thickness of the water film, the presence of an overlying impermeable layer above the sand, the thickness of impervious layer, magnitude and duration of the earthquake, the physical and mechanical properties of the soils involved. Several computer tests are presented on a wide range of very loose to very dense sands. Among the parameters involved, the void ratio is important in determining the settlement of the sandy soil layer. Large settlements is associated with high void ratio leading to large deformation, whereas small settlements is associated with lower void ratio. These numerical test results indicate that the model is able to present quantitatively the behavior of real soil of what is observed in earthquake-induced sites.

6.2 RECOMMENDATIONS FOR FURTHER RESEARCH

1. The proposed model has strong potential for application to the analysis of certain types of geotechnical problems. However, it is important to verify that the proposed model works correctly and to validate the computational results with well-documented case studies before one can rely on the results of such analytical tool for

practical purposes. It is also important to examine the validity of the two hypotheses, which are the foundations of the model. Certain modifications may prove to be necessary.

2. The studies regarding the wave action should be extended by means of more sophisticated techniques (probably a hybrid of the finite element and the finite difference methods). The solution presented in the present study is an approximation that is statically admissible.

3. The solution for the sand layer subjected to seismic load assumes infinite permeability for the sand layer. This provides an upper bound for the magnitude of the settlement of the layer and hence from an engineering point of view, it is conservative. Future research should incorporate the effect of the permeability of the soil layer.

REFERENCES

1. **Altaee, A. and Fellenius, B.H.** (1994), "Physical modeling in sand," Canadian Geotechnical Journal, Vol. 31, pp. 420-431.

2. **Anandarajah, A. and Dafalias, Y.F.** (1986), "Bounding surface plasticity III: Application to anisotropic cohesive clays," Journal of the Engineering Mechanics, ASCE, Vol. 112, No. 12, pp. 1292-1318.

3. **Arthur, J.R.F., Chua, K.S., Dunstan, T. and Rodriguez del C.J.I.** (1980), "Principal stress rotation: A missing parameter", Journal of Geotechnical Engineering, ASCE, Vol. 106, No. GT4, pp. 419-433.

4. **Atkinson, J.H. and Bransby, P.L.** (1978), "*The mechanics of soils–An introduction to critical state soil mechanics*," McGraw-Hill, London, 375 pp.

5. **Bardet, J.P.** (1986), "A bounding surface model for sands," Journal of Engineering Mechanics Division, ASCE, Vol. 112, No. 11, pp. 1198-1217.

6. **Bardet, J.P., Idriss, I.M., O'Rourke, T.D., Adachi, N., Hamada, M.and Ishihara, K.** (1997), "North America-Japan workshop on the geotechnical aspects of the Kobe, Loma Prieta, and Northridge earthquakes", A report to the National Science Foundation and Japanese Geotechnical Society, Osaka, Japan, 128 p.

7. **Been, K. and Jefferies, M.G.** (1985), "A state parameter for sands," Geotechnique, Vol.35, No. 2, pp. 99-112.

8. **Been, K., Jefferies, M.G. and Hachey, J.** (1991), "The critical state of sands," Geotechnique, Vol. 41, No. 3, pp. 365-381.

9. **Been, K., Jefferies, M.G. and Hachey, J.** (1992), Discussion on "The critical state of sands," Geotechnique, Vol. 42, No. 4, pp. 655-663.

10. **Biot, M.A.** (1941), "General theory of three dimensional consolidation", Journal of Applied Physics, Vol. 12, pp. 155-164.

11. **Biot, M.A.** (1955), "Theory of elasticity and consolidation for a porous anisotropic solid", Journal of Applied Physics, Vol. 26, pp. 182-185.

12. **Biot, M.A.** (1956), "Theory of propagation of elastic waves in a fluid-saturated porous solid, Part I: Low frequency range and Part II: Higher frequency range", J. Acoust. Soc. of America, Vol. 28, pp. 168-191.

13. **Biot, M.A.** (1962), "Mechanics of deformation and acoustic propagation in porous media", Journal of Applied Physics, Vol. 33, pp. 1482-1498.

14. **Britto, A.M. and Gunn, M.J.** (1987), "*Critical state soil mechanics via finite elements*", Ellis Horowood Ltd., Chichester.

15. **Burland, J.B.** (1965), "The yielding and dilation of clay," Correspondence, Geotechnique, Vol. 15, No. 2, pp. 211-214.

16. **Calladine, C.R.** (1963), "Correspondence on a paper by Roscoe and Poorooshasb: A theoretical and experimental study of strains in triaxial tests on normally consolidated clays," Geotechnique, Vol. 13, No. 3, p. 250.

17. **Casagrande, A.** (1936), "Characteristics of cohesionless soils affecting the stability of earth fills", Journal of the Boston Society of Civil Engineers, Vol. 23, No.1, pp. 13-32.

18. **Casagrande, A.** (1975), " Liquefaction and cyclic deformation of sands: A critical review," Proceedings of the 5th Pan-American Conference on Soil Mechanics and Foundations Engineering, Buenos Aires, Argentina, Vol. 5, pp. 80-133.

19. **Castro, G.** (1969), "Liquefaction of sands," Harvard University, Cambridge, Harvard Soil Mechanics Series, No. 81.

20. **Castro, G.** (1987), "On the behavior of soils during earthquakes–Liquefaction," Developments in Geotechnical Engineering 42, Soil Dynamics and Liquefaction, Cakmak, A.S. (ed.), Elsevier, pp. 169-204.

21. **Castro, G. and Poulos, S.J.** (1977), "Factors affecting liquefaction and cyclic mobility," Journal of the Geotechnical Engineering Division, ASCE, Vol. 103, No. GT 6, pp. 501-516.

22. **Castro, G., Seed, R.B., Keller, T.O. and Seed, H.B.** (1992), "Steady state strength analysis of Lower San Fernando Dam slide", Journal of the Geotechnical Engineering, ASCE, Vol. 118, No. GT 3, pp. 406-427.

23. **Chen, W.F. and Huang, T.K.** (1994), "Plasticity analysis in geotechnical engineering: From theory to practice," Developments in Geotechnical Engineering, Balasubramaniam, et al. (eds.), Balkema, pp. 49-79.

24. **Christian, J.T., Taylor, P.K., Yen, J.K. and David, R.E.** (1974), "Large diameter underwater pipeline for nuclear power plant designed against soil liquefaction", Proceedings, Sixth Annual Offshore Technology Conference, Houston, Texas, Paper No. OTC 2094, pp. 597-606.

25. **Coulomb, C.A.** (1773), "Essai sur une application des regles de maximis et minimis a quelques problemes de statique, relatifs a l'architecture," Memoires de Mathematique de l'Academie Royal des Sciences, Paris, Vol. 7, pp. 343-382.

26. **Crouch, R.S. and Wolf, J.P.** (1994, a), "Unified 3D critical state bounding-surface plasticity model for soils incorporating continuous plastic loading under cyclic paths, Part I: Constitutive relations," International Journal for Numerical and Analytical Methods in Geomechanics, Vol. 18, No. 11, pp. 735-758.

27. **Crouch, R.S. and Wolf, J.P.** (1994, b), "Unified 3D critical state bounding-surface plasticity model for soils incorporating continuous plastic loading under cyclic paths, Part II: Calibration and simulations," International Journal for Numerical and Analytical Methods in Geomechanics, Vol. 18, No. 11, pp. 759-784.

28. **Crouch, R.S., Wolf, J.P. and Dafalias, Y.F.** (1994), "Unified critical state bounding surface plasticity model for soil," Journal of Engineering Mechanics, ASCE, Vol. 120, No. 11, pp. 2251-2270.

29. **Dafalias, Y.F.** (1979), "A bounding surface plasticity model," Proceedings of the 7th Canadian Congress of Applied Mechanics, Sherbrooke, Canada.

30. **Dafalias, Y.F. and Herrmann, L.R.** (1980), "A bounding surface soil plasticity model," International Symposium on Soils Under Cyclic and Transient Loading, Swansea, U.K., Vol. 1, pp. 335-345.

31. **Dafalias, Y.F. and Herrmann, L.R.** (1982), "Bounding surface formulation of soil plasticity," Soil Mechanics-Cyclic and Transient Loads, Pande, G.N. and Zienkiewicz, O.C. (eds.), John Wiley and Sons, Chapter 10, pp. 253-282.

32. **Dafalias, Y.F. and Herrmann, L.R.** (1986), "Bounding surface plasticity II: Application to isotropic cohesive soils," Journal of the Engineering Mechanics Division, ASCE, Vol. 112, No. EM12, pp. 1263-1291.

33. **Dafalias, Y.F. and Popov, E.P.** (1976), "Plastic internal variables formalism of cyclic plasticity," Journal of Applied Mechanics, Vol. 98, No. 4, pp. 645-650.

34. **Dafalias, Y.F. and Popov, E.P.** (1975), "A model of nonlinearly hardening materials for complex loading, Acta Mechanica, Vol. 21, pp. 173-192.

35. **de Saint-Venant, B.** (1870), "Memoire sur l'etablissement des equations differentielles mouvements interieurs operes dans les corps solids ductiles au dela des limites ou l'elasticite pourrait les ramener a leur premier etat," Comptes Rendus, Acad. Sci., Paris, Vol. 70, pp. 1323-1325.

36. **Desai, C.S., Sharma, K.G., Wathugala, G.W. and Rigby, D.B.** (1991), "Implementation of hierarchical single surface δ_o and δ_1 models in finite element procedure" International Journal for Numerical and Analytical Methods in Geomechanics, Vol. 15, pp. 649-680.

37. **Desai, C.S., Somasundaram, S. and Frantziskonis, G.** (1986), "A hierarchical approach for constitutive modeling of geologic materials," International Journal for Numerical and Analytical Methods in Geomechanics, Vol. 10, pp. 225-257.

38. **Dickmen, S.U. and Ghaboussi, J.** (1984), "Effective stress analysis of seismic response and liquefaction: Theory," Journal of the Geotechnical Engineering Division, ASCE, Vol. 110, No. 5, pp. 628-644.

39. **DiMaggio, F.L. and Sandler, I.S.** (1971), "Material models for granular soils," Journal of the Engineering Mechanics Division, ASCE, Vol. 97, No. EM3, pp. 935-950.

40. **Dobry, R., Ladd, R.S., Yokel, F.Y., Chung, R.M. and Powell, D.** (1982), "Prediction of pore water pressure build up and liquefaction of sands during earthquakes by cyclic strain method," National Bureau of Standards, Building Science series 138, U.S. Department of Commerce.

41. **Drucker, D.C.** (1959), "A definition of stable inelastic material," ASME Transactions, Journal of Applied Mechanics, Vol. 26, No. 1, pp. 101-106.

42. **Drucker, D.C. and Prager, W.** (1952), "Soil mechanics and plastic analysis or limit design," Quarterly of Applied Mathematics, Vol. 10, No. 2, pp. 157-165.

43. **Drucker, D.C., Gibson, R.E. and Henkel, D.J.** (1957), "Soil mechanics and work-hardening theories of plasticity," ASCE Transactions, Vol. 122, pp. 338-346.

44. **Drucker, D.C., Greenberg, H.J. and Prager, W.** (1951), "The safety factor of an elastic-plastic body in plane strain," Journal of Applied Mechanics, Vol. 18, p. 371.

45. **Drucker, D.C., Greenberg, H.J. and Prager, W.** (1952), "Extended limit design theorems for continuous media," Quarterly Journal of Applied Mathematics, Vol. 9, p. 381.

46. **Elgamal, A.W., Zeghal, M. and Parra, E.** (1996), "Liquefaction of reclaimed island in Kobe, Japan," Journal of the Geotechnical Engineering, ASCE, Vol. 122, No. 1, pp. 33-49.

47. **El-Zahaby, K. and Rahman, M.S.** (1993), "The seabed response under a plane progressive wave", Proceedings of the 3rd International Offshore and Polar Engineering Conference, Singapore, Vol. 1, pp. 660-666.

48. **Finn, W.D.L.** (1993), "Evaluation of liquefaction potential," Proceedings of the Seminar on Soil Dynamics and Geotechnical Earthquake Engineering, Lisbon, Portugal, pp. 127-157.

49. **Finn, W.D.L.** (1997), "Earthquake engineering in Canada: A selective overview," Geotechnical News, Vol. 15, No. 4, pp. 129-136.

50. **Finn, W.D.L., Lee, W.K. and Martin, G.R.** (1977), "An effective stress model for liquefaction," Journal of the Geotechnical Engineering Division, ASCE, Vol. 103, No. GT 6, pp. 517-533.

51. **Finn, W.D.L., Siddharthan, R. and Martin, G.R.** (1983), "Response of seafloor to ocean waves", Journal of Geotechnical Engineering Division, Vol. 109, No. GT4, pp. 556-572.

52. **Florin, V.A. and Ivanon, P.L.** (1961), "Liquefaction of saturated sandy soil", Proceedings of the 5th International Conference on Soil Mechanics and Foundation Engineering, Paris, France.

53. **Frantziskonis, G. and Desai, C.S.** (1987), "Constitutive model with strain softening," International Journal of Solids and Structures, Vol. 23, No. 6, pp. 733-750.

54. **Frantziskonis, G., Desai, C.S. and Somasundaram, S.** (1986), "Constitutive model for non-associative behavior", Journal of Engineering Mechanics, ASCE, Vol.9, pp. 932-946.

55. **Fung, Y.C.** (1965), "*Foundation of Solid Mechanics*", Prentice-Hall, Englewood Cliffs, NJ, pp. 195-197.

56. **Gatmiri, B.** (1990), "A simplified finite element analysis of wave-induced effective stress and pore pressures in permeable seabeds", Geotechnique, Vol. 40, No. 1, pp. 15-30.

57. **Gatmiri, B.** (1991), "Wave-induced stresses and pore pressures in sloping seabeds", International Journal for Numerical and Analytical Methods in Geomechanics, Vol. 15, pp. 355-373.

58. **Gatmiri, B.** (1992), "Response of cross-anisotropic seabed to ocean waves", Journal of Geotechnical Engineering, ASCE, Vol. 118, No. 9, pp. 1295-1314.

59. **Gatmiri, B.** (1994), "Wave-induced pore pressure and effective stress distributions in a nonlinear seabed", Proceedings of 13th International Conference on Soil Mechanics and Foundation Engineering, Vol. 4, New Delhi, India, pp. 1665-1668.

60. **Ghaboussi, J. and Momen, H.** (1982), "Modeling and analysis of cyclic behavior of sands," Soil Mechanics-Transient and Cyclic Loads, Pande, G.N. and Zienkiewicz, O.C. (eds.), John Wiley and Sons, Chapter 12, pp. 313-342.

61. **Ghaboussi, J. and Momen, H.** (1979), "Plasticity model for cyclic behavior of sands," Proceedings of the 3rd International Conference on Numerical Methods in Geomechanics, Aachen, Vol. 1, pp. 423-434.

62. **Gutierrez, M., Ishihara, K. and Towhata, I.** (1989), "A plasticity model for the deformation of sand during rotation of principal stress directions", Proceedings of the 3rd International Symposium on Numerical Models in Geomechanics (NUMOG-III), Edited by S. Pietruszczak and G.N. Pande, pp. 53-60.

63. **Gutierrez, M., Ishihara, K. and Towhata, I.** (1991a), "Non-coaxiality and stress-dilatancy relations for granular materials", Computer Methods and Advances in Geomechanics, Proceedings of the 7th International Conference on Computer Methods and Advances in Geomechanics, Edited by G. Bear et al., pp. 625-630.

64. **Gutierrez, M., Ishihara, K. and Towhata, I.** (1991b), "Flow theory for sand during rotation of principal stress direction", Soils and Foundations, Vol. 31, No. 4, pp. 121-132.

65. **Gutierrez, M., Ishihara, K. and Towhata, I.** (1993), "Model for the deformation of sand during rotation of principal stress directions", Soils and Foundations, Vol. 33, No. 3, pp. 105-117.

66. **Hardin, B.O. and Drnevich, V.P.** (1972), "Shear modulus and damping of soils: design equations and curves", Journal of Soil Mechanics and Foundation Division, ASCE, Vol. 98, No. SM7, pp. 667-692.

67. **Hashigushi, K.** (1979), "Constitutive equations of granular media with anisotropic hardening", Proceedings of the Third International Conference on Numerical Methods in Geomechanics, Aachen, p. 345.

68. **Hashigushi, K.** (1986), "A mathematical description of elastoplastic deformation in normal-yield and subyield states", Proceedings of the Second International Conference on Numerical Model in Geomechanics, Pande, G.N. and van Impe, W.F. (eds.), M. Jackson and Son, pp. 17-24.

69. **Hazen, A.** (1920), "Hydraulic fill dams", ASCE Transactions, Vol. 83, pp. 1713-1745.

70. **Henkel, D.J.** (1970), "The role of waves in causing submarine landslides", Geotechnique, Vol. 20, No. 1, pp. 75-80.

71. **Hill, R.** (1950), *"The mathematical theory of plasticity,"* Oxford University Press, 355 pp.

72. **Hodgson, E.A.** (1945), "Industrial earthquake hazards in eastern Canada," Bulletin of the Seismological Society of America, Vol. 35, pp. 151-174.

73. **Hodgson, E.A.** (1950), "The St. Lawrence earthquake of March 1st, 1925," Publications of the Dominion Observatory, Vol. 7, pp. 361-436.

74. **Holtz, R.D. and Kovacs, W.D.** (1981), *"An introduction to geotechnical engineering",* Prentice-Hall Inc., Civil Eng. and Engineering Mechanics Series, Englewood Cliffs, New Jersey, U.S.A., p. 733.

75. **Horikawa, K.** (1978), "*Coastal Engineering*", University of Tokyo Press, Tokyo.

76. **Housner, G.W.** (1958), "The mechanism of sand blows", Bulletin of the Seismological Society of America, No. 48, pp. 155-161.

77. **Huang, W.** (1980), "Effect of work hardening rules on the elasto-plastic matrix," Proceedings of International Symposium on Soils under Cyclic and Transient Loading, Balkema, Rotterdam, pp. 277-282.

78. **Inel, S. and Lade, P.V.** (1997), "Rotational kinematic hardening model for sand, Part II: Characteristic work hardening law and predictions," Computers and Geotechnics, Vol. 21, No. 3, pp. 217-234.

79. **Ishihara, K.** (1983), "Soil response in cyclic loading induced by earthquakes, traffic and waves", Proceedings of the 7th Asian Regional Conference, Haifa, Israel, Vol. 2, pp. 42-66.

80. **Ishihara, K.** (1993), "Liquefaction and flow failure during earthquakes," The 33rd Rankine Lecture, Geotechnique, Vol. 43, No.3, pp. 351-415.

81. **Ishihara, K. and Towhata, I.** (1982), "Dynamic response of level ground based on effective stress method," Chapter 7, Soil Mechanics-Transient and Cyclic Loads, Pande, G.N. and Zienkiewicz, O.C., (eds.), John Wiley and Sons Ltd., New York, pp. 133-172.

82. **Ishihara, K. and Towhata, I.** (1983), "Sand response to cyclic rotation of principal stress direction as induced by wave loads", Soils and Foundations, Vol. 23, No. 4, pp. 11-26.

83. **Ishihara, K. and Towhata, I.** (1983), "Cyclic behavior of sand during rotation of principal stress axes", Mechanics of Granular Materials: New Models and Constitutive Relations, Edited by J.T. Jenkins, and M. Satake, Elsevier Science Publications, Amsterdam, pp. 53-73.

84. **Ishihara, K. and Towhata, I.** (1984), "Effects of rotation of principal stress directions on cyclic response of sand", Mechanics of Engineering Materials, Edited by C.S. Desai and R.H. Gallagher, John Wiley and Sons, pp. 319-333.

85. **Ishihara, K. and Yamazaki, A.** (1984), "Analysis of wave-induced liquefaction in seabed deposits of sand", Soils and Foundations, Vol. 24, No. 3, pp. 85-100.

86. **Ishihara, K. and Yamazaki, A.** (1984), "Wave-induced liquefaction in seabed deposits of sand", Proceedings of the International Union of Theoretical and Applied Mechanics (IUTAM) in Seabed Mechanics (edited by B. Denness), Graham and Trotman, pp. 139-148.

87. **Ishihara, K., Tatsuoka, F. and Yasuda S.** (1975), "Undrained deformation and liquefaction of sand under cyclic stresses," Soils and Foundations, Vol. 15, No. 1, pp. 29-44.

88. **Ishihara, K., Verdugo, R. and Acacio, A.A.** (1991), "Characterization of cyclic behavior of sand and post-seismic stability analyses," Proceedings of the 9th Asian Regional Conference on Soil Mechanics and Foundation Engineering, Bangkok, Thailand, Vol. 2, pp. 45-67.

89. **Iwan, W.D.** (1967), "On a class of models for the yielding behavior of continuous and composite systems," Journal of Applied Mechanics, ASME, Vol. 34, No. E3, pp. 612-617.

90. **Joyner, W.B. and Chen, A.T.F.** (1976), "Calculation of nonlinear ground response in earthquakes," Bulletin of Seismological Society of America, Vol. 65, No. 5, pp. 1315-1336.

91. **Kim, M.K. and Lade, P.V.** (1988), "Single hardening constitutive model for frictional materials: I: Plastic potential function," Computers and Geotechnics, Vol. 5, pp. 307-324.

92. **Ko, H.Y. and Scott, R.F.** (1968), "Deformation of sand at failure," Journal of Soil Mechanics and Foundation Division, ASCE, Vol. 94, No. SM4, pp. 883-898.

93. **Krieg, R.D.** (1975), "A practical two-surface plasticity theory," Journal of Applied Mechanics, Transactions of ASME, Vol. 42, pp. 641-646.

94. **Kuerbis, R., Negussey, D. and Vaid, Y.P.** (1988), "Effect of gradation and fine content on the undrained response of sand," ASCE Specialty Conference on Hydraulic Fill Structures, Fort Collins Co., pp. 330-345.

95. **Lacy, S.L. and Prevost, J.H.** (1987), "Constitutive model for geomaterials," Proceedings of the 2nd International Conference on Constitutive Laws for Engineering Materials, Desai, C.C., et al. (eds.), Tucson, Arizona, Vol. 1, pp. 149-160.

96. **Lade, P.V.** (1977), "Elasto-plastic stress-strain theory for cohesionless soil with curved yield surfaces," International Journal of Solids and Structures, Vol. 13, pp. 1019-1035.

97. **Lade, P.V.** (1988), "Effects of voids and volume changes on the behavior of frictional materials," International Journal for Numerical and Analytical Methods in Geomechanics, Vol. 12, pp. 351-370.

98. **Lade, P.V. and Duncan, J.M.** (1973), "Cubical triaxial tests on cohesionless soil," Journal of Soil Mechanics and Foundation Division, ASCE, Vol. 99, No. SM10, pp. 793-812.

99. **Lade, P.V. and Duncan, J.M.** (1975), "Elasto-plastic stress-strain theory for cohesionless soil," Journal of the Geotechnical Engineering Division, ASCE, Vol. 101, No. GT10, pp. 1037-1053.

100. **Lade, P.V. and Duncan, J.M.** (1976), "Stress-path dependent behavior of cohesionless soil," Journal of the Geotechnical Engineering Division, ASCE, Vol. 102, No. GT1, pp. 51-68.

101. **Lade, P.V. and Inel, S.** (1997), "Rotational kinematic hardening model for sand, Part I: Concept of rotating yield and plastic potential surfaces," Computers and Geotechnics, Vol. 21, No. 3, pp. 183-216.

102. **Lade, P.V. and Kim, M.K.** (1988, a), "Single hardening constitutive model for frictional materials: II: Yield criterion and plastic work contours," Computers and Geotechnics, Vol. 6, pp. 13-29.

103. **Lade, P.V. and Kim, M.K.** (1988, b), "Single hardening constitutive model for frictional materials: III: Comparisons with experimental data," Computers and Geotechnics, Vol. 6, pp. 31-47.

104. **Lee, K.L.** (1965), "Triaxial compressive strength of saturated sands under seismic loading conditions," Ph.D. dissertation, University of California at Berkeley, U.S.A., p. 521.

105. **Lee, K.L. and Seed, H.B.** (1967), "Drained characteristics of sand," Journal of Soil Mechanics and Foundation Division, ASCE, Vol. 93, No. 6, pp. 117-141.

106. **Lee, K.L., Focht, J.A.** (1975), "Liquefaction potential of Ekofisk tank in North sea", Journal of the Geotechnical Engineering Division, ASCE, Vol. 101, No. GT1, pp. 1-18.

107. **Levy, M.** (1871), "Extrait du memoire sur les equations generales des mouvements interieurs des corps solides ductiles au dela des limites out l'elasticite pourrait les ramener a leur premier etat," Journal Math. Pure Appl., Vol. 16, p. 369.

108. **Liu, P.L.F** (1977), "On gravity waves propagated over a layered permeable bed", Journal of Coastal Engineering, Vol. 1, pp. 135-148.

109. **Madsen, O.S.** (1978), "Wave-induced pore pressures and effective stresses in a porous bed", Geotechnique, Vol. 28, No. 4, pp. 377-393.

110. **Manzari, M.T. and Dafalias, Y.F.** (1997), "A critical state two-surface plasticity model for sands," Geotechnique, Vol. 47, No. 2, pp. 255-272.

111. **McRoberts, E.C. and Sladen, J.A.** (1992), "Observations on static and cyclic sand liquefaction methodologies," Canadian Geotechnical Journal, Vol. 29, pp. 650-665.

112. **Mei, C.C. and Foda, M.A.** (1981), "Wave-induced responses in a fluid-filled poro-elastic solid with a free surface: A boundary layer theory", Geophysics Journal for Royal Astronomical Society, Vol. 66, pp. 597-637.

113. **Meyerhof, G.G.** (1951), "The ultimate bearing capacity of foundations," Geotechnique, Vol. 2, pp. 301-332.

114. **Moshagen, H. and Torum, A** (1975), "Wave-induced pressures in permeable seabeds", Journal of Waterways, Harbor and Coastal Engineering, ASCE, Vol 101, No. WW1, pp. 49-57.

115. **Mroz, Z.** (1967), "On the description of anisotropic work-hardening," Journal of the Mechanics and Physics of Solids, Vol. 15, pp. 163-175.

116. **Mroz, Z.** (1969), "An attempt to describe the behavior of metals under cyclic loads using a more general work-hardening model," Acta Mechanica, Vol. 7, pp. 199-212.

117. **Mroz, Z.** (1972), "A description of work hardening of metals with application to variable loading," Proceedings of International Symposium on Foundations of Plasticity, Sawczuk, A. (ed.), Noordhoff International Publishing Company.

118. **Mroz, Z. and Norris, V.A.** (1982), "Elastoplastic and viscoplastic constitutive models for soils with application to cyclic loading, "Soil Mechanics - Transient and Cyclic Loads, Pande, G.N. and Zienkiewicz, O.C. (eds.), John Wiley and Sons, Chapter 8, pp. 173-217.

119. **Mroz, Z. and Pietruszczak, S.,** (1983), "A constitutive model for sand with an anisotropic hardening rule," International Journal of Numerical and Analytical Methods in Geomechanics, Vol. 7, pp. 305-320.

120. **Mroz, Z., Norris, V.A. and Zienkiewicz, O.C.** (1975), "Application of an anisotropic hardening model in the analysis of elastoplastic deformation of soils," Geotechnique, Vol. 29, No. 1, pp. 1-34.

121. **Mroz, Z., Norris, V.A. and Zienkiewicz, O.C.** (1978), "An anisotropic hardening model for soils and its application to cyclic loading," International Journal for Numerical and Analytical Methods in Geomechanics, Vol. 2, pp. 203-221.

122. **Mroz, Z., Norris, V.A. and Zienkiewicz, O.C.** (1979), "Application of an anisotropic hardening model in the analysis of elastoplastic deformation of soils," Geotechnique, Vol. 29, No. 1, pp. 1-34.

123. **Mroz, Z., Norris, V.A. and Zienkiewicz, O.C.** (1981), "An anisotropic critical state model for soils subjected to cyclic loading," Geotechnique, Vol. 31, No. 4, pp. 451-469.

124. **Muir, S.G. and Scott, R.F.** (1981), "Earthquake generated sand blows formed during the 15 October 1979 Imperial Valley main shock", U.S. Geological Survey Professional paper 1254, U.S. Department of Interior, Washington, D.C.

125. **Nago, H., Maeno, S., Matsumoto, T. and Hachiman, Y.** (1993), "Liquefaction and densification of loosely deposited sand bed under water pressure variation", Proceedings of the Third International Offshore and Polar Engineering Conference, Singapore, Vol. 1, pp. 578-584.

126. **Nataraja, M.S. and Gill, H.S.** (1983), "Ocean wave-induced liquefaction analysis", Journal of Geotechnical Engineering, ASCE, Vol. 109, No. 4, pp. 573-590.

127. **Noorzad, A. and Poorooshasb, H.B.** (1997), "Yielding and flow of sand," Trends in Structural Mechanics: Theory, Practice, Education, Roorda, J. and Srivastava, N.K. (eds.), Kluwer Academic Publishers, Netherlands, pp. 51-56.

128. **Nova, R. and Wood, D.M.** (1979), "A constitutive model for sand in triaxial compression," International Journal for Numerical and Analytical Methods in Geomechanics, Vol. 3, pp. 255-278.

129. **Oka, F., Yashima, A. and Kato, M.** (1993), "Numerical analysis of wave-induced liquefaction in seabed", Proceedings of the Third International Offshore and Polar Engineering Conference, Singapore, Vol. 1, pp. 591-598.

130. **Okusa, S.** (1985), "Wave-induced stresses in unsaturated submarine sediments", Geotechnique, Vol. 35, No. 4, pp. 517-532.

131. **Okusa, S. and Yoshimura, M.** (1987), "Wave-induced instability in sandy submarine sediments", Soils and Foundations, Vol. 27, No. 4, pp. 62-72.

132. **Pande, G.N. and Pietruszczak, S.** (1982), "Reflecting surface model for soils," Proceedings of the International Symposium on Numerical Methods in Geomechanics, Dungar, R., Pande, G.N. and Studer, J.A. (eds.), Balkema Pub., Rotherdam, Zurich, pp. 50-64.

133. **Pastor, M.** (1991), "Modeling of anisotropic sand behavior," Computers and Geotechnics, Vol. 11, pp. 173-208.

134. **Pastor, M. and Zienkiewicz, O.C.** (1986), "A generalized plasticity, hierarchical model for sand under monotonic and cyclic loading," Proceedings of the 2nd International Conference on Numerical Models in Geomechanics, (NUMOG II), Pande, G.N., van Impe, W.F., M. Jackson and Son, pp. 131-150.

135. **Pastor, M. Zienkiewicz, O.C. and Chan, A.H.C.** (1990), "Generalized plasticity and the modeling of soil behavior," International Journal for Numerical and Analytical Methods in Geomechanics, Vol. 14, pp. 151-190.

136. **Pastor, M., Zienkiewicz, O.C. and Leung, K.H.** (1985), "Simple model for transient soil loading in earthquake analysis, Part II: Non-associative models for sands," International Journal for Numerical and Analytical Methods in Geomechanics, Vol. 9, pp. 477-498.

137. **Philips, A. and Tang, T.L.** (1972), "The effect of loading path on the yield surface at elevated temperatures," International Journal of Solids and Structures, Vol. 8, p. 463.

138. **Pietruszczak, S. and Krucinski, S.** (1989), "Consideration on soil response to the rotation of principal stress directions", Computers and Geotechnics, Vol. 8, pp. 89-110.

139. **Pietruszczak, S.T. and Mroz, Z.** (1983), "On hardening anisotropy of K_o-consolidated clays," International Journal for Numerical and Analytical Methods in Geomechanics, Vol. 7, pp. 19-38.

140. **Pietruszczak, S.T. and Stolle, D.F.E.** (1987), "Modeling of sand behavior under earthquake excitation," International Journal for Numerical and Analytical Methods in Geomechanics, Vol. 11, No. 3, pp. 221-240.

141. **Poorooshasb, H.B.** (1961), "The properties of soils and other granular media in simple shear," Ph.D. thesis, University of Cambridge, U.K.

142. **Poorooshasb, H.B.** (1971), "Deformation of sand in triaxial compression," Proceedings of the 4th Asian Regional Conference on Soil Mechanics and Foundation Engineering, Bangkok, Vol. 1, pp. 63-66.

143. **Poorooshasb, H.B.** (1989), "Description of flow of sand using state parameters," Computers and Geotechnics, Vol. 8, pp. 195-218.

144. **Poorooshasb, H.B.** (1991), "Critical state, steady state of deformation and the ultimate state of cohesionless media," Proceedings of the 3rd International Conference on Constitutive Laws for Engineering Materials: Theory and Applications, Arizona, USA, pp. 167-172.

145. **Poorooshasb, H.B.** (1994), "CANAsand and its application", Applications of Computational Mechanics in Geotechnical Engineering, Vargas et al. (eds.), Balkema, Rotterdam, pp. 213-241.

146. **Poorooshasb, H.B.** (1995), "One gravity model testing," Soils and Foundations, Vol.35, No.3, pp. 35-59.

147. **Poorooshasb, H.B. and Fletcher, E.B.** (1987), "Earthquake induced instability of the Persian Gulf coastal plains", Proceedings of 8th Asian Regional Conference on Soil Mechanics and Foundation Engineering, Vol. 1, pp. 261-264.

148. **Poorooshasb, H.B. and Pietruszczak, S.** (1985), "On yielding and flow of sand; A generalized two-surface model," Computer and Geotechnics, Vol. 1, pp. 35-58.

149. **Poorooshasb, H.B. and Pietruszczak, S.** (1986), "A generalized flow theory for sand," Soils and Foundations, Vol. 26, No. 2, pp. 1-15.

150. **Poorooshasb, H.B., Alamgir, M. and Miura, N.** (1996, a), "Negative skin friction on rigid and deformable piles," Computers and Geotechniques, Vol. 18, No. 2, pp. 109-126.

151. **Poorooshasb, H.B., Alamgir, M. and Miura, N.** (1996, b), "Application of an integro-differential equation to the analysis of geotechnical problems," Structural Engineering and Mechanics, Vol. 4, No. 3, pp. 227-242.

152. **Poorooshasb, H.B., Holubec, I. and Sherbourne, A.N.** (1966), "Yielding and flow of sand in triaxial compression," Canadian Geotechnical Journal, Vol. 3, No. 4, Part I, pp. 179-190.

153. **Poorooshasb, H.B., Holubec, I. and Sherbourne, A.N.** (1967), "Yielding and flow of sand in triaxial compression," Canadian Geotechnical Journal, Vol. 4, No. 4, Part II and III, pp. 376-399.

154. **Poorooshasb, H.B., Ishihara, K. and Yang, Q.S.** (1987), "Action of standing waves on seabed sands", Proceedings of the International Conference on Computational Engineering Mechanics, Beijing, China, pp. 146-151.

155. **Poorooshasb, H.B., Miura, N. and Alamgir, M.** (1996, c), "Refinement of a numerical technique for solution of geotechnical problems," Proceedings of the 3rd Asian-Pasific Conference on Computational Mechanics, Seoul, Korea, pp. 2145-2150.

156. **Poorooshasb, H.B., Miura, N. and Noorzad, A.** (1997), "Load carried by buried culverts," Proceedings of the 4th International Conference on Civil Engineering, Tehran, Iran, Vol. 2, pp. 167-177.

157. **Poorooshasb, H.B., Miura, N. and Noorzad, A.** (1998), 'Analysis and design of inclined piles used to prevent downhill creep of unsaturated clay formation," to appear in " Structural Engineering and Mechanics."

158. **Poorooshasb, H.B., Noorzad, A.** (1996), "The compact state of the cohesionless granular media," International Journal of Science and Technology: Scientia Iranica, Vol. 3, Nos. 1, 2, 3, pp. 1-8.

159. **Poorooshasb, H.B., Noorzad, A., Miura, N.** (1995), "Analysis of piled-raft foundation," Proceedings of the 5th International Symposium on Numerical Models in Geomechanics (NUMOG-V), Davos, Switzerland, pp. 213-241.

160. **Poorooshasb, H.B., Yang, Q.S. and Clark, J.I.** (1990), "Non-linear analysis of a seabed deposit subjected to the action of standing waves", Mathl. Comput. Modeling, Vol. 13, No. 4, pp. 45-58.

161. **Poulos, H.G.** (1988), "*Marine Geotechnics*", Unwin Hyman Ltd., London, U.K.

162. **Poulos, S.J.** (1981), "The steady state of deformation," Journal of the Geotechnical Engineering, ASCE, Vol. 107, No. GT 5, pp. 553-562.

163. **Poulos, S.J., Castro, G. and France, J.W.** (1985), "Liquefaction evaluation procedures," Journal of the Geotechnical Engineering, ASCE, Vol. 111, No. GT 6, pp.772-792.

164. **Poulos, S.J., Castro, G. and France, J.W.** (1988), Closure of discussion of "Liquefaction evaluation procedures," Journal of the Geotechnical Engineering, ASCE, Vol. 114, No. GT 2, pp. 251-259.

165. **Pradel, D., Ishihara, K. and Gutierrez, M.** (1990), "Yielding and flow of sand under principal stress axes rotation", Soils and Foundations, Vol. 30, No. 1, pp. 87-99.

166. **Prager, W.** (1955), "The theory of plasticity - A survey of recent achievements," Proceedings of the Institution of Mechanical Engineers, London, Vol. 169, pp. 41-57.

167. **Prager, W.** (1956), "A new method of analyzing stresses and strains in work-hardening plastic solids," Journal of Applied Mechanics, ASME, Vol. 23, pp. 493-496.

168. **Prandtl, L.** (1924), "Spannungsverteilung in plastischen korerpern," Proceedings of the First International Congress on Applied Mechanics, Delft, p. 43.

169. **Prevost, J.H.** (1977), "Mathematical modeling of monotonic and cyclic undrained clay behavior," International Journal for Numerical and Analytical Methods in Geomechanics, Vol. 1, No. 2, pp. 195-216.

170. **Prevost, J.H.** (1978), "Plasticity theory for soil stress-strain behavior," Journal of the Engineering Mechanics Division, ASCE, Vol. 104, No. EM5, pp. 1177-1194.

171. **Prevost, J.H.** (1982), "Nonlinear transient phenomena in saturated porous media", Computer Methods in Applied Mechanics and Engineering, Vol. 20, No. 1, pp. 3-18.

172. **Prevost, J.H.** (1985), "A simple plasticity theory for frictional cohesionless soils," Journal of Soil Dynamics and Earthquake Engineering, Vol. 4, No.1, pp. 9-17.

173. **Prevost, J.H. and Griffiths, D.V.** (1988), "Parameter identification and implementation of a kinematic plasticity model for frictional soils," Proceedings of the Workshop on Constitutive Laws for the Analysis of Fill Retention Structures, Evgin, E. (ed.), Department of Civil Engineering, University of Ottawa, pp. 285-358.

174. **Prevost, J.H., Eide, O. and Andersen, K.** (1975), Discussion of "wave-induced pressures in permeable seabeds", by H. Moshegan and A. Torum, Journal of the Waterways, Harbors and Coastal Engineering Division, ASCE, Vol. 101, No. WW4, pp. 464-465.

175. **Putnam, J.A.** (1949), "Loss of wave energy due to percolation in a permeable sea bottom", Transactions, American Geophysical Union, Vol. 30, No. 3, pp. 349-356.

176. **Rahman, M.S.** (1991), "Wave-induced instability of seabed: Mechanism and Conditions", Marine Geotechnology, Vol. 10, pp. 277-299.

177. **Rahman, M.S.** (1992), "Wave-induced liquefaction of seabed: Mechanism and Conditions", Proceedings of the Second International Offshore and Polar Engineering Conference, San Francisco, USA, Vol. 1, pp. 403-409.

178. **Rahman, M.S. and Jaber, W.Y.** (1986), "A simplified drained analysis for wave-induced liquefaction in oceanfloor sands", Soils and Foundations, Vol. 26, No. 3, pp. 57-68.

179. **Reuss, A.** (1930), "Beruecksichtigung der elastischen formaenderungen in der plastizitaets theorie," Z. Angen. Math. Mech., Vol. 10, p. 266.

180. **Roscoe, K.H. and Burland, J.B.** (1968), "On the generalized stress-strain behavior of "wet" clay," In: Engineering Plasticity, Heyman, J. and Leckie, F.A. (eds.), Cambridge University Press, Cambridge, England, pp. 535-609.

181. **Roscoe, K.H. and Poorooshasb, H.B.** (1963), "A fundamental principle of similarity in model tests for earth pressure problems", Proceedings of the 2nd Asian Regional Conference on Soil Mechanics and Foundation Engineering, Bangkok, Thailand, Vol. 1, pp. 134-140.

182. **Roscoe, K.H. and Poorooshasb, H.B.** (1963, a), "A theoretical and experimental study of strains in triaxial tests on normally consolidated clays," Geotechnique, Vol. 13, No. 1, pp. 12-38.

183. **Roscoe, K.H., Schofield, A.N. and Thurairajah, A.** (1963), "Yielding of clays in states wetter than critical," Geotechnique, Vol. 13, No. 3, pp. 211-240.

184. **Roscoe, K.H., Schofield, A.N. and Wroth, C.P.** (1958), "On yielding of soils," Geotechnique, Vol.8, pp. 22-53.

185. **Rowe, P.W.** (1962), "The stress-dilatancy relation for static equilibrium of an assembly of particles in contact," Proceedings of Royal Society, Series A, Vol. 269, pp. 500-527.

186. **Sandler, I.S., DiMaggio, F.L. and Baladi, G.Y.** (1976), "Generalized cap model for geological materials," Journal of Geotechnical Engineering Division, ASCE, Vol. 102, No. GT7, pp. 683-699.

187. **Sasitharan, S.** (1994), "Collapse behavior of very loose sand," Ph.D. thesis, Department of Civil engineering, University of Alberta, Edmonton, Canada.

188. **Schofield, A.N. and Wroth, C.P.** (1968), "*Critical state soil mechanics*," McGraw-Hill, New York, NY, 310pp.

189. **Scott, R.F.** (1988), "Centrifuge and model technology: A survey," Address to Centrifuge' 88 Conference, Paris, France.

190. **Scott, R.F.** (1989), "Essais en centrifuge et technique et de la modelisation," Revenue Francaise de Geotechnique, Paris, No. 48, pp. 15-34.

191. **Scott, R.F. and Zuckerman, K.A.** (1973), "Sand blows and liquefaction", The Great Alaskan Earthquake of 1964-Engineering Volume, Committee on the Alaska of Sciences, Washington, D.C., pp. 179-189.

192. **Seed, H.B. and Idriss, I.M.** (1967), "Analysis of soil liquefaction: Niigata earthquake," Journal of the Soil Mechanics and Foundations Division, ASCE, Vol.93, No. SM 3, pp. 83-108.

193. **Seed, H.B. and Idriss, I.M.** (1981), "Evaluation of liquefaction potential of sand deposits based on observations and performance in previous earthquakes," Pre-print

No. 81-544, In situ testing to evaluate liquefaction susceptibility, ASCE Annual Convention, St. Louis, USA.

194. **Seed, H.B. and Lee, K.L.** (1966), "Liquefaction of saturated sands during cyclic loading", Journal of Soil Mechanics and Foundation Division, ASCE, Vol. 92, No. SM9, pp. 1249-1273.

195. **Seed, H.B. and Rahman, M.S.** (1977), "Analysis for wave-induced liquefaction in relation to ocean floor stability", Geotechnical Engineering Report No. UBC/TE-77/02, University of California, Berkeley, pp. 1-84.

196. **Seed, H.B. and Rahman, M.S.** (1978), "Wave-induced pore pressure in relation to ocean floor stability of cohesionless soils", Marine Geotechnology, Vol. 3, No. 2, pp. 123-150.

197. **Seed, H.B., Martin, P.P. and Lysmer, J.** (1976), "Pore water pressure changes during soil liquefaction", Journal of Geotechnical Engineering Division, ASCE, Vol. 102, No. GT4, pp. 323-346.

198. **Siddharthan, R.** (1987), "Wave-induced displacements in seafloor sands", International Journal for Numerical and Analytical Methods in Geomechnics, Vol. 11, pp. 155-170.

199. **Siddharthan, R. and Finn, W.D.L.** (1979), "STAB-MAX: Analysis of instantaneous instability induced in seafloor sands by large waves", Soil Dynamic Group, Faculty of Graduate Studies, University of British Columbia, Vancouver, British Columbia, Canada.

200. **Siddharthan, R. and Finn, W.D.L.** (1979), "STAB-W: Analysis of instability in seafloor sands by cumulative effects of waves", Soil Dynamic Group, Faculty of Graduate Studies, University of British Columbia, Vancouver, British Columbia, Canada.

201. **Silver, M.I. and Seed, H.B.** (1971), "Volume changes in sand during cyclic loading," Journal of the Soil Mechanics and Foundations Division, ASCE, Vol. 97, No. SM 9, pp. 1171-1182.

202. **Sleath, J.F.A.** (1970), "Wave-induced pressures in permeable seabeds", Journal of Waterways, Harbor and Coastal Engineering, ASCE, Vol. 96, No. HY2, pp. 367-378.

203. **Tatsuoka, F. and Ishihara, K.** (1974), "Yielding of sand in triaxial compression," Soils and Foundations, Vol. 14, No. 2, pp. 63-76.

204. **Terzaghi, K.** (1943), "*Theoretical soil mechanics,*" John Wiley, New York, NY, 510 pp.

205. **Terzaghi, K.** (1956), "Varieties of submarine slope failures," Proceedings of the 8th Texas Conference on Soil Mechanics and Foundation Engineering, University of Texas, Austin, pp. 1-41.

206. **Towhata, I. and Ishihara, K.** (1985), "Modeling soil deformation undergoing cyclic rotation of principal stress axes", Proceedings of 5th International Conference on Numerical Methods in Geomechanics, Nagoya, Vol. 1, pp. 523-530.

207. **Tresca, H.** (1864), "Sur l'ecoulement des corps solides soumis a de fortes pressions," Comptes Rendus Acad. Sci., Paris, Vol. 59, p. 574.

208. **Truesdell, C. and Toupin, R.A.** (1960), "The classical field theories", in Handbuch der Physic, Editor, S. Flugge, Springer-Verlage, Berlin, Vol. III/1.

209. **Tsui, Y. and Helfrich, S.C.** (1983), "Wave-induced pore pressures in submerged sand layer", Journal of Geotechnical Engineering Division, ASCE, Vol. 109, No. 4, pp. 603-618.

210. **U.S. Army Corps of Engineers** (1984), "*Shore protection manual*", Coastal Engineering Research Center, Vicksburg, Mississippi.

211. **Uthayakumar, M.** (1996), "Liquefaction of sands under multi-axial loading," Ph.D. thesis, The University of British Columbia, British Columbia, Canada.

212. **Vaid, Y.P. and Thomas, J.** (1995), "Liquefaction and post-liquefaction behavior of sand," Journal of the Geotechnical Engineering, ASCE, Vol. 121, No. GT 2, pp. 163-173.

213. **Vaid, Y.P., Chung, E.K.F. and Kuerbis, R.H.** (1990), "Stress path and steady state," Canadian Geotechnical Journal, Vol. 27, No. 1, pp. 1-7.

214. **Verdugo, R. and Ishihara, K.** (1996), " The steady state of sandy soils," Soils and Foundations, Vol. 36, No. 2, pp. 81-91.

215. **Vermeer, P.A.** (1978), "A double hardening model for sand," Geotechnique, Vol. 28, No.4, pp. 413-433.

216. **Verruijt, A.** (1982), "Approximations of cyclic pore pressures caused by sea waves in a poro-elastic half-plane", Soil Mechanics - Transient and Cyclic Loads, Edited by G.N. Pande and O.C. Zienkiewicz, John Wiley and Sons Ltd., London, U.K., pp. 37-51.

217. **von Mises, R.** (1913), "Mechanik der festen lorper in plastisch deformabllem zustand," Nachr. Gess. Wess. Gottingen, p. 582.

218. **von Mises, R.** (1928), "Mechanik der plastischen formanderung von kristallen," Z. Angen. Math. Mech., Vol. 8, p. 161.

219. **Wood, D.M.** (1990), "*Soil behavior and critical state soil mechanics*", Cambridge University Press, Cambridge, U.K.

220. **Wood, D.M., Belkheir, K. and Liu, D.F.** (1994), "Strain softening and state parameters for sand modeling," Geotechnique, Vol. 44, No. 2, pp. 335-339.

221. **Wroth, C.P.** (1958), "The behavior of soils and other granular media when subjected to shear," Ph.D. thesis, Cambridge University, U.K.

222. **Yamada, Y. and Ishihara, K.** (1979), "Anisotropic deformation characteristics of sand under three-dimensional stress conditions," Soils and Foundations, Vol. 19, No. 2, pp. 79-94.

223. **Yamada, Y. and Ishihara, K.** (1981), "Undrained deformation characteristics of loose sands under three-dimensional stress conditions," Soils and Foundations, Vol. 21, No. 1, pp. 97-107.

224. **Yamamoto, T.** (1978), "Seabed instability from waves", Proceedings of the 10th Annual Offshore Technology Conferences, paper 3262, Houston, Texas, pp. 1819-1824.

225. **Yamamoto, T.** (1983), "On the response of a Coulomb-damped poroelastic bed to water ways", Marine Geotechnology, Vol. 5, No. 2, pp. 93-130.

226. **Yamamoto, T., Koning, H.L., Sellmeijer, H. and Hijum, E.V.** (1978), "On the response of a poro-elastic bed to water waves", Journal of Fluid Mechanics, Vol. 87, No. 1, pp. 193-206.

227. **Yang, Q.S.** (1990), "Wave-induced response of seafloor desposits: a simple model for sands and nonlinear analysis by finite element method", Ph.D. thesis, Concordia University, Montreal, Quebec, 197 p.

228. **Yang, Q.S., Poorooshasb, H.B., Cheung, S.C.H.** (1994), "Travelling wave-induced liquefaction of sand deposits", Canadian Journal of Civil Engineering, Vol. 21, pp. 186-194.

229. **Youd, T.L.** (1972), "Compaction of sands by repeated shear straining," Journal of the Soil Mechanics and Foundations Division, ASCE, Vol. 98, No. SM 7, pp. 709-725.

230. **Zen, K. and Yamazaki, H.** (1990a), "Mechanism of wave-induced liquefaction and densification in seabed", Soils and Foundations, Vol. 30, No. 4, pp. 90-104.

231. **Zen, K. and Yamazaki, H.** (1990b), "Oscillatory pore pressures and liquefaction in seabed induced by ocean waves", Soils and Foundations, Vol. 30, No. 4, pp. 147-161.

232. **Zen, K. and Yamazaki, H.** (1991), "Field observation and analysis of wave-induced liquefaction in seabed", Soils and Foundations, Vol. 31, No. 4, pp. 161-179.

233. **Zen, K., Yamazaki, H. and Lee, I.H.** (1991), "Wave-induced liquefaction and instability of breakwaters", Proceedings of the International Conference on Geotechnical Engineering for Coastal Development (Geo-Coast '91), Yokohama, Japan, Vol. 1, pp. 673-678.

234. **Zhang, H.** (1997), "Steady state behavior of sands and limitations of the triaxial test," Ph.D. thesis, University of Ottawa, Ottawa, Canada.

235. **Zhang, H. and Garga, V.K.** (1997), "Quasi-steady state: a real behavior?" Canadian Geotechnical Journal, Vol. 34, No.5, pp. 749-761.

236. **Ziegler, H.** (1959), "A modification of Prager's hardening rule," Quarterly Applied Mathematics, Vol. 17, pp. 55-65.

237. **Zienkiewicz, O.C. and Bettess, P.** (1982), "Soils and other saturated media under transient, dynamic conditions: General formulation and the validity of various simplifying assumptions", Soil Mechanics - Transient and Cyclic Loads, Edited by G.N. Pande and O.C. Zienkiewicz, John Wiley and Sons Ltd., London, U.K., pp. 1-16.

238. **Zienkiewicz, O.C. and Mroz, Z.** (1984), "Generalized plasticity formulation and applications to geomechanics," Mechanics of Engineering Materials, Desai, C.S. and Gallagher, R.H. (eds.), John Wiley, Chapter 33, pp. 655-679.

239. **Zienkiewicz, O.C. and Shiomi, T.** (1984), "Dynamic behavior of saturated porous media; The generalized Biot formulation and its numerical solution", International Journal for Numerical and Analytical Methods in Geomechanics, Vol. 8, pp. 71-96.

240. **Zienkiewicz, O.C., Chan, A.H.C., Pastor, M., Paul, D.K. and Shiomi, T.** (1990), "Static and dynamic behavior of geomaterials: Rational approach to quantitative solutions, Part I: Fully saturated problems," Proceedings of Royal Society, Series A., Vol. 429, pp. 285-309.

241. **Zienkiewicz, O.C., Chang, C.T. and Bettess, P.** (1980), "Drained, undrained, consolidating and dynamic behavior assumptions in soils", Geotechnique, Vol. 30, No. 4, pp. 385-395

242. **Zienkiewicz, O.C., Chang, C.T. and Hinton, E.** (1978), "Nonlinear seismic response and liquefaction," International Journal for Numerical and Analytical Methods in Geomechanics, Vol. 2, No.4, pp. 381-404.

243. **Zienkiewicz, O.C., Leung, K.H. and Pastor, M.** (1985), "A simple model for transient soil loading in earthquake analysis, Part I: Basic model and its application," International Journal for Numerical and Analytical Methods in Geomechanics, Vol. 9, pp. 953-976.